

Medizinische Klinik und Poliklinik I,
Klinikum der Ludwig-Maximilians-Universität München
Vorstand: Univ. Prof. Dr. Steffen Massberg



The role of mechanosensing in platelet function

Dissertation
zum Erwerb des Doktorgrades der Medizin
an der Medizinischen Fakultät der
Ludwig-Maximilians-Universität zu München

vorgelegt von

Ben Heinrich Raude

aus

Berlin

2021

Mit Genehmigung der Medizinischen Fakultät
der Universität München

Berichterstatter: Prof. Dr. Steffen Massberg

Mitberichterstatter: Prof. Dr. Alexander Bartelt
PD Dr. Christian Wichmann
Prof. Dr. Hans-Ulrich Kreider-Stempfle

Mitbetreuung durch den
promovierten Mitarbeiter: Dr. Dr. Florian Gärtner

Dekan: Prof. Dr. med. dent. Reinhard Hickel

Tag der mündlichen Prüfung: 01.07.2021

Danksagung

Besonderer Dank gilt Herrn Prof. Dr. med. Steffen Massberg für die Möglichkeit in seinem Labor arbeiten zu können und Teil einer so innovativen Forschungsgruppe zu sein, die mich nachhaltig für die Grundlagenforschung begeisterte. Zudem möchte ich mich bei Dr. med. Florian Gärtner bedanken, der mein Projekt exzellent betreute und mich mit zahlreichen Ideen inspirierte.

Auch die übrigen Mitglieder der Arbeitsgruppe möchte ich erwähnen, ohne die dieses Projekt in diesem Umfang nicht hätte realisiert werden können und die mir stets in Rat und Tat zur Seite standen.

Zuletzt möchte ich mich für die Unterstützung und Motivation bei meinen Eltern und Geschwistern bedanken.

Table of contents

| | |
|---|-----------|
| Index of abbreviations | iv |
| List of figures | vi |
| 1 Introduction | 1 |
| 1.1 The functional role of platelets in hemostasis and atherothrombosis | 1 |
| 1.2 The structure and function of the $\alpha_{IIb}\beta_3$ integrin | 6 |
| 1.3 Principles of platelet migration | 10 |
| 1.4 Platelet mechanosensing | 13 |
| 1.5 Thesis aim | 15 |
| 2 Material and Methods | 16 |
| 2.1 Technical setup for optimal image acquisition | 16 |
| 2.1.1 The inverted fluorescence microscope | 16 |
| 2.1.2 The camera | 16 |
| 2.1.3 The lens | 17 |
| 2.1.4 The filter cubes | 18 |
| 2.1.5 Definition of fluorescence | 21 |
| 2.1.6 The fluoroscein-5-isothiocyanate (FITC) | 22 |
| 2.1.7 The sulfoindocyanine Cy3 | 23 |
| 2.1.8 Image acquisition and live cell imaging | 24 |
| 2.2 Preparation of washed platelets | 25 |
| 2.2.1 Preparation of modified Tyrode buffer | 25 |
| 2.2.2 Isolation of human and murine platelets | 25 |
| 2.3 Setup of the biomechanical microenvironment to study platelet function | 26 |
| 2.3.1 Surface synthesis and – properties | 26 |
| 2.3.2 Coating Substrates | 28 |
| 2.4 Flow cytometry | 31 |
| 2.5 Pharmacological inhibition | 32 |
| 2.6 Data analysis | 33 |
| 2.7 Statistics | 34 |
| 3 Results | 35 |
| 3.1 A precise assay to investigate platelet mechanobiology | 35 |
| 3.2 The effect of plasma activators and divalent cations on platelet function | 37 |
| 3.3 Platelet function on low ligand densities | 40 |
| 3.4 Platelet function on high-tension tolerance - PLL-g-PEG-RGD | 43 |
| 3.5 Platelet function on the tension gauge tether | 45 |
| 3.5.1 Human platelet mechanobiology on the tension gauge tethering system – a tension threshold ≥ 55 pN is required to alter platelet function | 45 |
| 3.5.2 Murine platelet mechanobiology on the tension gauge tethering system | 53 |
| 3.6 The influence of pharmacologically inhibiting the contractile machinery of human platelets | 54 |
| 3.7 Pharmacological blockage of the mechanosensitive channels Piezo1 of human platelets | 57 |
| 4 Discussion | 59 |
| 5 Summary | 66 |
| 6 Bibliography | 70 |
| 7 Eidesstaatliche Erklärung | 88 |

Index of abbreviations

A

| | |
|---------|---|
| ACD | acid-citrate-dextrose |
| ADMIDAS | adjacent to the metal ion–dependent adhesion site |
| ADP | adenosine diphosphate |
| AFM | atomic force microscopy |

B

| | |
|----|------------|
| bp | base pairs |
|----|------------|

C

| | |
|--------|-------------------------------|
| COX | cyclooxygenase |
| Cy3 | cyanine 3 |
| CHO-K1 | Chinese hamster ovary cells 1 |

E

| | |
|-----|-------------------------|
| ECM | extracellular matrix |
| EGF | epidermal growth factor |

F

| | |
|------|-------------------------------------|
| FA | focal adhesion |
| FACS | fluorescence activated cell sorting |
| FITC | fluorescein isothiocyanate |

G

| | |
|------|-------------------------------------|
| GFP | green fluorescence protein |
| GPCR | g-protein-coupled-receptors (GPCRs) |
| g | gram |

H

| | |
|---------------------|---|
| h | hour |
| HSA | human serum albumin |
| HCL _(aq) | hydrochloric acid |
| HEPES | 2-(4-(2-hydroxyethyl)-1-piperazineethanesulfonic acid |

K

| | |
|-----|------------|
| kDA | kilodalton |
|-----|------------|

L

| | |
|-------|--------------------------------------|
| LIMBS | ligand-associated metal binding site |
|-------|--------------------------------------|

M

| | |
|------|------------|
| mbar | millibar |
| μg | microgram |
| μl | microliter |
| μm | micrometre |
| μM | micromolar |

| | |
|------------------|-----------------------------------|
| MIDAS | metal-ion-dependent adhesion site |
| min | minute |
| ml | millilitre |
| MRP | multidrug resistance protein |
| ms | milliseconds |
| MSC | mechanosensitive channel |
| N | |
| NA | numerical aperture |
| nm | nanometre |
| nN | nanonewton |
| P | |
| PH | phase contrast |
| pN | piconewton |
| PRP | platelet rich plasma |
| PSI | plexin-semaphorin-integrin |
| R | |
| RFP | red fluorescence protein |
| RT | room temperature |
| T | |
| TGT | tension gauge tether |
| T _{tol} | tension tolerance |
| TXA ₂ | thromboxane A ₂ |
| V | |
| VWF | von willebrand factor |

List of figures

| | |
|--|----|
| Figure 1.1: Cascade of events showing platelet recruitment to sites of vascular injury | 3 |
| Figure 1.2: Structure of $\alpha V\beta 3$ -Mn complexed with cyclo(RGDf- $\{Me\}V$)..... | 8 |
| Figure 1.3: Basic principle of platelet migration | 12 |
| Figure 2.1: The inverted microscope Olympus IX83 and its technical constitution | 16 |
| Figure 2.2: Architecture and basic working principle of a charge-coupled device | 17 |
| Figure 2.3: The numerical aperture and the collection of emitted fluorescence with different immersion media..... | 18 |
| Figure 2.4: The filter cube | 20 |
| Figure 2.5: The Jablonski diagram..... | 22 |
| Figure 2.6: Fluorescein-5-isothiocyanate | 23 |
| Figure 2.7: Cyanine3..... | 24 |
| Figure 2.8: Low-pressure plasma system Zepto | 28 |
| Figure 2.9: Architecture of the tension gauge tether..... | 30 |
| Figure 2.10: DNA geometry | 31 |
| Figure 2.11: Basic principle of flow cytometry | 32 |
| Figure 3.1.1: The effect of ligand density on fluorescence intensity..... | 35 |
| Figure 3.1.2: The effect of platelet function on untreated glass surfaces and PLL-g-PEG coated surfaces | 36 |
| Figure 3.2.1: The effect of activators and divalent cations on the integrin activation and P-Selectin expression | 37 |
| Figure 3.2.2: The effect of varying concentrations of PLL-g-PEG-Biotin-NA-FITC-Biotin-cRGD with physiological concentrations of Ca^{2+} and Mg^{2+} 1 mM on platelet migration | 38 |
| Figure 3.2.3: The effect of activators and divalent cations on migration on PLL-g-PEG-Biotin-NA-FITC-Biotin-cRGD 10%..... | 39 |
| Figure 3.3.1: Platelet function on <i>PLL-g-PEG-Biotin-NA-FITC-Biotin-cRGD 10%</i> with physiological concentrations of Ca^{2+} and Mg^{2+} 1 mM and exogenous integrin activation with Mn^{2+} 200 μM | 40 |
| Figure 3.3.2: Representative images of platelet migration on <i>PLL-g-PEG-Biotin-NA-FITC-Biotin-cRGD 10%</i> with physiological concentrations of Ca^{2+} and Mg^{2+} 1 mM and external integrin activation with Mn^{2+} 200 μM | 41 |
| Figure 3.3.3: Human platelet function on <i>PLL-g-PEG-Biotin - NA-FITC - Biotin-cRGD 5%</i> with physiological concentrations of Ca^{2+} and Mg^{2+} 1 mM and external integrin activation with Mn^{2+} 200 μM | 42 |
| Figure 3.3.4: Murine platelet function on <i>PLL-g-PEG-Biotin - NA-FITC - Biotin-cRGD 5%</i> with physiological concentrations of Ca^{2+} 1 mM and external integrin activation with Mn^{2+} 200 μM | 43 |
| Figure 3.4.1: Human platelet function on <i>PLL-g-PEG-RGD 10%</i> with physiological concentrations of Ca^{2+} and Mg^{2+} 1 mM and external integrin stimulation with Mn^{2+} 200 μM | 44 |
| Figure 3.4.2: Comparison of human platelet function on <i>PLL-g-PEG-Biotin - NA-FITC - Biotin-cRGD 10 %</i> and <i>PLL-g-PEG-Biotin - NA-FITC - Biotin-RGD 10%</i> | 44 |
| Figure 3.5.1.1 Human platelet mechanobiology on <i>PLL-g-PEG-Biotin - NA - Biotin-TGT-cRGD 10 %</i> and the control <i>PLL-g-PEG-Biotin - NA-FITC - Biotin-cRGD 10 %</i> | 46 |
| Figure 3.5.1.2: Human platelet mechanobiology on <i>PLL-g-PEG-Biotin - NA - Biotin-TGT-cRGD 10 %</i> and the control <i>PLL-g-PEG-Biotin - NA-FITC - Biotin-cRGD 10 %</i> under physiological conditions of Ca^{2+} 1mM and Mg^{2+} 1mM..... | 48 |

| | |
|--|----|
| Figure 3.5.1.3: Live imaging of human platelets and investigating mechanobiology on <i>PLL-g-PEG-Biotin - NA - Biotin-55pN-cRGD 10 %</i> under physiological conditions of Ca^{2+} 1mM and Mg^{2+} 1mM. | 49 |
| Figure 3.5.1.4: Human platelet mechanobiology on <i>PLL-g-PEG-Biotin - NA - Biotin-TGT-cRGD 10 %</i> and the control <i>PLL-g-PEG-Biotin - NA-FITC - Biotin-cRGD 10 %</i> with integrin activation by Mn^{2+} 200 μM | 52 |
| Figure 3.5.2.1: Murine platelet function on <i>PLL-g-PEG-Biotin - NA - Biotin-TGT-cRGD 10 %</i> and <i>PLL-g-PEG-Biotin - NA-FITC - Biotin-cRGD 10%</i> | 54 |
| Figure 3.6: Pharmacological inhibition of myosin IIa by Blebbistatin..... | 56 |
| Figure 3.7: Pharmacological inhibition of Piezo1 by GsMTx-4 for human platelets..... | 58 |

1 Introduction

1.1 The functional role of platelets in hemostasis and atherothrombosis

In a complex fashion of events platelets derive from the cytoplasm of megakaryocytes in the bone marrow and are released into the circulation. (Italiano, Lecine et al. 1999) (Junt, Schulze et al. 2007) Platelets measure a size of 2 – 4 μm and adapt a discoid shape in the resting state – upon activation, they undergo actin-dependent morphological shape changes. (Hartwig 2013) Approximately one trillion platelets circulate in the human blood with a lifespan of about seven to ten days and constantly scan the vasculature for tissue injury. (Varga-Szabo, Pleines et al. 2008) Besides the fact that platelets are anucleate cellular fragments they reveal a sophisticated cytoskeleton, a variety of different surface receptors and multiple secretory granules. (Jackson 2011) (Hartwig 2013)

For the past few decades platelet function was assumed to be limited to the formation of physiological blood clots in hemostasis and leading to pathological conditions such as in atherothrombosis. (Italiano, Lecine et al. 1999) (Ruggeri 2002) (Nieswandt, Aktas et al. 2005) (Jackson 2011) However, platelets exert a more diverse role such as in immunological processes and antimicrobial host defence. Platelets are among the first cells to be encountered at sites of endothelial injury or inflammation and seem to follow a similar recruiting cascade of events as well understood as in arterial thrombosis. (Brass, Zhu et al. 2005) (Jackson 2011) (Semple, Italiano et al. 2011) (Wong, Jenne et al. 2013) (Yeaman 2014) (Gaertner, Ahmad et al. 2017) Although previous works described a position change of platelets at sites of injury or inflammation, platelet migration has only recently been identified by Gärtner et al. to be an autonomous process in vivo. (Pitchford, Momi et al. 2008) (Kraemer, Borst et al. 2010) (Gaertner, Ahmad et al. 2017)

During the initial steps of clot formation platelets interact with several adhesive proteins and agonists and are exposed to a highly dynamic microenvironment all of which trigger activation and adhesion. (Offermanns 2006) (Ruggeri 2007) (Qiu, Brown et al. 2014) The synergy of biochemical – as well as biophysical stimuli allow platelets to precisely probe the mechanical properties of the vessel wall. (Kroll, Hellums et al. 1996) (Offermanns 2006) (Sheriff, Bluestein et al. 2010) (Brass, Wannemacher et al. 2011) The initial capture of a

circulating, resting platelet at the site of tissue injury is referred to as “tethering” and mediated through the two membrane glycoproteins GPVI and GPIb. The GPIb-V-IX complex predominantly interacts with von Willebrand factor and indirectly with collagen. (Ruggeri 1997) (Savage, Almus-Jacobs et al. 1998) (Varga-Szabo, Pleines et al. 2008) This highly abundant surface receptor complex works independent of platelet activation and is unique to platelets and megakaryocytes. (Sakariassen, Nievelstein et al. 1986) Besides the broad range of macromolecular components such as laminin, fibronectin or vWF, collagen is considered to be the most potent thrombogenic substrate to be encountered at sites of vascular injury. (Baumgartner 1977) (Clemetson and Clemetson 2001) The transmembrane glycoprotein GPVI was identified to be the central platelet collagen receptor, thus playing the main role for the initiation of platelet attachment. (Moroi, Jung et al. 1989) (Gibbins, Okuma et al. 1997) (Clemetson and Clemetson 2001) (Nieswandt, Bergmeier et al. 2000) (Massberg, Gawaz et al. 2003) (Dubois, Panicot-Dubois et al. 2006) The “tethering” is characterised by a relatively short-lived – and weak interaction that is unable to support permanent attachment. (Savage, Almus-Jacobs et al. 1998) (Varga-Szabo, Pleines et al. 2008) However, the underlying function of this mechanism is to recruit platelets from the bloodstream by reducing their speed. This initial interaction with the vessel wall enables additional surface receptors to bind. (Savage, Saldivar et al. 1996) (Varga-Szabo, Pleines et al. 2008) The initial “tethering” is followed by platelet “rolling” on the vascular wall that will support permanent attachment (see figure 1.1A)). (Savage, Saldivar et al. 1996)

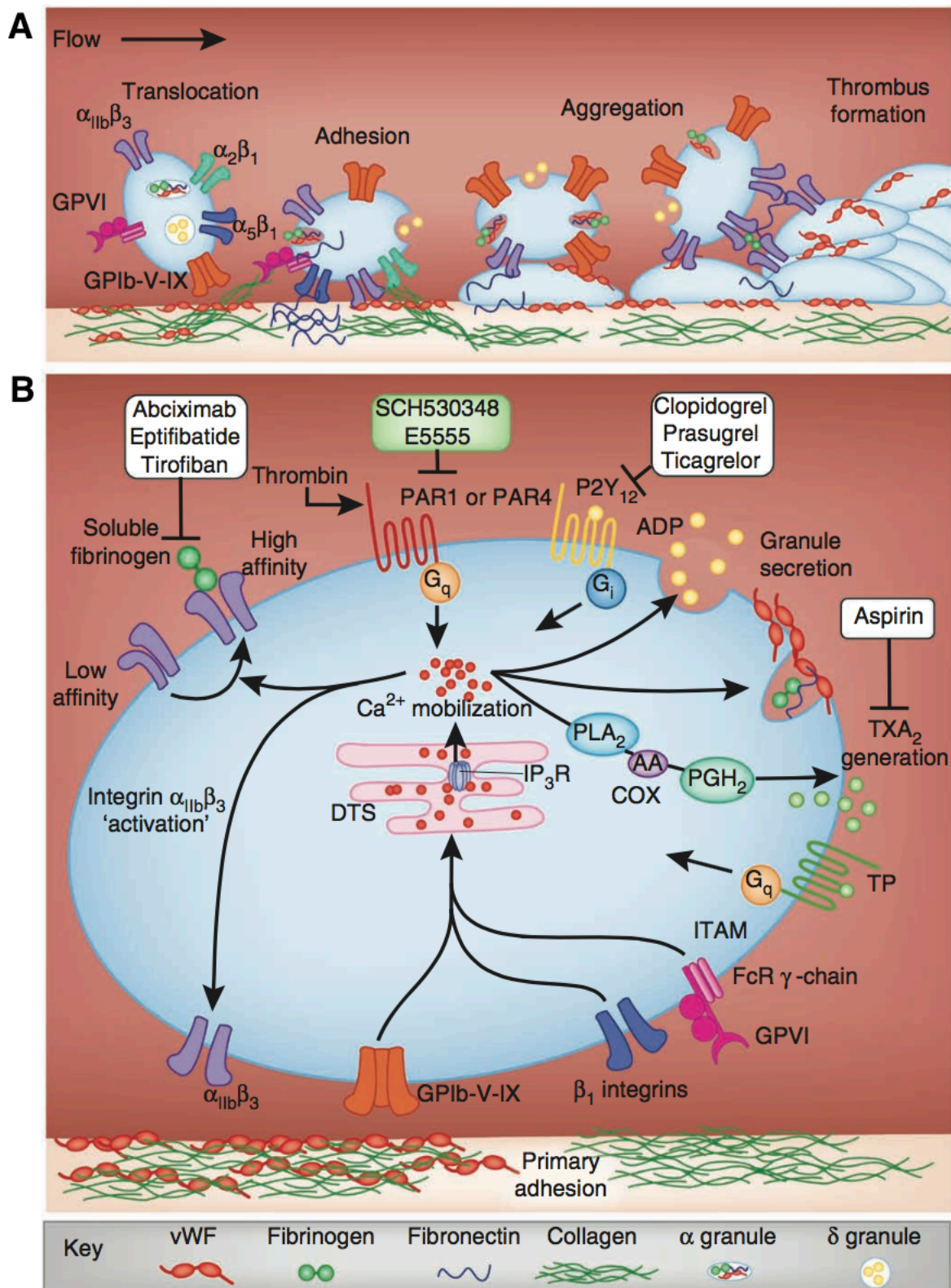


Figure 1.1: Cascade of events showing platelet recruitment to sites of vascular injury

A: Simplified scheme showing the events leading to thrombus formation. B: Interplay of surface receptors and downstream signaling cascades. The different steps will be described in detail throughout the text (Jackson 2011)

A prerequisite of firm platelet adhesion is the activation of integrins acting as bidirectional surface receptors linking cytoplasmic regulators to extracellular stimuli. A quiescent platelet expresses multiple copies of integrins on the plasma membrane that remain in an inactive, low affinity conformational configuration (see figure 1.1B)). (Beglova, Blacklow et al. 2002) (Xiong, Stehle et al. 2001) (Nishida, Xie et al. 2006) The receptor-specific platelet activation through the exposed ligands of the ECM drives further downstream signaling cascades that lead to “outside-in” signaling. Simultaneously the two main intracellular activators talin and kindlin bind to the cytoplasmic domain of the β subunit of the integrin. This process termed “inside-out” signaling induces conformational changes of the extracellular domain of the integrin resulting in a switch to the high affinity state. (Carman and Springer 2003) (Li, Delaney et al. 2010) (Shattil, Kim et al. 2010) This leads to the additional surface expression from intracellular granules of the major integrin $\alpha_{IIb}\beta_3$ mainly binding to fibrinogen, but also von Willebrand factor and fibronectin and the integrin $\alpha_2\beta_1$ binding to collagen. (Hynes 2002) (Qiu, Brown et al. 2014) These two crosslinking processes mediate firm adhesion, aggregation as well as thrombus formation – additionally they induce the release of intracellular granules and morphological shape changes. (Clark and Brugge 1995)

The induced heterogeneous downstream signaling pathways that promote initial adhesion and activation via several positive feedback loops, also trigger the release of a variety of different mediators that act in an autocrine - and paracrine fashion. (Kroll and Schafer 1989) (Davi and Patrono 2007) The complex mechanism orchestrating platelet activation combines the translation of biochemical – and biophysical stimuli at the site of tissue injury with the main effector serine protease – thrombin – of the coagulation cascade. The generation of thrombin from prothrombin in a tissue-factor dependent manner is spatially concentrated on the platelet membrane favouring the interaction with the two protease-activated receptors PAR 1 and PAR 4 in humans (see figure 1.1B)). (Kahn, Nakanishi-Matsui et al. 1999) (Weiss, Hamilton et al. 2002) (Coughlin 2005) (Cornelissen, Palmer et al. 2010) Thrombin as a multifunctional agonist is considered to be the most potent platelet activator inducing a broad range of cellular actions including shape change, exocytosis of alpha-, dense- and lysosomal granules and an additional affinity change of the integrin $\alpha_{IIb}\beta_3$. (Davey and LÜScher 1967) (Stenberg, McEver et al. 1985) (Hughes and Pfaff 1998) (McNicol and Israels 1999) The “alpha granules” are the most abundant granules and release a variety of high molecular polypeptides that contribute to primary – and secondary hemostasis. (Blair and Flaumenhaft 2009) Upon platelet activation the alpha granules coalesce with the platelet membrane

thereby increasing the surface area approximately two to four fold. The alpha granule membrane largely mirrors the platelet membrane boosting the expression of additional “(GP) IIb-IIIa; fibrinogen receptor; CD 36; the thrombospondin and collagen receptor; CD9; PECAM1; and Rap1b, a guanosine triphosphate (GTP)-binding protein.” (Berger, Masse et al. 1996) The “dense granules” mainly contain Adenosindiphosphat (ADP), Adenosindiphosphat (ATP), Serotonin and Calcium that accounts for approximately 60-70% of the total platelet calcium. (Holmsen and Weiss 1979) (McNicol and Israels 1999)

The release of the “secondary mediators” such as Thromboxane (TXA₂) and ADP will lead to an increase of intracellular Ca²⁺ thereby amplifying and sustaining the platelet response. (Davi and Patrono 2007) The cyclooxygenase I (COX I) catalyses the reaction, where TXA₂ is produced from arachidonic acid that originates from phospholipids of the plasma membrane and is then actively transported and secreted by the multidrug resistance protein 4 (MRP4). (Reid, Wielinga et al. 2003) (Rius, Thon et al. 2005) (Jedlitschky, Greinacher et al. 2012) ADP in turn binds to the P2Y₁ receptor that mainly leads to the mobilization of calcium, whereas the P2Y₁₂ receptor represents the final common path to complete platelet aggregation initiated by all known platelet agonists. (Boarder and Hourani 1998) (Kunapuli 1998) (Gachet 2006) (Gachet 2008) TXA₂ and ADP exert their function through “G-Protein-Coupled-Receptors” (GPCRs) and play a central role for platelet aggregation and recruitment of additional platelets to the site of injury. (Offermanns 2006)

Serotonin accumulates in dense granules by passively diffusing from the blood plasma. Its role as a weak agonist for platelet activation and aggregation is considered to be secondary to the vasoactive effects on endothelium and vascular smooth muscle causing increased permeability and reduced blood flow. (Vanhoutte and Cohen 1983) (De Clerck, Xhonneux et al. 1984) (De Clerck 1986) (Li, Wallen et al. 1997)

Similar to the paracrine reactions induced by serotonin, platelets also secrete a number chemotactic cytokines that act on monocytes as well as endothelial – and smooth muscle cells. (Gleissner, von Hundelshausen et al. 2008) This is of particular interest considering the involvement of platelets in inflammation, antimicrobial host defence and angiogenesis. (Klinger and Jelkmann 2002) (May, Seizer et al. 2008) (Blair and Flaumenhaft 2009)

The synergising mechanism triggering platelet activation via the initial adhesion of GPIIb to von VWF followed by aggregation mainly mediated by $\alpha_{IIb}\beta_3$ integrin, not only coats the endothelium with a platelet monolayer, but also amplifies the recruitment of additional platelets to sites of vascular injury. (Smyth, Reis et al. 2001) (Bergmeier, Piffath et al. 2006) The locally high concentrations of soluble proteins such as VWF, fibrinogen and fibronectin

are the main mediators promoting clot maturation by firm platelet-platelet cohesion. (Ni, Denis et al. 2000) (Ni, Yuen et al. 2003) (Jackson 2007) The interaction of a firm fibrin network and the active process of clot retraction create a robust architectural scaffold that resists shear forces by the blood flow. (Chou, Mackman et al. 2004) (Ono, Westein et al. 2008)

1.2 The structure and function of the $\alpha_{IIb}\beta_3$ integrin

Integrins constitute a large family of membrane receptors transmitting signals bidirectionally across the membrane and can be identified on a variety of cell lines mainly mediating cell-matrix and cell-cell adhesion. (Hynes 1992) The term “integrin” derives from its action by integrating the extracellular compartment to the innards of the platelet’s cytoskeletal architecture and signaling pathways. (Luo, Carman et al. 2007)

The $\alpha_{IIb}\beta_3$ integrin is restricted to the megakaryocyte cell line and with approximately 40,000-80,000 copies the most abundant platelet integrin in the resting state. (Duperray 1987) (Wagner, Mascelli et al. 1996) (Adair and Yeager 2002) It is expressed on the platelet’s plasma membrane and upon activation additional integrins are translocated from the membranes of platelet α granules. (Niiya, Hodson et al. 1987) (Vorchheimer, Badimon et al. 1999) (Bennett 2005) In a Ca^{2+} -dependent manner the heterodimeric transmembrane protein is formed by the noncovalent association of an α – and β subunit, both consisting of a large extracellular headpiece, a transmembrane helix and a short cytoplasmic tail. (Phillips and Baughan 1983) (Fitzgerald and Phillips 1985) (Kieffer and Phillips 1990) (Weisel, Nagaswami et al. 1992) (Bennett 1996) (Beglova, Blacklow et al. 2002) (Springer and Wang 2004) (Kononova, Litvinov et al. 2017) The extracellular portion carries binding sites for fibrinogen, fibronectin and vWF as well as divalent cations required to complete the ligand-binding pocket. (Smith, Piotrowicz et al. 1994)

In the past few decades advances in the understanding of the complex crystal structure gave detailed insights into the extracellular portion of the $\alpha_{IIb}\beta_3$ integrin. The headpiece of the α_{IIb} subunit is formed by the β -propeller - and thigh domains followed by the tailpiece consisting of the Calf-1 – and Calf-2 domains. The structure of the β subunit is more complex where the β_3 βA (I-like) domain loops out from a hybrid domain which in turn is inserted into the PSI domain (*p*lexin, *s*emaphoring, *i*ntegrin) while the tailpiece consists of four tandem epidermal-growth-factor (EGF) like repeats connected to an unique βTD domain (see figure 1.2A)).

(Xiong, Stehle et al. 2001) (Xiong, Stehle et al. 2002) (Xiao, Takagi et al. 2004) (Bennett 2005) The flexibility of both subunits that enables the conformational relocation upon activation, is constituted by segments that are termed the α -genu between the thigh and calf-1 of the α -subunit and β -genu between the EGF-1 and EGF-2 of the β subunit. (Arnaout, Mahalingam et al. 2005) (Bennett 2005) (Bennett, Berger et al. 2009) The ligand-binding pocket located in the head domain is formed by the interface between the β -propeller of the α -subunit with the β 3 β A domain and hybrid domain of the β -subunit. (Craig, Gao et al. 2004) (Bennett, Berger et al. 2009) Additionally three divalent cation binding sites on the β 3 β A-domain seem to be involved in ligand-binding: a centrally located metal-ion-dependent adhesion site (MIDAS) and two allosteric sites, termed synergistic metal ion-binding site (SyMBS) and adjacent to the metal ion-dependent adhesion site (ADMIDAS). (Lee, Rieu et al. 1995) (Tozer, Liddington et al. 1996) (Shimaoka, Takagi et al. 2002) (Xiong, Stehle et al. 2002) (Xiong, Stehle et al. 2003) (Chen, Salas et al. 2003) (Mould, Barton et al. 2003) (Craig, Gao et al. 2004) (Xiao, Takagi et al. 2004) (Arnaout, Mahalingam et al. 2005) (Zhu, Luo et al. 2008) (Coller 2015) The MIDAS mainly coordinate a Mg^{2+} ion and is indispensable for ligand binding. (Xiong, Stehle et al. 2002) (Chen, Salas et al. 2003) (Mould, Barton et al. 2003) (Shimaoka, Xiao et al. 2003) Previous literature proved the pivotal role of the MIDAS by mutations that lead to an abolished ligand binding. (Tozer, Liddington et al. 1996) (Chen, Salas et al. 2003) (Valdramidou, Humphries et al. 2008) The SyMDS instead is occupied by Ca^{2+} that acts as an allosteric activator stabilizing the MIDAS, important but expandable for ligand binding. The ADMIDAS coordinate both Ca^{2+} and Mn^{2+} , where Mn^{2+} activates integrins by competing with Ca^{2+} . While Ca^{2+} seems to stabilize different conformational configurations, Mn^{2+} leads to large conformational changes between the unliganded-closed and liganded-open conformations thereby promoting ligand binding (see figure 1.2.B)). (Xiong, Stehle et al. 2002) (Chen, Salas et al. 2003) (Mould, Barton et al. 2003) (Xiao, Takagi et al. 2004) (Valdramidou, Humphries et al. 2008) In the unliganded-closed state only the ADMIDAS was occupied, while all three β 3 A-domain contained a cation in the liganded-open state. (Zhu, Zhu et al. 2010) The ion at the MIDAS was in direct contact with the ligand, thus playing a pivotal role in ligand binding. In contrast, the ion did not interact with the ligand at either the ADMIDAS or SyMDS suggesting a regulatory role of these two sites. (Xiong, Stehle et al. 2001) (Xiong, Stehle et al. 2002) (Mould, Barton et al. 2003) (Springer, Zhu et al. 2008) The collaborate interaction of the divalent cation binding sites play a pivotal role in mediating ligand binding and still remains a matter of research.

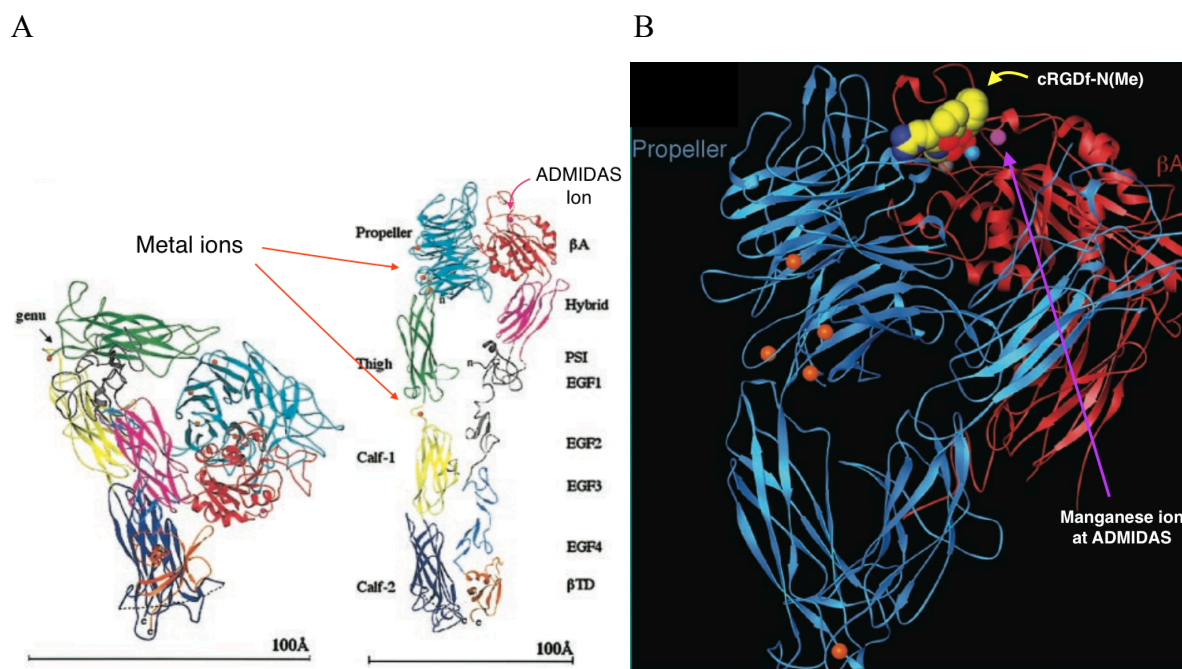


Figure 1.2: Structure of $\alpha V\beta 3$ -Mn complexed with cyclo(RGDf- $\{Me\}V$)

A) Ribbon diagram showing unliganded extracellular $\alpha V\beta 3$ integrin in the bent and the extended configuration. The ADMIDAS ion visible at the top of the βA domain (Xiong, Stehle et al. 2003).

B) Ribbon drawing of the $\alpha V\beta 3$ -Mn complexed with cyclo(RGDf-N $\{Me\}V$). ADMIDAS with the Manganese ion (magenta) and the metal ions at the MIDAS (cyan) and LIMBS (gray) (Xiong, Stehle et al. 2002).

In a quiescent platelet, the $\alpha_{IIb}\beta_3$ integrin resides in a low-affinity state, where the ligand-binding pocket faces the cell membrane to avoid platelet aggregation under physiological conditions that shifts to a high-affinity state upon activation. (Savage, Almus-Jacobs et al. 1998) (Hynes 2002) (Shimaoka, Takagi et al. 2002) (Nishida, Xie et al. 2006) Although often conceptually separated, the complex events leading to integrin activation may influence one another and thereby amplify signaling. The mechanism termed “outside-in” signaling involves ECM substrates, antibodies and ligands directly targeting the $\alpha_{IIb}\beta_3$ integrin that initiate several downstream signaling cascades. (Schwartz, Schaller et al. 1995) (Ma, Qin et al. 2007) This in turn will trigger “inside-out” signaling, in which binding to the cytoplasmic segment of the $\beta 3$ subunit by the two major regulatory proteins talin and kindlins induce intramolecular rearrangements. (Tadokoro, Shattil et al. 2003) (Coller and Shattil 2008) (Moser, Nieswandt et al. 2008) (Shattil, Kim et al. 2010) Despite the broad range of extracellular activators in the microenvironment and intracellular regulatory proteins, the external force applied on the substrate via the integrin induces allosteric signaling pathways. This stabilizes bonds by decreasing the dissociation time. (Puklin-Faucher, Gao et al. 2006) (Puklin-Faucher and Sheetz 2009) (Kee, Myers et al. 2015) The resulting conformational changes expose the ligand binding sites leading to the high affinity-state of the integrin. (Li,

Delaney et al. 2010) (Ye, Kim et al. 2011) Up to date, the conformational changes may be explained by two mechanistic models: the favoured mechanism for the $\alpha_{IIb}\beta_3$ integrin - the “switchblade model” - describes a shift from the bent to the extended conformation, in which large conformational rearrangement of the entire heterodimer induce straightening of the knees and separation of the α – and β subunits. A swing out movement will expose the ligand-binding pocket thereby switching to a high affinity state. (Hantgan, Paumi et al. 1999) (Beglova, Blacklow et al. 2002) (Hynes 2002) (Shimaoka, Takagi et al. 2002) (Takagi, Petre et al. 2002) (Askari, Buckley et al. 2009) (Bennett, Berger et al. 2009) (Zhu, Zhu et al. 2010) Takagi et al. showed that integrins in the presence of the superagonist Mn^{2+} or the ligand cyclic Arg-Gly-Asp (RGD) peptides adapted the extended conformation. (Takagi, Petre et al. 2002) The “deadbolt” model describes the allosteric rearrangements in the β subunit thereby exposing the ligand binding sites in the bent conformation without extending the opening of the headpiece. (Xiong, Stehle et al. 2003) (Arnaout, Goodman et al. 2007) (Mehrbod, Trisno et al. 2013)

The cytoplasmic domain of the integrin lacks enzymatic activity and thus relies on the recruitment of adapter molecules and signaling proteins. (Geiger, Bershadsky et al. 2001) (Arnaout, Goodman et al. 2007) Talin mechanically links the integrin’s cytoplasmic β tail to the cytoskeleton and despite carrying binding sites for the β subunit also contains multiple binding sites for actin and vinculin. (Calderwood, Zent et al. 1999) (Calderwood, Yan et al. 2002) (Tadokoro, Shattil et al. 2003) (Wegener, Partridge et al. 2007) (Gingras, Bate et al. 2008) (Critchley 2009) (Gingras, Bate et al. 2010) Its indispensable role was revealed in talin-null platelets that showed impaired integrin activation and platelet aggregation with otherwise normal configuration. (Nieswandt, Moser et al. 2007) (Kim, Ye et al. 2011) It seems to be the final regulatory checkpoint for integrin activation. (Tadokoro, Shattil et al. 2003) (Nieswandt, Moser et al. 2007)

The other regulatory proteins, the Kindlins play an equally important role in integrin activation. They also bind to the cytoplasmic part of the β subunit and may be further subdivided into three different members (Kindlin-1, Kindlin-2, Kindlin-3). (Ussar, Wang et al. 2006) (Mory, Feigelson et al. 2008) Kindlin-3 is particularly abundant in megakaryocytes and platelets and Moser et al. identified that kindlin-3-deficient platelets showed impaired integrin activation and defective aggregation. (Ussar, Wang et al. 2006) (Moser, Nieswandt et al. 2008)

The activated $\alpha_{IIb}\beta_3$ integrin predominantly binds the trinodular fibrinogen molecule and selectively targets two peptide motifs: firstly the two RGD sequences at positions 95-97 and

572–574 on the $\text{A}\alpha$ chain and secondly a C-terminal AGDV-containing dodecapeptide (γC -12) sequence at position 400–411 of the γ chain. (Ruoslahti and Pierschbacher 1986) (D'Souza, Ginsberg et al. 1990) (Beer, Springer et al. 1992) (Farrell, Thiagarajan et al. 1992) (Ruoslahti 1996) (Hantgan, Paumi et al. 1999) (Sanchez-Cortes and Mrksich 2009) (Kononova, Litvinov et al. 2017) While the γ chain of fibrinogen predominately binds the α subunit, the RGD and RGD-like peptides bind to both the α and β subunits of integrin $\alpha_{\text{IIb}}\beta_3$. Cierniewski et al. even reported different binding sites among RGD and RGD-derivatives. (Santoro and Lawing 1987) (Cierniewski, Byzova et al. 1999) Hu et. al described that the binding sites are spatially separated from one another, which was confirmed by Xiao et al. in crystal structures who located the cross-linking of the gamma chain to be distally to the RGD binding sites. (Hu, White et al. 1999) (Xiao, Takagi et al. 2004)

The ligand behaviour of these two sequences still remains a controversial topic particularly because several other studies showed that there was considerable competition at the ligand binding sites. (Santoro and Lawing 1987) (Bennett 2001) The binding properties of the fibrinogen molecule in a soluble – or immobilized condition are considerably different. The γ chain mediates the binding to soluble fibrinogen required for platelet aggregation, while binding to the RGD sequence is only favoured to immobilized fibrinogen or as polymerized fibrin in a maturing blood clot. (Litvinov, Farrell et al. 2016) (Kononova, Litvinov et al. 2017) The hypothesis that fibrinogen immobilization undergoes conformational changes cannot fully be supported since activated platelets bind soluble fibrinogen; however, Qiu et al. suggested that platelets sense the mechanical differences between soluble – and immobilized fibrinogen. (Balasubramanian and Slack 2002) (Jiroušková, Jaiswal et al. 2007) (Qiu, Ciciliano et al. 2015)

1.3 Principles of platelet migration

Generally, cell locomotion is the functional ability for a position change by precisely regulating cellular processes involved in spatio-temporal (re-) organisation. The prerequisites are congruent between cell lines and predominantly dependent on the interplay of extracellular surface receptors, the cytoskeletal network as well as intracellular trafficking. (Fukata, Nakagawa et al. 2003) (Keren, Pincus et al. 2008) (Barnhart, Lee et al. 2011) Despite these complex mechanisms accounting for cell migration, Lauffenburger et al. described a sequence of events trailing in four sequential steps: 1) membrane extensions as

lamelli- and filopodia at the leading edge 2) ligand adhesion 3) actomyosin mediated contraction 4) substrate release at the rear (see figure 1.3). (Lauffenburger and Horwitz 1996) When adhering to a given substrate platelets generate isotropic traction forces pointing towards the cell centre thereby probing the mechanical resistance. (Schwarz Henriques, Sandmann et al. 2012) However, in order to be able to migrate platelets have to reorganise the cytoskeleton in such a way that a polarised phenotype is adapted and asymmetry achieved. (Ridley et al., 2003) (Lombardi et al., 2007) A quiescent platelet changes form the resting into an asymmetric, migrating phenotype by generating high traction forces at the rear, with low traction at the front leading to protrusions (see figure 1.3). (Lombardi et al., 2007)

The spatio-temporal reorganisation at the leading edge is primarily dependent on the interplay of actin polymerization with cell-matrix-assembly. The morphological cell shape changes at the rear, however, are driven by myosin IIa-mediated contraction and adhesion-disassembly. (Gaertner, Ahmad et al. 2017) These mechanisms influencing the complex intracellular processes leading to differing migratory behaviours, largely dependent on the biochemical – as well as biophysical microenvironment. (Palecek, Loftus et al. 1997) (Gupton and Waterman-Storer 2006) (Yam, Wilson et al. 2007) (Lämmermann, Bader et al. 2008) Based on the principles of cell locomotion by Lauffenberger et al., Gaertner et al. only recently identified autonomous platelet migration *in vitro* and *in vivo* by dynamic visualization. (Lauffenburger and Horwitz 1996) (Gaertner, Ahmad et al. 2017)

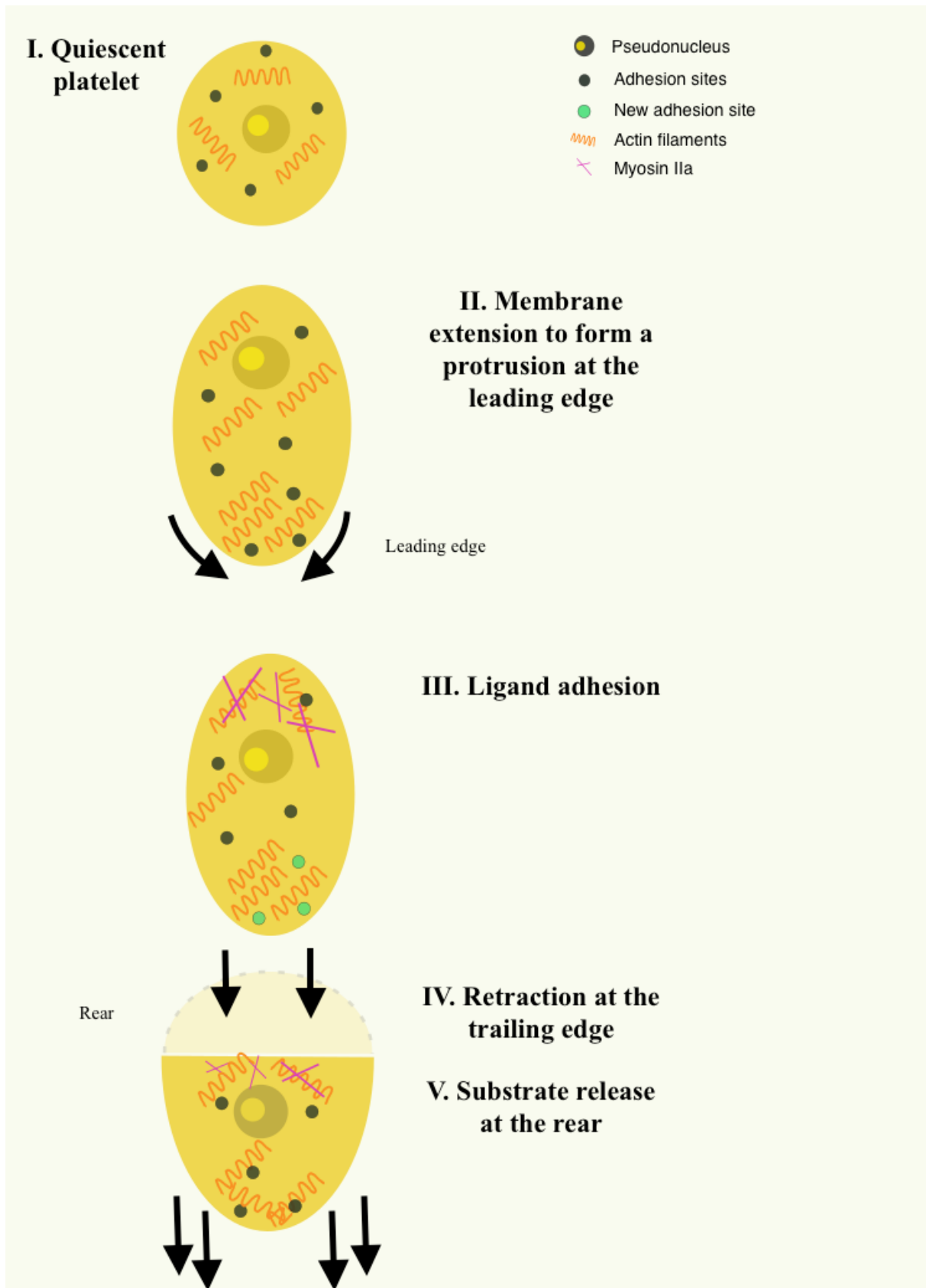


Figure 1.3: Basic principle of platelet migration
 (modified from (Lauffenburger and Horwitz 1996), (Gaertner, Ahmad et al. 2017))

1.4 Platelet mechanosensing

Platelets are ideal candidates to study the complex mechanisms accounting for mechanobiology due to their high integrin density and relatively basic cytoskeletal constitution. (Doggett, Girdhar et al. 2002) (Mody and King 2008) (Ciciliano, Tran et al. 2014) The integrins act as mechanosensitive surface receptors and are directly linked to the contractile machinery. The mechanosensitive forces are bidirectionally transduced via the integrin and seem to be a critical step in reaching a specific tension threshold to induce platelet activation, spreading and migration. (Wang and Ha 2013) (Qiu, Brown et al. 2014) Platelet force is determined by the contractile apparatus composed of actomyosin and believed to be able to generate a maximum force of up to ~ 30 nN per platelet. (Pollard, Fujiwara et al. 1977) (Jen and McIntire 1982) (Léon, Eckly et al. 2007) (Schwarz Henriques, Sandmann et al. 2012) (Zhang, Qiu et al. 2018) Individual platelets are considered to carry $\sim 12,000$ myosin II heads, each producing a force of $\sim 1,3$ pN in vivo. (Finer 1994, Michelson 2007) Earlier studies by Carr et. al and Jen et al. intended to study single platelet forces in large aggregates, however the experimental conditions using blood plasma and external forces applied to the maturing clot were difficult to control. (Jen and McIntire 1982) (Carr and Zekert 1991) However, Liang et al. combined platelet contractile forces with microclot volume and estimated the force per platelet to be ~ 2.1 nN after 60 min of clotting. (Liang, Han et al. 2010) These experimental setups up to this point were not able to accurately determine quantitative measures due to technological hindrance.

In an approach to investigate single cell forces Lam et al. conducted experiments with an atomic force microscope (AFM) and reported a maximum contractile force of ~ 29 nN after 15 min and adhesions stronger than ~ 70 nN. However, the generated force was only measured in an uniaxial contraction. (Lam, Chaudhuri et al. 2011) Myers et al. implanted microchips into hydrogels thereby measuring contractile forces of individual platelets by precisely controlling the mechanical-, chemical- and shear microenvironment. (Myers, Qiu et al. 2017)

Furthermore Jirouskova et al. examined the effect of low- and high-density fibrinogen on platelet function and revealed that ligand density fundamentally determines $\alpha_{IIb}\beta_3$ mediated outside-in signalling mechanisms. (Jirouskova, Jaiswal et al. 2007) Consistent with this study Qui et al. outlined the significance of substrate stiffness of the mechanical microenvironment

during clot formation, where high substrate stiffness maximized $\alpha_{\text{IIb}}\beta_3$ affinity and outside-in signaling. (Qiu, Brown et al. 2014) Additionally Kee et al. identified that $\alpha_{\text{IIb}}\beta_3$ integrin activity regulated by GP-VI-collagen interaction is not mediated by substrate stiffness. (Kee, Myers et al. 2015)

However, as to this date the mechanosensitive effects on platelet migration has not been investigated and will give insight in how platelets mechanically probe their microenvironment during clot formation. (Zhang, Qiu et al. 2018)

1.5 Thesis aim

Based on the current introductory evidence, platelets play a fundamental role in vascular injury and are among the first cells to be encountered at sites of inflammation. True autonomous migration of platelets in vitro and in vivo has only recently been shown by Gärtner et al. and previously been seen with scepticism. As to this date, little is known about how platelets probe the mechanical microenvironment and the processes accounting for mechanobiology.

Here, we aim to establish a novel migration assay that allows to quantify molecular forces and to study platelet mechanobiology using dynamic visualization. Furthermore, we aim to study the alteration of platelet function by pharmacological blocking the contractile apparatus as well as mechanosensitive ion channels.

2 Material and Methods

2.1 Technical setup for optimal image acquisition

2.1.1 The inverted fluorescence microscope

All live cell imaging experiments were performed by using the Olympus IX83 microscope (see figure 2.1). The characteristic feature of this inverted microscope is that the specimen is placed above the objective – the space in between the objective and the specimen spans a specific oil immersion. The stage contains a water basin, a critical feature for live cell imaging and may be heated to 37°C. The objective with the maximal resolution of 100x was used in the phase contrast - and fluorescence channels.

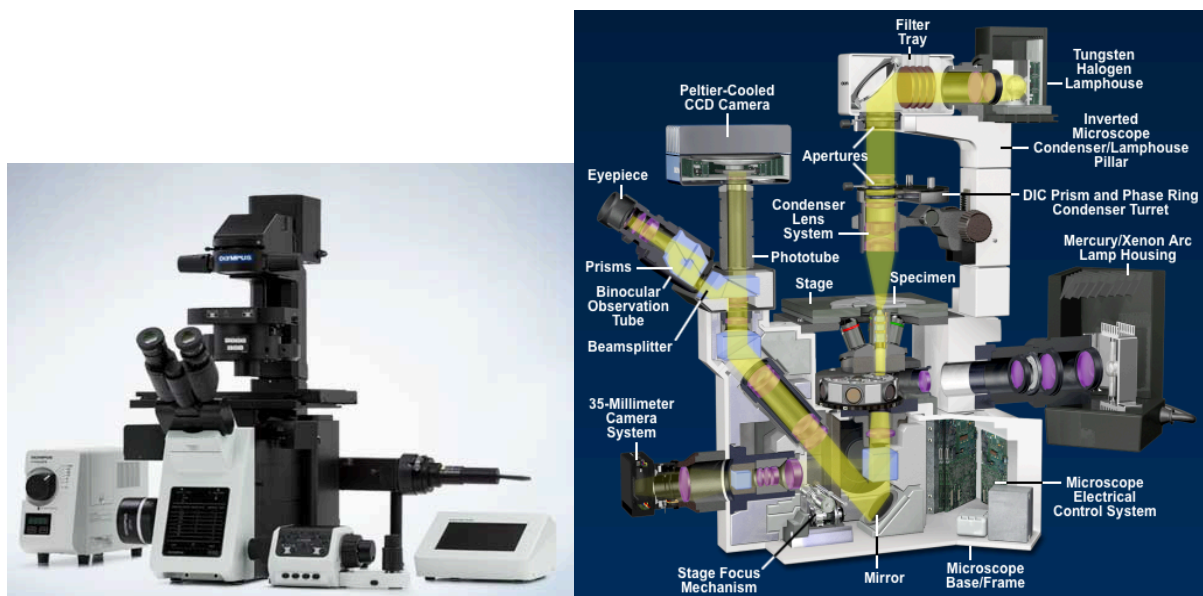


Figure 2.1: The inverted microscope Olympus IX83 and its technical constitution
(adapted from Abramowitz and Davidson (2020))

2.1.2 The camera

Images may either be depicted by the ocular or detected by a camera, where the vast majority of modern fluorescence microscopes contain charge-coupled devices (CCD-camera). The underlying principle of the CCDs is the conversion of light energy transmitted by a photon

into an electrical charge. (see figure 2.2) The CCD sensor is composed of a photosensitive silicon body with a matrix of photodiodes. The shape of the diodes and the area covered by a pixel strongly affect image resolution. The bigger the area covered by a pixel, the higher the photosensitivity, but with a decrease in overall resolution. (Abramowitz and Davidson 2020) The physical process where a photon interacts with the silicon body releasing negatively charged electrons is described as the photoelectric effect. (Janesick, 2001) (Abramowitz and Davidson 2020) This will excite an electron into a potential well of the diode in which the charge is proportional to the amount of photons. (Janesick, Elliott et al. 1987) (Abramowitz and Davidson 2020) The silicon diode photosensors (pixel) are arranged in vertical columns and horizontal rows. Each individual row is read out one after the other. The charge will pass down the vertical columns until reaching the final horizontal row (the readout register) that will measure a value for each individual pixel (see figure 2.2). Finally, a video signal is generated by reading the amount of electrons per pixel. (Janesick, Elliott et al. 1987) (Janesick, 2001) (Pawley, 2006) (Abramowitz and Davidson 2020) Images were acquired by a CCD-Camera of the company Olympus. (XM10, Olympus, Shinjuku, prefecture Tokio, Japan)

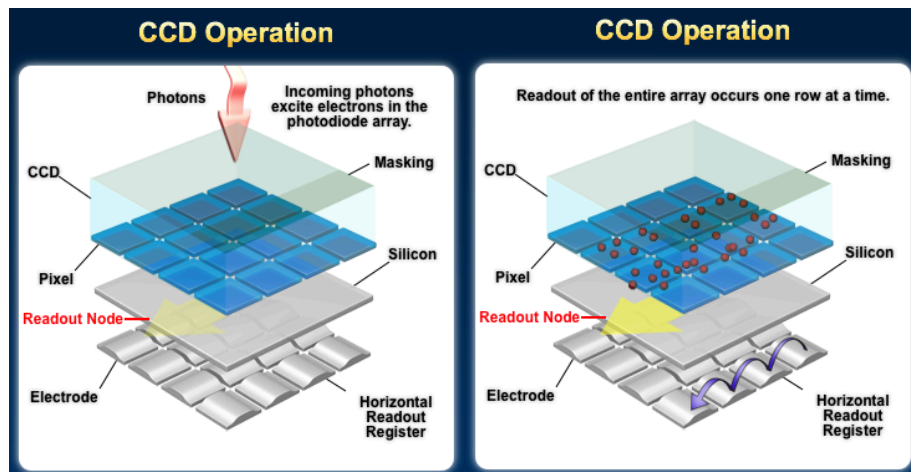


Figure 2.2: Architecture and basic working principle of a charge-coupled device
(adapted from Abramowitz and Davidson (2020))

2.1.3 The lens

The objective constitutes a critical component for optimal image acquisition – it influences magnification, light gathering ability as well as transmitted wavelength and differs in the immersion medium required.

The resolution of a microscope is defined as the smallest distance between two objects that still can be optically discriminated as two separate points. (Herman 1998) The larger the numerical aperture (NA), the more emitted fluorescence may be collected, thus resulting in a higher resolution. The NA is defined as the product of the refractive index = n (medium between specimen and objective) and the sinus of the aperture angle α . (Herman 1998)

The NA is proportional to the refractive index of the immersion medium – air has a refractive index = 1, water of around 1,3 and immersion oil of around 1,5. (Zhou, Chan et al. 2013)

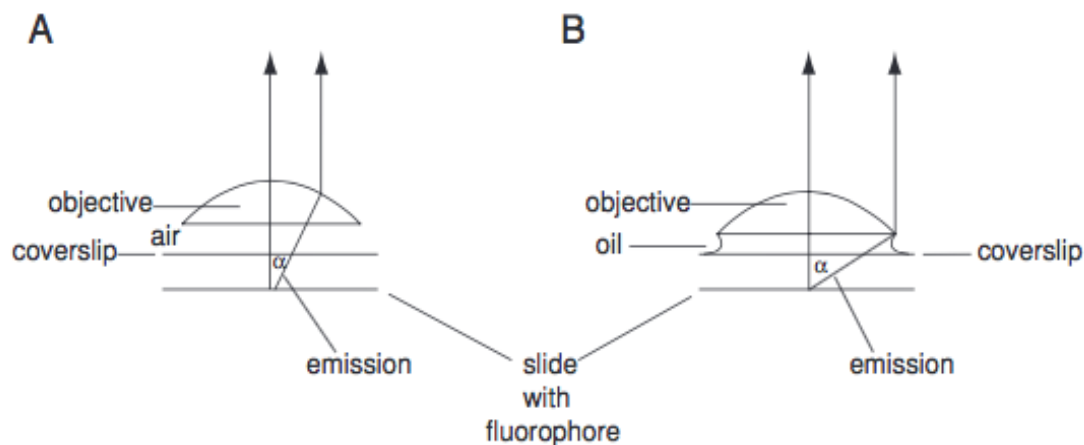


Figure 2.3: The numerical aperture and the collection of emitted fluorescence with different immersion media (Herman 1998)

Figure 2.3 evidences that immersion oil results in a shorter working distance and larger emission angle thereby increasing the collection of emitted fluorescence. (Herman 1998) (Stephens and Allan 2003) (Lichtman and Conchello 2005)

2.1.4 The filter cubes

The key why epifluorescence microscopy is so powerful, is due to specific filter cubes consisting of three fundamental elements: the excitation filter, dichromatic beamsplitters (dichroic mirrors) and the barrier filter (see figure 2.4). A full-spectrum light beam generated by the light source of the microscope encountering the excitation filter will be filtered in the way that only the exciting wavelength (blue light of wavelength $\approx 450 - 500$ nm for FITC and green light of wavelength $\approx 500 - 570$ nm for Cy3) of the particular fluorophore of interest will pass through (see figure 2.4). (Reichmann 2017) The maximum of the absorption spectrum may not overlap with the maximum of the emission spectrum of that particular fluorophore. The dichroic mirror angled at 45° reflects the exciting short-wavelength light.

The exciting light will now reach the object of interest. In epifluorescence the objective not only magnifies and images the specimen, but also works as a condenser illuminating it. (Lichtman and Conchello 2005) The now emitted longer-wavelength light passes through the dichroic mirror, while the remaining exciting light of shorter wavelength yet again will be reflected. The shift from the peak of the absorption – to the peak of the emission spectrum is called the Stoke's shift. The emitted light now encounters the barrier filter which selectively only allows the targeted spectral wavelength of the fluorophore (FITC \approx 518 nm and Cy3 \approx 563) to pass through. (see figure 2.4) (Wiederschain 2011) The targeted wavelength will either reach the eyepiece or be detected by the camera.

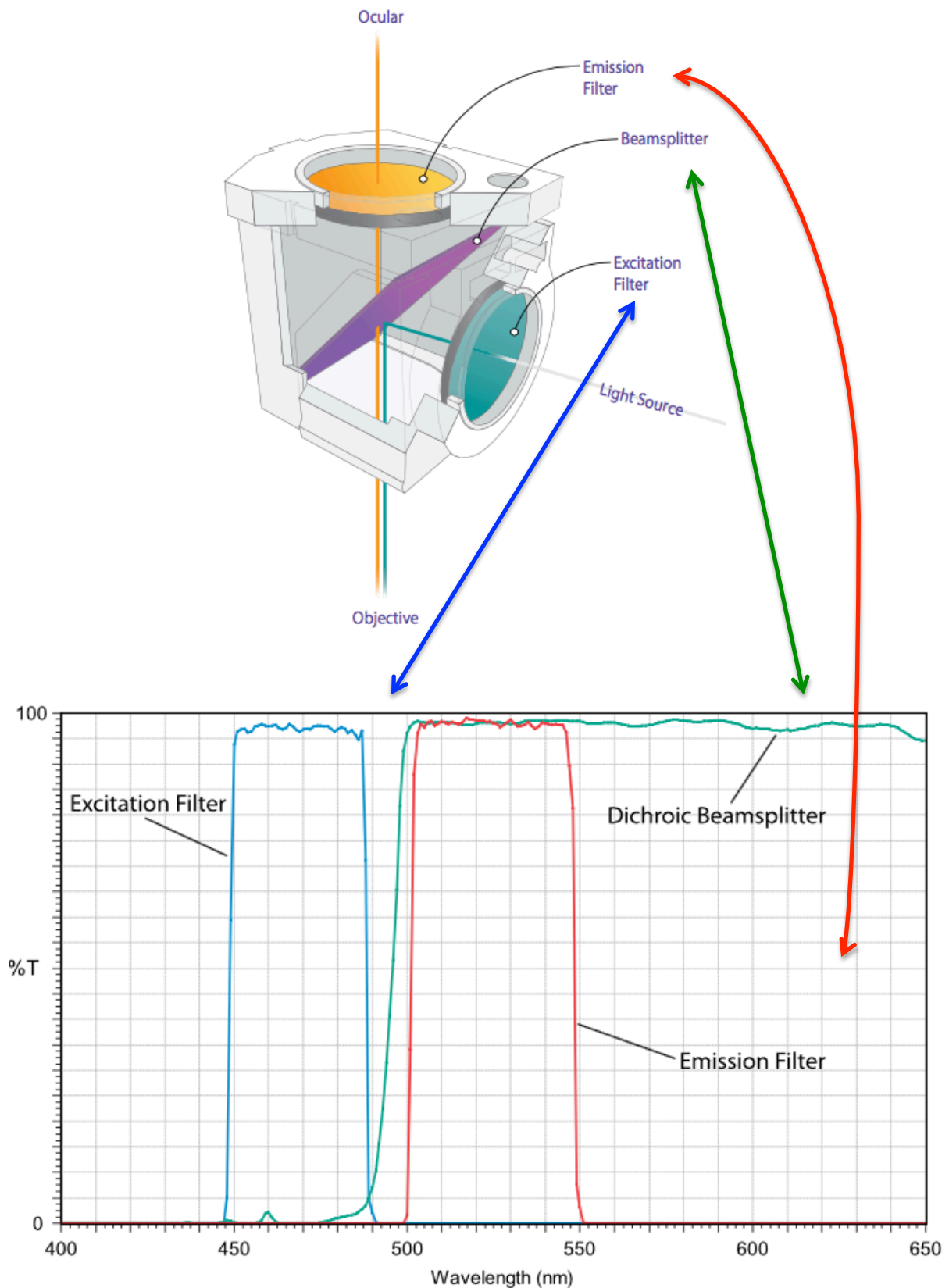


Figure 2.4: The filter cube

Technical setup of a filter cube in an epifluorescence microscope and the effect of individual components of the filter cube on absorption - and emission wavelength (detailed explanation throughout the text) (Reichmann, 2017)

2.1.5 Definition of fluorescence

A fluorophore is defined as a molecule with fluorescent properties that emits light within nanoseconds after the absorption of light that is mainly of shorter wavelength. (Lichtman and Conchello 2005) The key to fluorescence microscopy lies in the fact that the exciting light is filtered out, while only the emitted longer wavelength fluorescence will be detected by the camera. This difference between the exciting - and emitted wavelengths is described as the Stoke's shift. (Lichtman and Conchello 2005)

A quiescent fluorophore is in the "ground-state" S_0 that is considered to be the lowest vibrational state. When a photon of a certain wavelength (light energy) is absorbed by a fluorophore it will transfer all its energy to that molecule causing transition of an electron to a higher energy level (higher orbital). The transition from S_0 to the lowest energetic level of S_1 is the minimum energy required for fluorescence. The excess energy triggers alterations of the electronic -, vibrational- and rotational states of the electron or boosts it into a different orbital of the excited singlet states S_2 - where $S_0 < S_1 < S_2$. (Lichtman and Conchello 2005) The singlet states are short-lived and defined as an electron pair with opposite spins in which the magnetic moment is mutually cancelled out. The spin represents an internal motion of an atomic electron, in which the "magnetic moment will be oriented parallel or antiparallel, with respect to the magnetic field." (Lichtman and Conchello 2005)

The fluorophore at any excited state has several different ways to return to the S_0 state: firstly by radiationless transition – such as internal conversion, vibrational relaxation or intersystem crossing; secondly by radiative transition – such as fluorescence and phosphoresence. Both transition modi are best described by the Jablonski diagram. (Lichtman and Conchello 2005) The preferred energy path is from S_2 to S_1 by internal transition followed by vibrational relaxation to the lowest energy level of S_1 . A photon is thereby expelled – causing fluorescence – in the gap between the lowest energy level of S_1 and any of the vibrational/rotational levels of the ground state (see figure 2.5). The internal transition and vibrational relaxation do not cause any emission of light. It may also occur that a molecule may transition from the excited state all the way to the ground state by internal transition - however, this is not a preferred energetic path. (Lichtman and Conchello 2005)

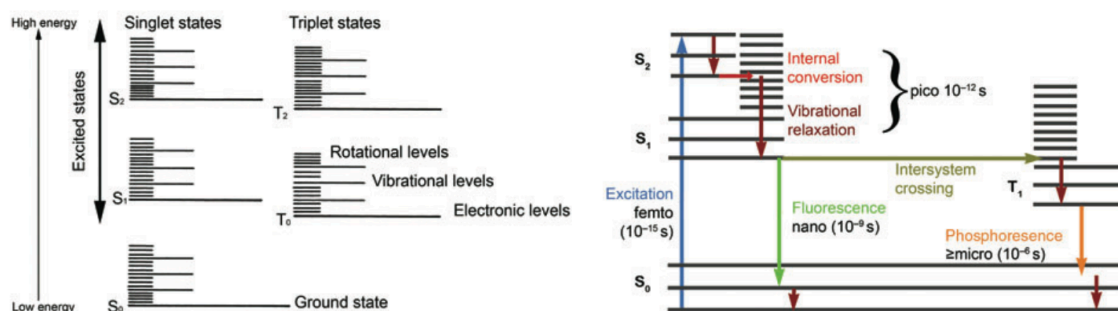


Figure 2.5: The Jablonski diagram: the correlation between ground state S_0 and excited states: singlet - and triplet states (Lichtman and Conchello 2005)

Via a forbidden transition an electron may pass from the singlet to the triplet state – a phenomenon termed intersystem crossing. It transfers from the lowest energy level of S_1 to the triplet state in which an electron is not only boosted to a new orbital, but also underwent a reversal in spin. This event where the electrons are now parallel has a low probability and is forbidden in quantum theory. (Lichtman and Conchello 2005)

Individual molecules may pass to the ground state without light emission. A more often observed event is the light emission in the form of phosphorescence in which the electron yet again undergoes intersystem crossing in order to reach the ground state. The time interval taken up by the phosphorescence photon to undergo the forbidden transition is too long, making it impossible to be detected by a laser scanning microscope. The triplet state as such weakens the fluorescence signal due to the fact that photons are unable to rapidly cycle through the different energy levels. (Lichtman and Conchello 2005)

An ubiquitous issue of fluorophores in the triplet state are photochemical reactions. One such reaction is the phenomenon of bleaching that causes irreversible fading of the fluorescent signal. Due to the long-lasting triplet state the excited electrons favour the interaction with other molecules. Oxygen, which itself is in the triplet state, may receive that excess energy exciting it into its singlet excited state. The resulting oxygen radical is highly active towards reaction with organic molecules causing phototoxicity of living cells or covalently binding to fluorophores thereby causing it to bleach. (Lichtman and Conchello 2005) (Boudreau, Wee et al. 2016) (Icha, Weber et al. 2017)

2.1.6 The fluorescein-5-isothiocyanate (FITC)

The fluorescence dye fluorescein-5-isothiocyanate is one of the most commonly used dyes and may be applied to a broad range of applications in biology and medicine. It has a

molecular formula of $C_{21}H_{11}NO_5S$ and belongs to the chemical class of xanthene. (see figure 2.6 A)) (Sabnis 2015) Fluorescein isocyanate was introduced by Coons et al. as a labelling antibody for tissue staining and further improved by Coons and Kaplan by conjugation to other proteins. (Coons 1942) (Coons and Kaplan 1950) Due to its complex synthesis, Riggs et al. then introduced the more stable fluorescein isothiocyanate which uses thiophosgene instead of the highly toxic phosgene. (Riggs, Seiwald et al. 1958)

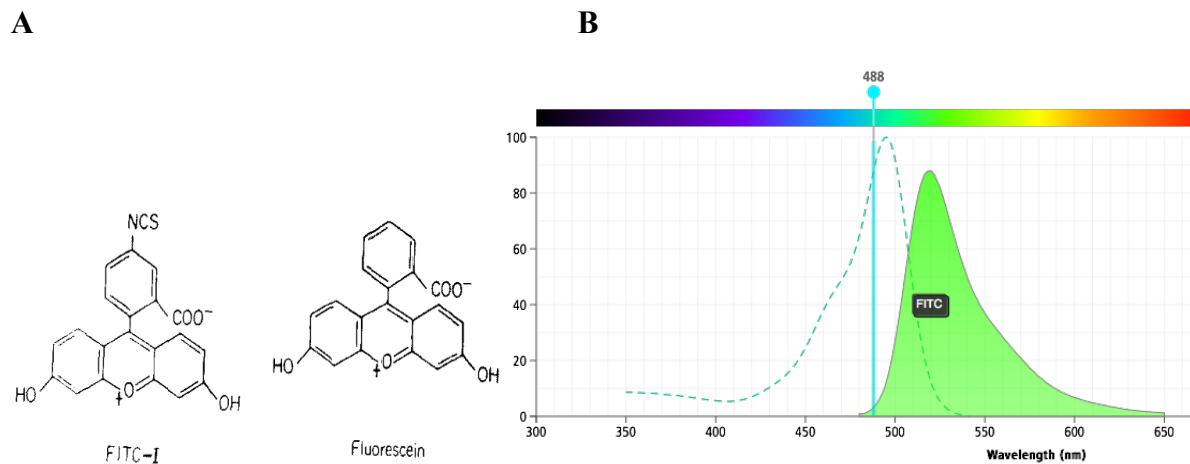


Figure 2.6: Fluorescein-5-isothiocyanate

A) Fluorescein and its derivate fluorescein-5-isothiocyanate (Maeda, Ishida et al. 1969) **B)** Absorption and emission spectrum (Biosciences 2018)

The fluorescence properties of FITC are largely influenced by pH, time and temperature and are believed to be due to its carboxyl – and one of the phenol groups. (Klugerman 1965) While an acidic solution inhibits fluorescence by favouring the formation of a cyclic ring of the carboxyl group, in an alkaline environment (optimal pH \approx 10.5) the carboxyl group remains in its open position, thus intensifying fluorescence. (Klugerman 1965) The maximum wavelength of the absorption spectrum of the dye is 490 nm that of the emission spectrum is 525 nm. (see figure 2.6 B)) We performed experiments using PLL(20)-g[3.5]- PEG(2)/FITC (1mg/ml in PBS, SuSoS AG, Dübendorf, Switzerland) where approximately 4% of the PLL-g-PEG was labelled with FITC and NeutrAvidin FITC (200ug/ml in PBS, Invitrogen, Carlsbad, USA).

2.1.7 The sulfoindocyanine Cy3

The sulfoindocyanine Cy3 with a molecular formula of $C_{34}H_{40}N_3BF_4O_4$ (for the Cy3 NHS ester) is one of the most commonly used fluorophores in the investigation of oligonucleotides

due to its stability against photobleaching and the commercial availability (see figure 2.7 A)). As described by Harvey et al. the fluorescence behaviour and lifetime significantly depend on the DNA sequence. (Harvey, Perez et al. 2009) Transition of the fluorophore to the first excited state may result in a trans-cis isomerization and the formation of a photoisomer, thus decreasing fluorescence quantum yields. Remarkable is the fact that Cy3-DNA interactions result in an enhancement of the fluorescence efficiency and lifetime, where ssDNA interactions were stronger than dsDNA. (Sanborn, Connolly et al. 2007, Harvey, Perez et al. 2009) The maximum wavelength of the absorption spectrum of the dye is 554 nm that of the emission spectrum is 568 nm (see figure 2.7 B)).

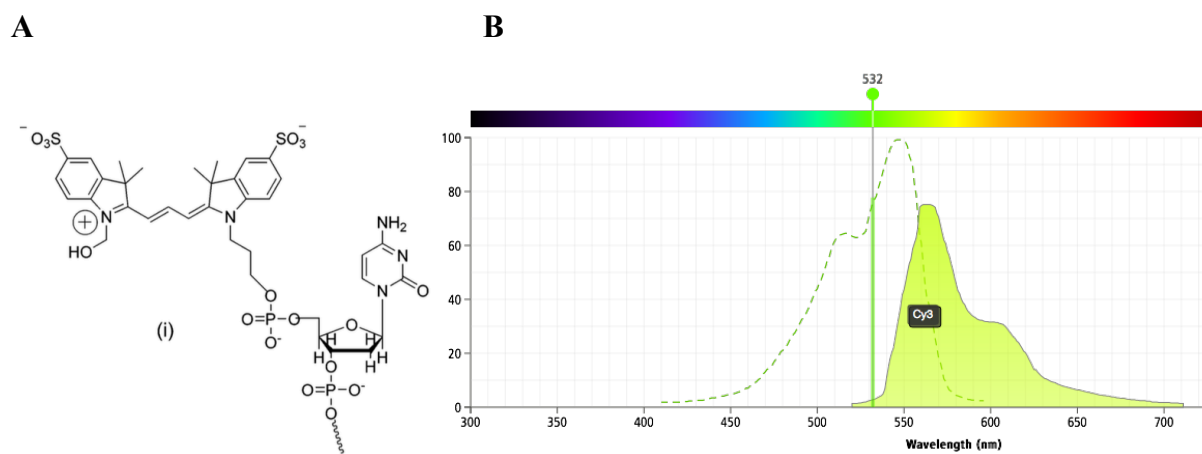


Figure 2.7: Cyanine3

a) Cy3-5'DNA (Sanborn, Connolly et al. 2007) b) Absorption and emission spectrum (Biosciences 2018)

The experiments involving Cy3 were performed with the TGTs where the fluorophore remained unchanged at the 5' end of the 21 base pair oligonucleotide among the different tethers. TGTs were purchased from Wang et al. and are not commercially available. (Wang and Ha 2013)

2.1.8 Image acquisition and live cell imaging

The Olympus IX 83 inverted epifluorescence microscope and the corresponding computer controlled software cellSense imaging were used for the majority of the experiments. In order to create a physiological environment at 37°C a stage – and objective heater was required for live cell imaging. For epifluorescence images the microscope is equipped with a fluorescence lamp and specific filter cubes. Images were acquired with a 100x objective in the phase contrast channel or fluorescence channels (red and green). Standard exposure times were: PH

= 120 ms and GFP/RFP = 600 ms. For live cell imaging time intervals of 20 or 30 seconds were chosen in the PH channel and/or GFP/RFP channels, respectively.

2.2 Preparation of washed platelets

2.2.1 Preparation of modified Tyrode buffer

In order to ensure a physiological setting for platelet isolation and further processing a modified Tyrode buffer on the basis of HEPES (Sigma-Aldrich Chemie GmbH, Taufkirchen, Deutschland) was produced. HEPES is characterised by membrane impermeability, its stability and limited effects on biochemical reactions. It has an acid dissociation constant of $pK_a = 7,55$ at 20°C with an optimal buffering capacity of $\text{pH} = 6,8 - 8,2$. (Good, Winget et al. 1966)

A stock solution of Tyrode buffer 10x (1000ml Aqua bidest, 80g NaCl (Fa. VWR International GmbH, Darmstadt), 10,15g NaHCO_3 (Fa. VWR International GmbH, Darmstadt) und 1,95g KCl (Fa. VWR International GmbH, Darmstadt) was prepared. Prior to each individual experiment the stock solution of the modified Tyrode buffer was diluted 1:10 in distilled water. D(+)-Glucose [0,1%] (Sigma-Aldrich Chemie GmbH, Taufkirchen, Deutschland) and HEPES [10mM] were added and the buffer solution titrated with 2M $\text{HCl}_{(\text{aq})}$ to $\text{pH} = 6,5$ and $\text{pH} = 7,4$, respectively.

2.2.2 Isolation of human and murine platelets

Blood donors were healthy voluntary individuals at the age of 25-35 years with informed consent obtained priorly. All subjects did not take any medication for at least two weeks, due to their influential effects on platelet function. (Mustard, Kinlough-Rathbone et al. 1989) (Konkle 2011) (Gaertner, Ahmad et al. 2017) Both gender were equally represented and experimental outcome was not influenced by gender-specific differences. Blood was drawn from the cubital vein, after discarding 1ml, into a 5ml syringe with 1/7 Acid-Citrate-Dextrose (ACD). ACD has a $\text{pH} = 4,5$ and is sodium-citrate [75mM] (Sigma-Aldrich Chemie GmbH, Taufkirchen), Dextrose [135mM] (Sigma-Aldrich Chemie GmbH, Taufkirchen) and citric acid [39mM] (Sigma-Aldrich Chemie GmbH, Taufkirchen) diluted in distilled water. Thus platelet aggregation is prevented firstly by the lowered $\text{pH} \approx 6,5$ of the anticoagulated blood and secondly by the Ca^{2+} chelating properties of citrate. The blood was then gently transferred into a 15ml Falcon, 1:1 diluted with modified Tyrode buffer $\text{pH} = 6,5$ and finally

centrifuged (Eppendorf Centrifuge 5804 R Kühlzentrifuge) at 22°C, 70 x g for 35 min without brake to prevent platelet activation through shear forces. The resulting platelet-rich-plasma (PRP) as a supernatant was gently pipetted into a second 15ml falcon and diluted 1/3 with modified Tyrode buffer pH=6,5 containing 0,1% human serum albumin (HSA) (Sigma-Aldrich Chemie GmbH, Taufkirchen) and Prostaglandin I₂ (PGI₂, 0,1ug/ml, Abcam). The second centrifugation step was performed at 22°C, 1200 x g, with brake for 10 min. Conclusively the platelet pellet was re-suspended in 1ml modified Tyrode's buffer pH=6,5.

Murine platelets were obtained from the C57BL/6 mice. Anaesthesia was initiated by placing the mice within a chamber to which isoflurane (Isofluran DeltaSelect, DeltaSelect GmbH, Dreieich) and oxygen were feed. Due to the limited analgetic properties of isoflurane, fentanyl was injected intraperitoneally. (0.05 mg/kg body weight; Fentanyl-Curamed, CuraMED Pharma GmbH, Karlsruhe). The platelets were isolated using the protocol above after blood was drawn intracardially from the anesthetized mice.

Platelets were kept at room temperature and used within 1 hour after isolation, while counts were obtained by an automated cell counter: final cell counts measured between 150.000 – 200.000/μl (ABX Micros ES60, Horiba Medical) (Massberg, Brand et al. 2002) (Gaertner, Ahmad et al. 2017).

2.3 Setup of the biomechanical microenvironment to study platelet function

In order to investigate the mechanosensitive effects on platelet function in-vitro, human – and murine platelets, plasma cleaned glass cover slips, a specific channel systems and different coatings at varying piconewton values were used. The individual steps will be described in more detail in the following chapters.

2.3.1 Surface synthesis and – properties

2.3.1.1 Acid treatment of glass cover slips

Prior to the plasma cleaning treatment, the glass cover slips (No. 1.5, D263T, Nexterion, Schott) were washed in HCO₃ (20%) at RT for 1h while slowly rocking with 100 rpm/min (Benchmark scientific Orbi-Shaker™ JR.); subsequently rinsed with distilled water for another hour at RT slowly rocking 100/min and finally dried on air under a chemical bench to avoid contamination. This procedure ensured the removal of contaminating particles.

2.3.1.2 The channel system

The channel system consists of an Ibidi sticky-Slide VI^{0.4} (Ibidi GmbH, Martinsried, Germany) and the plasma treated glass cover slip that are commercially purchasable. The sticky slide is delivered as a sterilely packed six channel bottomless slide that was manually cut into six individual channels and then assembled with the pre-treated glass cover slip. The channels are for single use only, take up a volume of 30 μ L and measures a size of *height x length x width* = 0,4 mm (+0,13 mm adhesive tape) x 17mm x 3,8 mm. The 130 μ m thick biocompatible double-faced adhesive tape seals the interface of the channel with the glass cover slip. The slides were immediately used for experiments after assembly, so that channel leakage did not represent a problem.

The channel consists of plastic, which after assembly with the glass cover slip allows fluorescence - and live imaging with highest optical features.

2.3.1.3 Low-pressure oxygen plasma treated glass cover slips

The surface activation by oxygen plasma provides a homogenous and reliable electrostatic negative charge to which the positively charged amine groups of the PLL-g-PEG bind. (Kenausis, Vörös et al. 2000) The plasma is generated by continuously applying energy through the high frequency generator to the low-flow oxygen gas in the vacuum. Reaching a certain threshold negatively charged electrons will break out of the atomic structure and move to the anode, while positively charged ions and radicals will move to the cathode. The chemically reactive species will thereby react and activate the surface generating a net negative, homogeneously distributed charge. (Liston, Martinu et al. 1993)

The low-pressure plasma system Zepto (Diener electronic GmbH + Co. KG, Ebhausen, Germany) was used, consisting of a vacuum chamber with a diameter of 105 mm, a length of 300 mm and a portable metal tray. Additional relevant components are the vacuum pump (rotary vane pump 3,5 m³/h), the high-frequency generator (40 kHz/100W) and the processing gas (oxygen). A 4 mm inlet tube supplies the O₂, while the processed gas is sucked off via a 10 mm exhaust tube.

The glass cover slips were placed on the tray inside the vacuum chamber (see figure 2.8 No.1) and the vacuum generated by the rotary vane pump (see figure 2.8 No.2) until a pressure of 0,3 mbar was reached. The oxygen gas under low flow (see figure 2.8 No.3) was fed into the chamber until a working pressure of 0,35 mbar was achieved, when the generator

(see figure 2.8 No.4) was switched on with a power of 90 W and a time frame of 20 seconds. Once the time was up the generator was switched off and the processed gas sucked off via the exhaust tube (see figure 2.8 No.5). The slides were immediately assembled with the channel under the chemical bench and coating procedure succeeded.



Figure 2.8: Low-pressure plasma system Zepto from Diener
(adapted from Diener Plasma-surface-technology 2020)

2.3.2 Coating Substrates

2.3.2.1 Poly(L-lysine)-graft-poly(ethylene glycol) (PLL-g-PEG) and conjugated biofunctional units

The PLL-g-PEG copolymer can be purchased from SuSoS AG (SuSoS AG, Dübendorf, Switzerland) and consists of a PLL backbone (mol wt 20 kDa), a graft ratio (3.5 lysine-mer/PEG side chain) and protein resistant PEG side chains (mol wt 2 kDa). The net negatively charged surface enables the adsorption of the cationic PLL backbone, thereby generating a dense aligned brush, which establishes a repellent layer for soluble particles - a phenomenon termed polymeric steric stabilisation. The water soluble poly non-ionic PEG side chains block cell-cell- and cell-surface interactions (Elbert and Hubbell 1998) (Kenausis, Vörös et al. 2000)

Different biofunctional peptides were covalently conjugated to the grafted PEG, specifically inducing cell-surface interactions (PLL(20)-g[3.5]- PEG(2)/PEG(3.4) - **RGD** (1mg/ml in PBS, SuSoS AG, Dübendorf, Switzerland) and PLL(20)-g[3.5]- PEG(2)/PEG(3.4) – **LGGAKQAGDV** (1mg/ml in PBS, custom peptide, SuSoS AG, Dübendorf, Switzerland)) or enabling further coating procedures (PLL(20)-g[3.5]- PEG(2)/PEG(3.4)- **biotin** (50%) (1mg/ml in PBS, SuSoS AG, Dübendorf, Switzerland)). (Pierschbacher et al., 1984a) (VandeVondele et al., 2003) The desired surface density of the biofunctional peptides was given as a percentage 5%, 10%, 15%, 25%, 50%, 75% or 100% with the remaining fraction being PLL-g-PEG. The surfaces were incubated for 30 min at RT, while slowly rocking with 60 rpm/min and then thoroughly rinsed with PBS for three times. While the PLL-g-PEG-RGD or PLL-g-PEG-LGGAKQAGDV were then seeded with cells, the PLL-g-PEG-Biotin was incubated with either NeutrAvidin (200ug/ml in PBS, Invitrogen, Carlsbad, USA) or NeutrAvidin-FITC (200ug/ml in PBS, Invitrogen, Carlsbad, USA) for 30 min at RT while slowly rocking 60 rpm/min and rinsed with PBS for three times.

The last coating step includes different substrates specifically binding certain integrin classes. All substrates contain a biotin tag that binds the NeutrAvidin and were incubated for 30 min at RT, while slowly rocking with 60 rpm/min. The cyclo RGDfk [Arg-Gly-Asp-D-Phe-Lys(Biotin-PEG-PEG)] (0,1 μ M in ddH₂O, Peptides International, Louisville, USA) contains two PEG spacer between the biotin tag in order to avoid unspecific binding and selectively targets the $\alpha_{IIb}\beta_3$ Integrin. A more sophisticated system consists of the biotin tag, the covalently bound cRGDfK and a 21bp double stranded DNA in between generating a model with differing rupture forces determined through DNA geometrics – this will be described in more detail below. The linear RGD (H-RGDfk(PEG-PEG-Biotin)-OH) (1mM in ddH₂O, Custom Peptide, ENZO life sciences GMBH, Lörrach, Germany) specifically bind the $\alpha_v\beta_{III}$ as well as the $\alpha_{IIb}\beta_3$. (Ruoslahti 1996)

2.3.2.2 The 21 base pair DNA-based Tension Gauge Tether (TGT)

In order to investigate the mechanosensitive effects of molecular forces on integrin signalling a DNA based tethering system initially described by Wang et al. was used. (Wang and Ha 2013) The base pair sequence of the upper single-stranded DNA consists of: 5- /5Cy3/CAC AGC ACG GAG GCA CGA CAC /3ThioMC3-D/ -3 in which Cy3 is the fluorophore, the cRGDfK is the substrate targeting $\alpha_{IIb}\beta_3$ and is covalently conjugated to the 3' end of the

DNA strand. The spatial distribution of all compounds remained unchanged in the upper ssDNA strand between different tethers.

The complementary ssDNA is 5-GTG TCG TGC CTC CGT GCT GTG-3 contains a biotin tag at varying positions determining the tension tolerance= T_{tol} . (see figure 2.9)

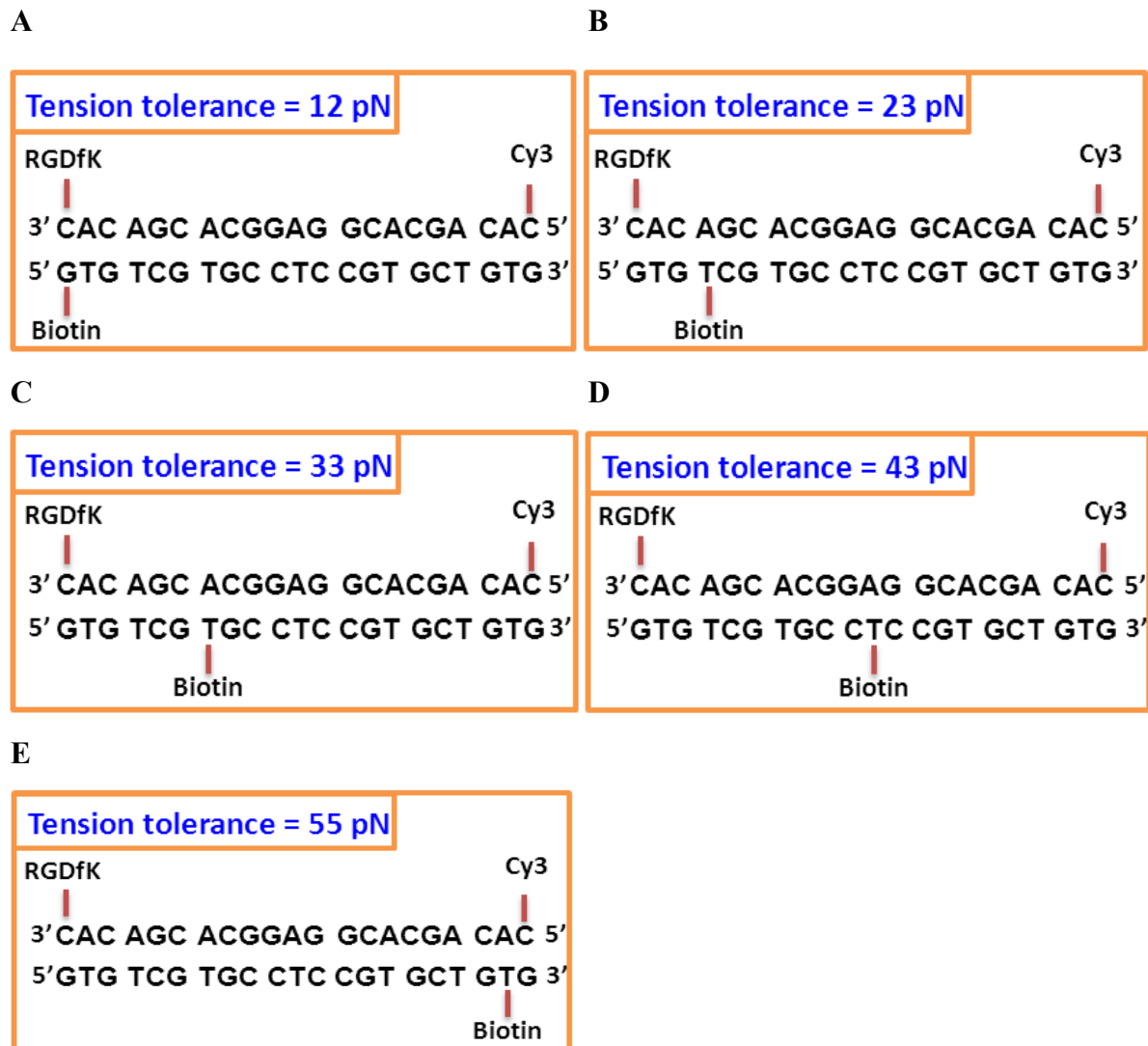


Figure 2.9: Architecture of the tension gauge tether

The position of the biotin tag in the lower DNA strand is responsible for the tuneable tension tolerance, while the upper DNA strand remains unchanged among the different tethers. (adapted from (Wang, Sun et al. 2015))

This tension force was measured via a constant force applied by magnetic tweezers and defined as “the lowest force that ruptures the DNA within 2 seconds if the force is applied at a constant level.” (Wang and Ha 2013)

The force applied to the varying positions of the biotin tag determines the DNA geometrical behaviour and results in three different modi: an unzipping-, an intermediate- and a shear mode. (see figure 2.10)

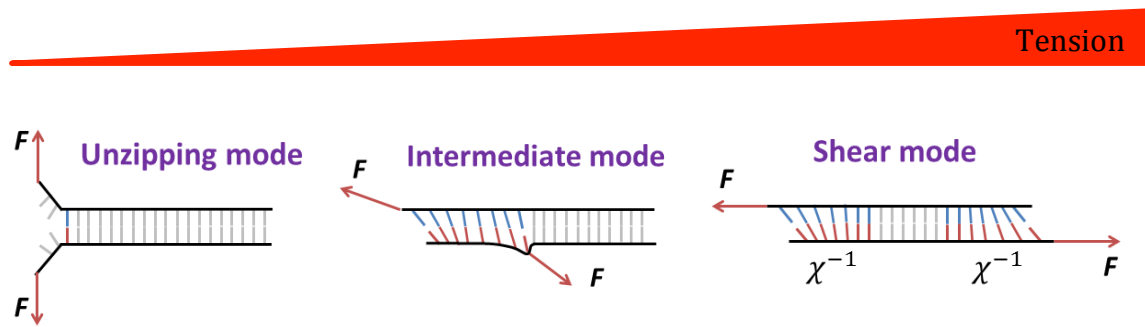


Figure 2.10: DNA geometry - determining different modi depending on the force applied

The coloured base pairs contribute to the T_{tol} , while the remaining base pairs are independent of rupture force. (adapted from (Wang and Ha 2013))

In our experiments we used five different TGTs with T_{tol} values of 12-, 23-, 33-, 43- and 55pN in which the DNA length, base pair sequence and thermal stability remained unchanged among the different tethers. The force that has to be overcome to rupture the tether is much smaller than the NeutrAvidin bond ($\sim 160\text{pN}$). (Moy, Florin et al. 1994)

The tension applied through the ligand-receptor engagement is the fundamental step for the tethering system. While a tension exceeding T_{tol} , ruptures the tether and abolishes signal activation, a molecular tension smaller than T_{tol} will endure and activate down stream signalling. Ligand and receptor density do not influence cell adhesion behaviour since each ligand is conjugated to an individual tether.

The surfaces were incubated with the TGTs ($0,1 \mu\text{M}$ in PBS – custom synthesis provided by Wang et al.) for 30 min while slowly rocking with 60 rpm/min, thoroughly rinsed with PBS for three times and the cells plated on.

2.4 Flow cytometry

Plasma activators and divalent cations induce variable intracellular trafficking pathways leading to degranulation and the expression of surface receptors on the plasma membrane. These effects on platelet function can be detected using flow cytometry. This technology measures and analyses how cells scatter incident laser light and emit fluorescence as they flow in a fluid stream. The side scatter detector gives information about the granularity of a cell, while the forward scatter detector measures cell size. (see figure 2.11) (Herzenberg, Sweet et al. 1976) (Perfetto, Chattopadhyay et al. 2004) (O'Neill, Aghaeepour et al. 2013)

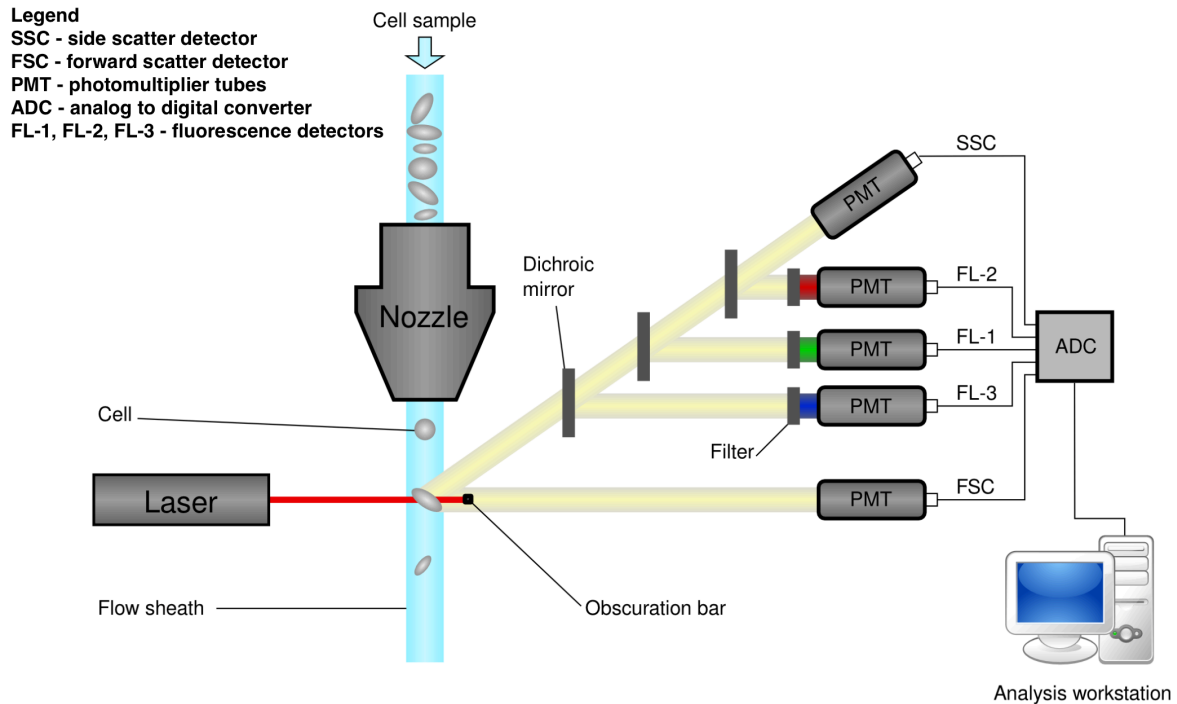


Figure 2.11: Basic principle of flow cytometry (O'Neill, Aghaeepour et al. 2013)

The experiments were performed to identify platelets (CD 42b-APC (BioLegend, San Diego, USA)) and measure the percentage of integrin $\alpha_{IIb}\beta_3$ activation (FITC Mouse Anti-Human PAC-1 (BD Biosciences, San Jose, USA)) as well as p-selectin (PE anti-human CD62P (BioLegend, San Diego, USA)) expression after degranulation.

Washed platelets were activated either with ADP and TXA_2 or Thrombin for 2 min. Following PAC-1 FITC as well as CD62P PE were added for 20 min at room temperature. Cells were then fixated with 4% PFA and CD 42b-APC added for 20 min at room temperature. The experiments were immediately performed.

The Beckman Coulter Gallios 3 Laser/10 colours bench-top flow cytometer was used to carry out the above mentioned experiments.

2.5 Pharmacological inhibition

The **Myosin IIa inhibition** was performed by incubating washed platelets with 50 μM Blebbistatin (-) (Cayman chemicals, Michigan, USA) in modified Tyrode buffer pH=7,4 for 30 min at RT. Platelets were then activated in solution and immediately plated onto the different coatings. Blebbistatin (+) (Cayman chemicals, Michigan, USA) acted as a negative control.

The **Piezo I inhibition** was performed by activating washed platelets and instantly adding 10 μM of GsMTx-4 (244 μM in H_2O , Bio-Techne GmbH, Wiesbaden-Nordenstadt, Germany) before the cells were plated onto the different coatings.

2.6 Data analysis

Platelet morphology, cell counts and function (adherence, spreading and migration) were manually evaluated and obtained by the advanced image processing program FIJI. (Schindelin, Arganda-Carreras et al. 2012) (Meijering, Dzyubachyk et al. 2012) Cell counts were obtained as absolute numbers, while spreading and migrating platelets were calculated as a percentage of adherent cells. Platelets with a solid lamellipodia were considered spread, while cells traveling a distance ≥ 1 cell diameter were considered as migrating. The migration distance was measured in μm using the FIJI software plugin “Manual tracking” in phase contrast videos, where the pseudonucleus served as a morphological landmark; each individual platelet was tracked manually. Alternatively phase contrast/fluorescent images were combined and the distance drawn by a segmented line. The FIJI software creates a value for each individual line/track that can then be used for further analysis.

In order to be able to analyse the impact of substrate architecture on cell morphology we performed the shape analysis of adherent platelets (spread and non-spread) by using the “celltool” software package. (Pincus and Theriot 2007) All cells from phase contrast images at magnification 100x were taken into consideration without prior shape preselection. Individual cells were manually masked and the image then converted into a 8-bit binary image using the FIJI software, in which all pixels of the cell had the intensity value=0, whereas all other pixels were set at intensity value = 255. The absolute numerical values of the binary image play a subordinate role, while the importance lies in the difference between the in- and outside the cell. (Schindelin, Arganda-Carreras et al. 2012) Contours were extracted from the binary mask. To ensure a more precise alignment, the pseudonucleus of each individual platelet was set as a well recognisable landmark – using the FIJI software, the pseudonucleus was manually marked and subsequently extracted to another set of binary images. By overlaying the extracted contour with the landmark to which an algorithm based on Procrustes analysis was applied, cells were optimally aligned using corresponding points. The alignment of each analysed set was manually verified. The aligned cells were further processed and principal component analysis, scaled by the standard deviation was performed

through which principal shape modes of shape variation could be measured. The different measured shape modes from the PCA included: (1) Area in mm² (mode 1) and (2) Aspect Ratio = long axis/short axis (mode 2). (Pincus and Theriot 2007) (Gaertner, Ahmad et al. 2017)

2.7 Statistics

The statistical analysis and the graphical illustrations were created using the statistic software “GraphPad Prism, Version 6.0c”. Throughout all experiments two statistical tests were used, depending on normal distribution: the Wilcoxon-Mann-Whitney-Test or an unpaired t-test. The Wilcoxon-Mann-Whitney-Test was used to test two independent variables – for example migration with and without an external integrin activation. This non-parametric test only requires an ordinal data set and can be applied if the requirements for a t-test are not given (for example normal distribution). However the Wilcoxon-Mann-Whitney-Test requires observations > 4 to receive a p-value < 0.05 . (Bland and Altman 2009)

An unpaired t-test was applied to compare velocities of individual cells. This statistical test investigates the mean values of two independent variables assuming normal distribution even in small sample sizes. A p-value of $< 0,05$ of the statistical test was considered significant revealing a difference between the groups.

The null hypothesis stating that there was no significant difference between the groups could be rejected with a probability of $\geq 0,95$.

3 Results

In an approach to investigate single molecular forces promoting mechanical signalling via integrins, Wang et. al introduced a DNA-based tethering system with tuneable tension tolerances and described that Chinese hamster ovary cells (CHO-K1) applied an universal peak tension of ~ 40 pN to single integrin-ligand bonds during initial adhesion. (Wang and Ha 2013) Based on this model we interrogated human – and murine platelets to investigate the influence of the biophysical microenvironment on platelet function.

3.1 A precise assay to investigate platelet mechanobiology

By using variable protein constructs, the experimental setup allowed to selectively control ligand densities and ligand mechanical resistance. In order to determine the accuracy of ligand densities at varying concentrations the fluorescence intensity of various ratios of unlabelled PLL-g-PEG and PLL-g-PEG-FITC/NeutrAvidin-FITC were investigated (see figure 3.1.1A) and B))

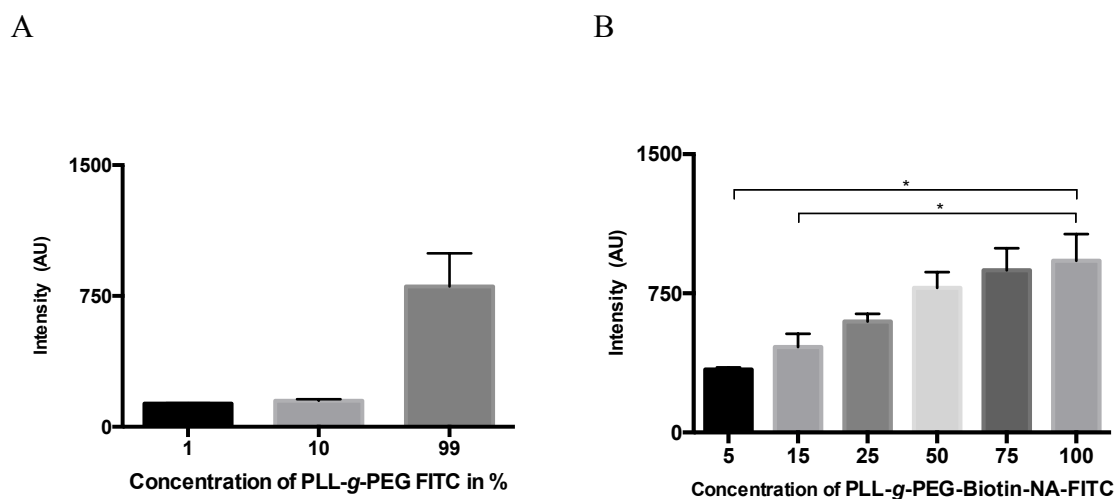


Figure 3.1.1: The effect of ligand density on fluorescence intensity

A) PLL-g-PEG-FITC at concentrations 1%, 10% and 99% with PLL-g-PEG. The results follow a typical log based exponential increase with increasing ligand density. **B)** PLL-g-PEG-Biotin-NeutrAvidin-FITC with PLL-g-PEG at varying concentrations (in per cent). Depicted is the effect on fluorescence intensity at fine tuneable ligand densities. Results from three and four independent experiments, respectively and their mean. * = $p < 0.05$.

The results clearly elucidate that ligand density can be precisely tuned and even small variances have a large effect on fluorescence intensity. This fundamental finding is an important tool to probe the effects of ligand density on platelet behaviour.

In order to outline the blocking properties of the water-soluble poly non-ionic PEG side chains, platelets were then seeded on untreated glass cover slips and PLL-g-PEG coated surfaces with a ligand density of 100%. The platelets readily adhered and more than 90 % spread on the untreated glass cover slips, while only a small percentage of platelets adhered on the PLL-g-PEG coated surfaces and none of them spread. Since spreading and consecutive polarization is required in order to promote migration the small percentage of adherent cells on the PLL-g-PEG coated surfaces were considered neglectable for further migration experiments (see figure 3.1.2).

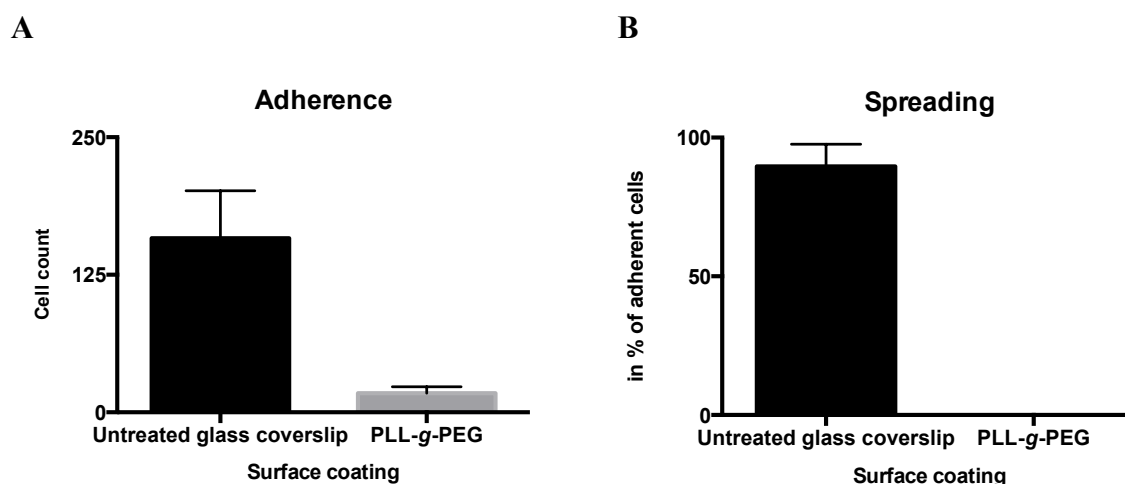


Figure 3.1.2: The effect of platelet function on untreated glass surfaces and PLL-g-PEG coated surfaces
A) The adherence of platelets assessed by absolute cell counts was reduced on PLL-g-PEG coated surfaces. **B)** Considerable difference in the spreading behaviour, where no platelets spread on the PLL-g-PEG coated surfaces. Depicted are three independent experiments and their mean. * = $p < 0.05$.

As to this point our assay allowed to precisely control ligand density and excluded that platelets would migrate on PLL-g-PEG coated surfaces. Platelet activation levels differ among activators and the encountered substrate – the following experiments gave insights of differing activation levels and its effects on substrate-coated surfaces.

3.2 The effect of plasma activators and divalent cations on platelet function

At sites of vascular injury or inflammation, platelets are exposed to a myriad of plasma activators and divalent cations essential for platelet activation. These induce variable intracellular trafficking pathways and consecutive expression of surface receptors. The following experiments were performed to subdivide and quantify these effects via fluorescence-activated cell sorting.

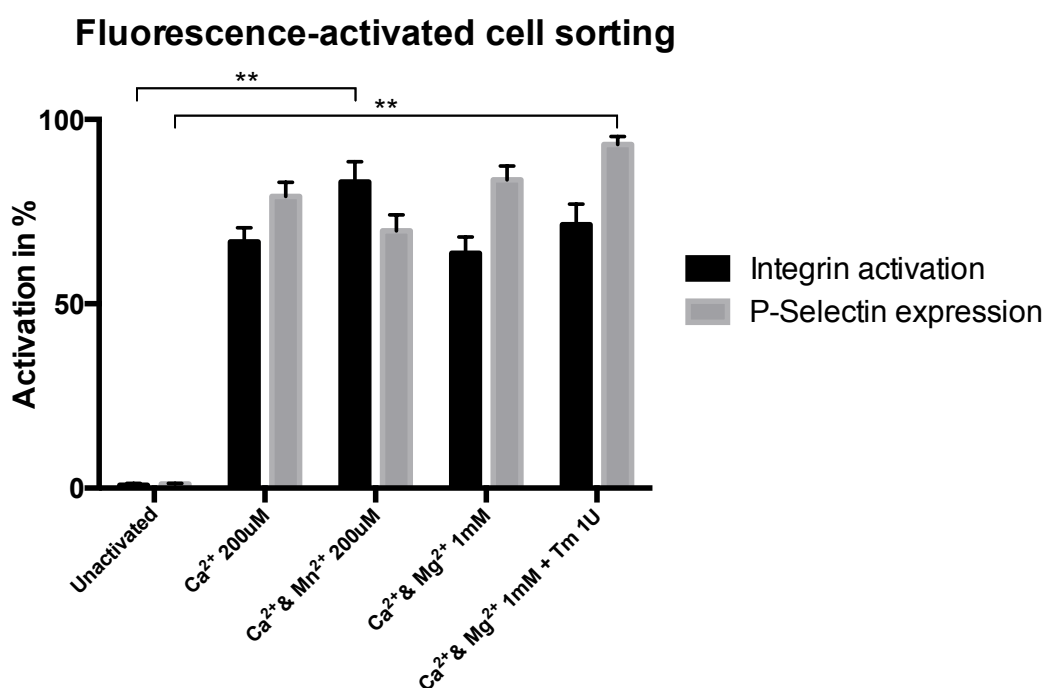


Figure 3.2.1: The effect of activators and divalent cations on the integrin activation and P-Selectin expression

Platelets were activated with ADP and TXA₂ excluding the unactivated - and thrombin group. Mn²⁺ significantly induced the strongest integrin activation while thrombin triggered the strongest P-Selectin expression. Depicted are five independent experiments and their mean. * = p < 0.05.

The data in figure 3.2.1 show that integrin activation was strongest with Manganese – this is due to the fact that Manganese directly binds the extracellular domain of the integrin thereby inducing a conformational change into the active state. (Xiong, 2002) Thrombin in turn induces the strongest degranulation of intracellular alpha – and dense granules – the coalescence of granules with the plasma membrane leads to the expression of P-Selectin. Although degranulation leads to an increase of integrin receptors on the plasma membrane,

the overall integrin activation only merely differs among the different groups (excluding external integrin activation by Manganese).

Based on the above-mentioned results, further experiments were performed by using physiological conditions of Ca^{2+} and Mg^{2+} with platelet activation through ADP and TXA_2 . In order to investigate the ligand integrin interaction platelets were firstly seeded onto varying concentrations of *PLL-g-PEG-Biotin - NA-FITC - Biotin-cRGD* (see figure 3.2.2).

Platelets have to overcome a force of ~ 160 pN to break the bond between the NeutrAvidin-FITC and the Biotin-cRGD in order to promote spreading and consecutive migration. (Moy, Florin et al. 1994) As evidenced by these experiments a ligand density of 10% was most favourable in promoting migration with physiological concentrations of 1mM Ca^{2+} and 1mM Mg^{2+} .

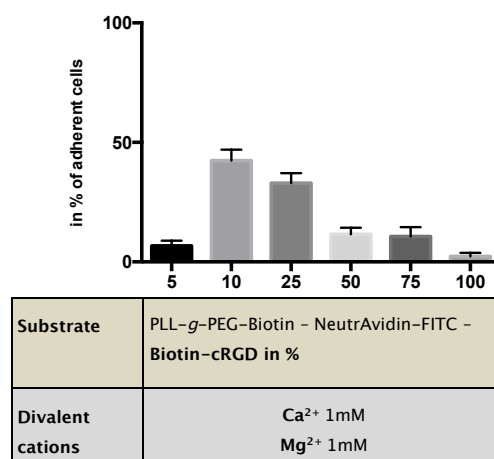


Figure 3.2.2: The effect of varying concentrations of PLL-g-PEG-Biotin-NA-FITC-Biotin-cRGD with physiological concentrations of Ca^{2+} and Mg^{2+} 1 mM on platelet migration.

Depicted are three independent experiments and their mean. * = $p < 0.05$.

The results also show that a ligand density of 5% Biotin-cRGD is too low to trigger migration and might be explained by the fact that a certain mechanosensitive threshold was not reached. However, a ligand density of 100% Biotin-cRGD is too high, where the platelets are unable to remove the substrate from the surface and firmly attach to the ligand. Thus platelet migration is only observed, if the ligand can be removed by the platelet which is consistent with the data published by Gärtner et al.. (Gaertner, Ahmad et al. 2017)

In order to translate the FACS experiment onto the *PLL-g-PEG-Biotin -NA-FITC - Biotin-cRGD 10%* surfaces, the influence of activators and different divalent cations was then

investigated (see figure 3.2.3). Ca^{2+} is required for many intra - and extracellular processes and links the integrins to the cytoskeletal machinery (particularly myosin activation) – in its absence there is only little migration observed.

The results underline the essential role of Ca^{2+} for platelet migration and also show that even thrombin, as the most potent platelet activator, did not enhance migration. Thus, the activation level of the platelet can be excluded as a limiting factor for migration in our assay; emphasis may be stressed on the ligand-integrin interaction and the central role of Ca^{2+} participating in a broad range of processes.

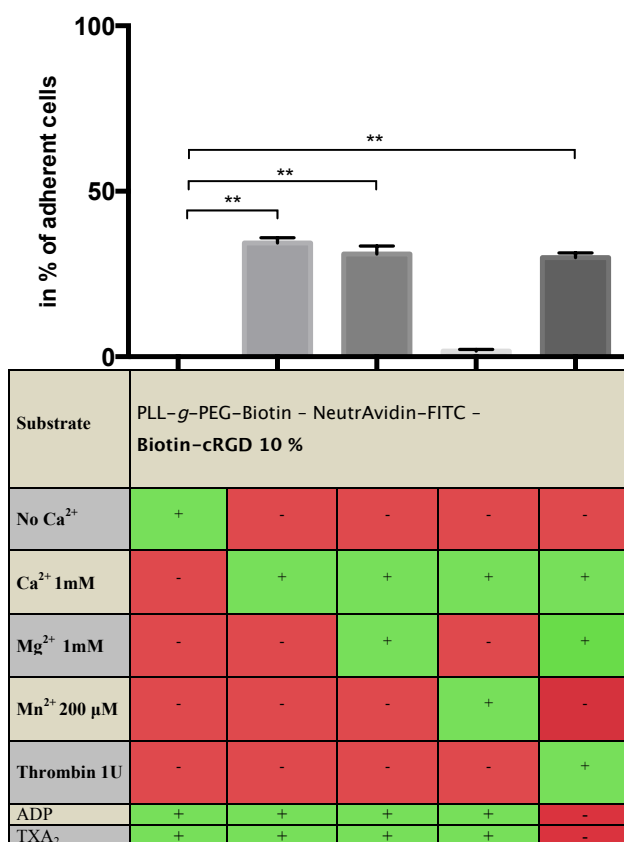


Figure 3.2.3: The effect of activators and divalent cations on migration on PLL-g-PEG-Biotin-NA-FITC-Biotin-cRGD 10%

The Ca^{2+} cation plays an important role for platelet migration. Thrombin as the most potent platelet activator did not enhance migration in relation to the other groups. Depicted are five independent experiments and their mean. * = $p < 0.05$.

3.3 Platelet function on low ligand densities

By identifying *PLL-g-PEG-Biotin - NA-FITC - Biotin-cRGD 10%* as the ideal concentration to promote migration, the effect whether external integrin stimulation with Mn^{2+} would alter platelet force was investigated. While Mn^{2+} did not alter the spreading behaviour, migration was significantly reduced (see figure 3.3.1).

One possible approach to explain this phenomenon would be the percentage of activated integrins by physiological activators versus the external integrin stimulation with Mn^{2+} . This would lead to the condition in which the majority of integrins on the platelet membrane with an external integrin activation remain in the ligand-integrin interaction. Consequently, the threshold and the required force to remove the ligand from the surface would increase. (Oria, Wiegand et al. 2017) Another approach is the spatial distribution of force on the plasma membrane – the peripheral zone seems to exert greater traction force than the central zone, where the pseudonucleus resides. (Wang, Sun et al. 2015)

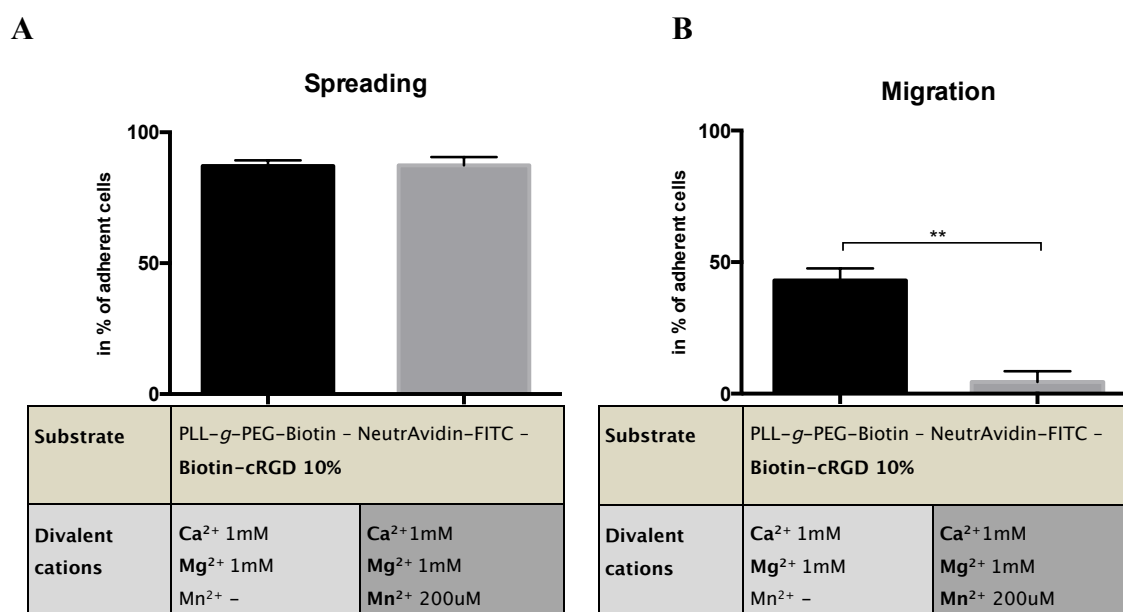


Figure 3.3.1: Platelet function on *PLL-g-PEG-Biotin-NA-FITC-Biotin-cRGD 10%* with physiological concentrations of Ca^{2+} and Mg^{2+} 1 mM and exogenous integrin activation with Mn^{2+} 200 μ M.

A) Spreading is not influenced by externally activating the integrins B) The external integrin activation significantly diminishes platelet migration. Depicted are five independent experiments and their mean. * = $p < 0.05$.

PLL-g-PEG-Biotin - NA-FITC - Biotin-cRGD 10%
 $Ca^{2+} + Mg^{2+} 1mM$

PLL-g-PEG-Biotin - NA-FITC - Biotin-cRGD 10%
 $Ca^{2+} + Mg^{2+} 1mM$ and $Mn^{2+} 200\mu M$

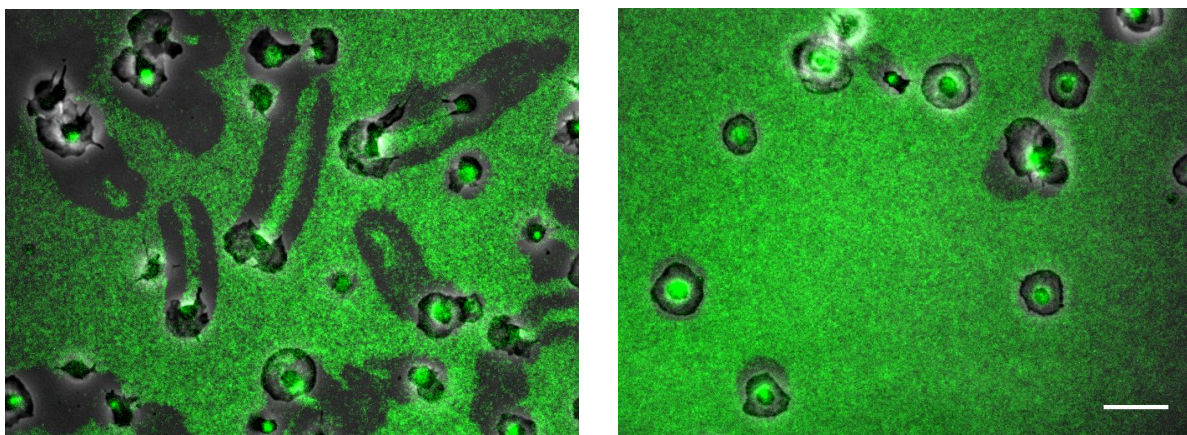


Figure 3.3.2: Representative images of platelet migration on *PLL-g-PEG-Biotin-NA-FITC-Biotin-cRGD 10%* with physiological concentrations of Ca^{2+} and $Mg^{2+} 1 mM$ and external integrin activation with $Mn^{2+} 200 \mu M$.

Two images taken by the Olympus IX 83 with a 100x objective in the green fluorescence protein (GFP) channel (exposure time: 600 ms), after 60 min incubation at 37°C. Visible is the significantly reduced migration. Scalebar = 10 μm

This led to the question of whether the external integrin activation would alter platelet function on ligand densities $\leq 5\%$. Platelets that were physiologically stimulated neither spread nor migrated. Interestingly the percentage of spreading - and migrating platelets was considerably increased on *PLL-g-PEG-Biotin - NA-FITC - Biotin-cRGD 5%* with Mn^{2+} . This supports our hypothesis that the mechanosensitive forces transmitted via the integrin play a fundamental role in influencing spreading – and migration behaviour (see figure 3.3.3).

An approach to explain this phenomenon would be that under physiological conditions, the reduced spatial ligand distribution is not sufficient to trigger spreading and consecutive migration. With an external integrin activation the majority of integrins is in contact with a ligand, thereby increasing the cumulative force on the substrate – platelets are able to overcome ligand resistance, thereby leading to migration.

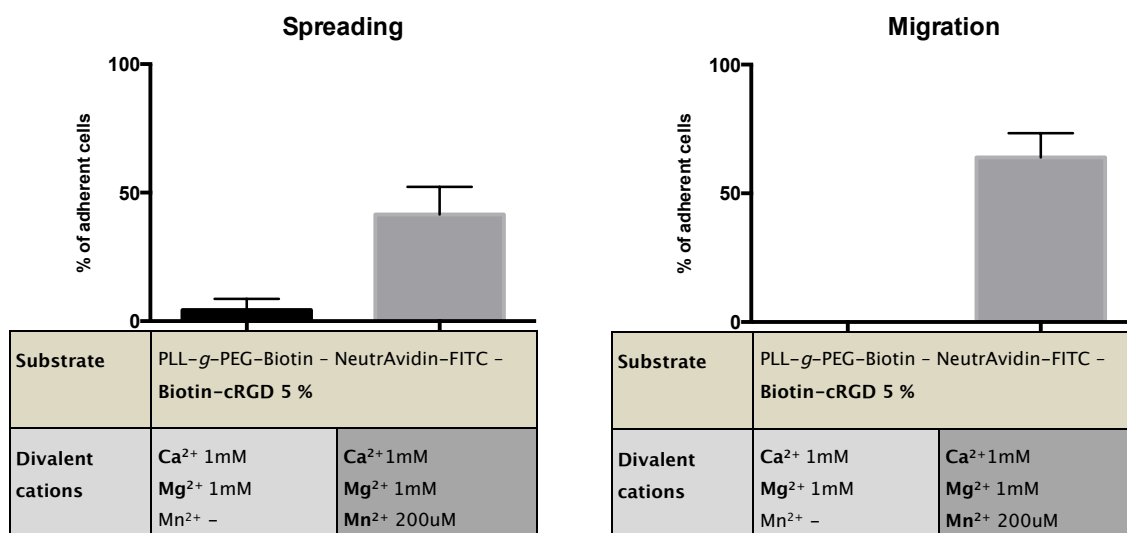


Figure 3.3.3: Human platelet function on *PLL-g-PEG-Biotin - NA-FITC - Biotin-cRGD 5%* with physiological concentrations of Ca^{2+} and Mg^{2+} 1 mM and external integrin activation with Mn^{2+} 200 μM . The external integrin activation considerably alters platelet function. Depicted are three independent experiments and their mean. * = $p < 0.05$.

Next the murine platelet function on these coatings was investigated, considering the migratory behaviour of human platelets. When comparing platelets from these two species, migration is considerably different. On *PLL-g-PEG-Biotin - NA-FITC - Biotin-cRGD 5%* human platelets do not spread nor migrate - murine platelets however, spread and migrate under physiological conditions. This may be explained by the phenomenon that murine platelets have less force, thus resulting in a lower tension threshold to trigger migration. This is consolidated by the fact that the addition of Mn^{2+} to murine platelets on *PLL-g-PEG-Biotin - NA-FITC - Biotin-cRGD 5%* leads to the abolishment of migration due to the firm attachment of the ligand-integrin interaction.

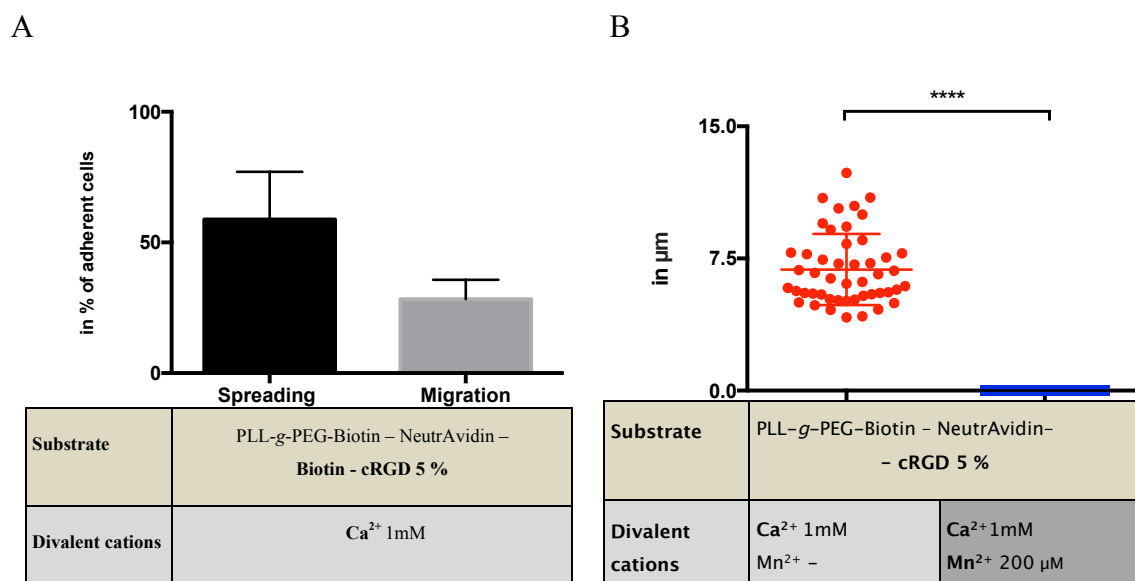


Figure 3.3.4: Murine platelet function on *PLL-g-PEG-Biotin - NA-FITC - Biotin-cRGD 5%* with physiological concentrations of Ca²⁺ 1 mM and external integrin activation with Mn²⁺ 200 μM, respectively.

Murine platelet function is considerably different from human platelet function. A) Murine platelets readily spread and migrate under physiological conditions. B) An external integrin activation completely ceases migration. A) Depicted are three independent experiments and their mean. B) Individual platelets and their migration distance in μm from two independent experiments * = p < 0.05.

3.4 Platelet function on high-tension tolerance - PLL-g-PEG-RGD

To investigate if human platelet function would be altered when the substrate is firmly attached to the surface, platelets were seeded onto *PLL-g-PEG-RGD 10%*. The attachment of the ligand to the surface exceeds the highest possible force generated by a single molecular force of a platelet. While platelets were able to fully spread under both conditions, there was no migration observed, due to the fact that the platelets were not able to remove the ligand from the surface.

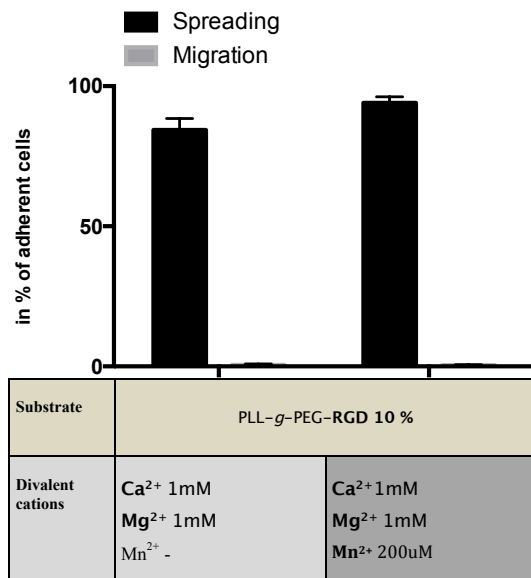


Figure 3.4.1: Human platelet function on PLL-g-PEG-RGD 10% with physiological concentrations of Ca²⁺ and Mg²⁺ 1 mM and external integrin stimulation with Mn²⁺ 200 μM.

While platelets spread under both conditions, migration is completely abolished due to the fact that platelets cannot remove the substrate from the surface. Depicted are five independent experiments and their mean. * = p < 0.05.

This led to the approach of whether the platelets would be able to migrate upon encountering **removable** *PLL-g-PEG-Biotin - NA-FITC - Biotin-RGD 10 %* on the surface. Spreading under physiological conditions was reduced in *- Biotin-RGD 10 %* and the platelets were not able to migrate. However, platelets were able to remove the *- Biotin-RGD 10 %* from the surface with an external integrin activation.

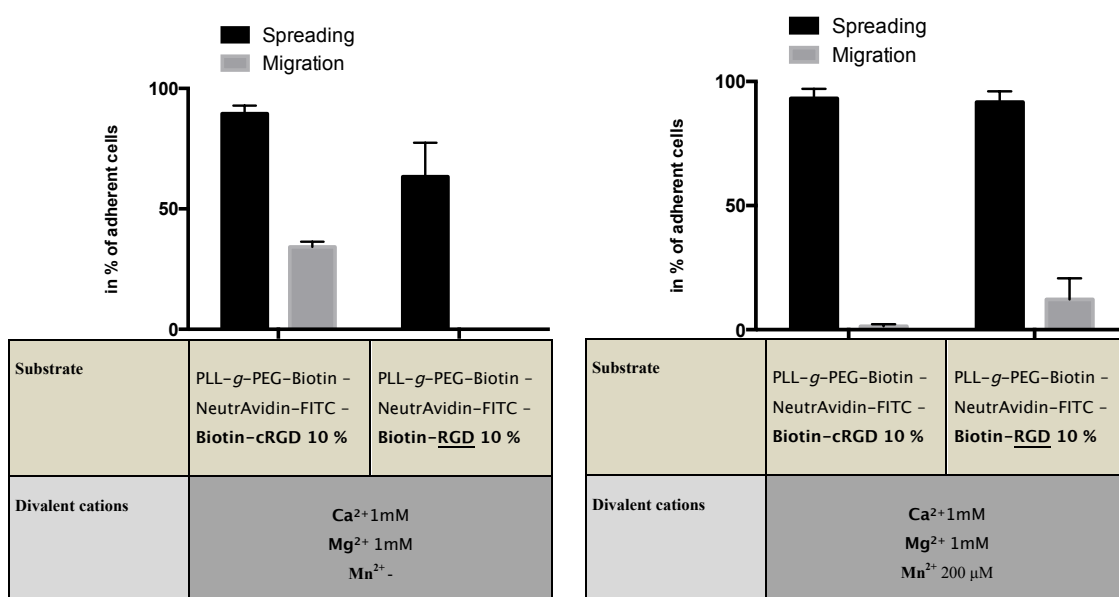


Figure 3.4.2: Comparison of human platelet function on *PLL-g-PEG-Biotin - NA-FITC - Biotin-cRGD 10 %* and *PLL-g-PEG-Biotin - NA-FITC - Biotin-RGD 10%*.

Interestingly ligand entity considerably alters mechanosensitive signalling among two ligands with the same tension threshold. While platelets are able to migrate on *PLL-g-PEG-Biotin - NA-FITC - Biotin-cRGD 10 %* under physiological conditions, an external integrin activation is required on *PLL-g-PEG-Biotin - NA-FITC - Biotin-RGD 10%*. Depicted are three independent experiments and their mean. * = $p < 0.05$.

The results suggest that although the force among these two experiments depicted in figure 3.4.2 remained the same, the mechanosensitive response by the ligand-integrin interaction considerably alters platelet function. Furthermore, it is evident that the – Biotin - cRGD specifically targeting the $\alpha_{11b}\beta_3$ integrin induces a stronger integrin activation.

3.5 Platelet function on the tension gauge tether

3.5.1 Human platelet mechanobiology on the tension gauge tethering system – a tension threshold $\geq 55\text{pN}$ is required to alter platelet function

Human - and murine platelets were investigated on *PLL-g-PEG-Biotin – NeutrAvidin – Biotin-TGT-cRGD 10 %* with tension tolerances of 12pN, 23pN, 33pN, 43pN and 55pN. The *PLL-g-PEG-Biotin – NA-FITC – Biotin-cRGD 10 %* with the tension tolerance of 160pN was identified as an ideal ligand to promote spreading and migration under physiological conditions and acted as a control in all experiments.

Gaertner et al. outlined the mechanism in which platelets adhere to a substrate, spread by forming filopodia and lamellipodia, polarize by adapting a half-moon shape and unidirectionally migrated by removing the ligand from the surface. (Gaertner, Ahmad et al. 2017) The results depicted in figure 3.5.1.1 show that under physiological conditions platelets require a tension tolerance $> 55\text{pN}$ in order to spread and promote migration. This phenomenon can be overcome by externally activating the integrin by which platelet function can be significantly altered. While the spreading behaviour was only considerably increased for $\geq 55\text{pN}$, migration showed a significantly gradually increasing trend from 12pN to 55pN and was completely abolished at 160pN.

These results also underline the fine tuneable differences in force and the considerable impact on platelet function.

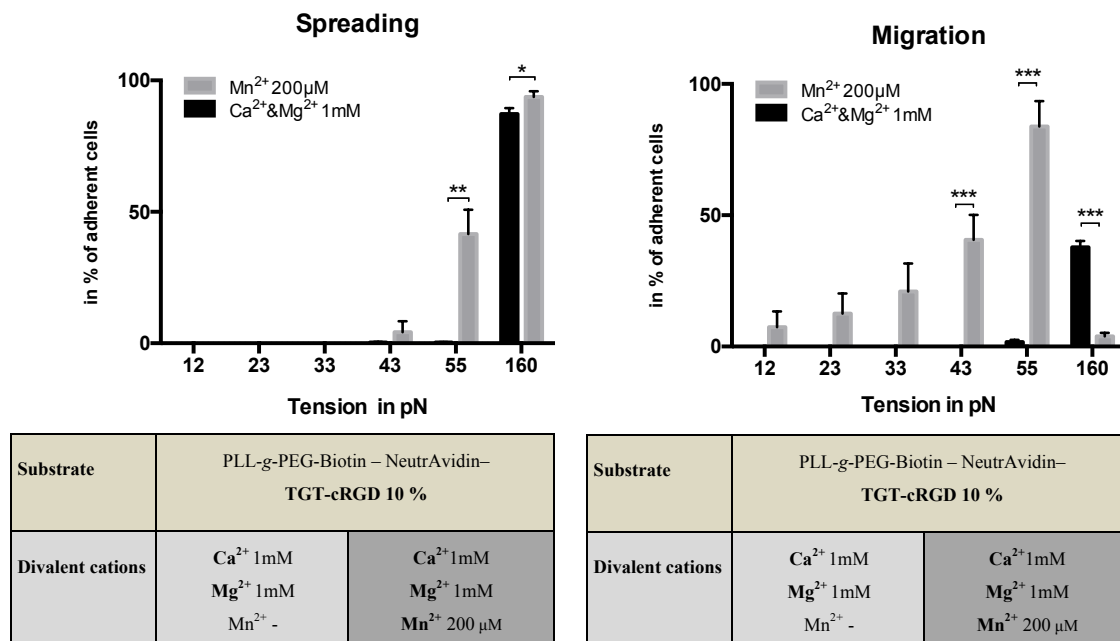
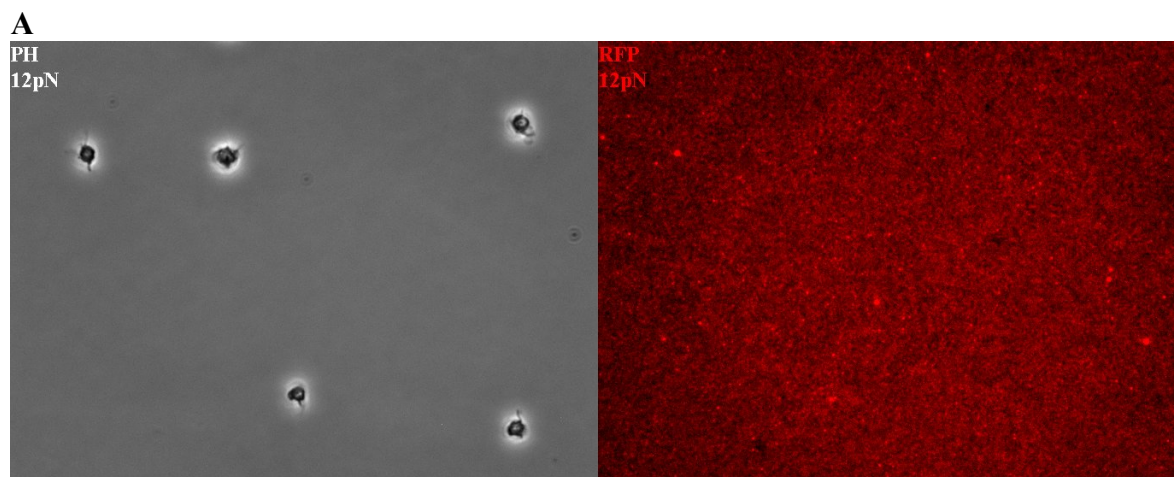
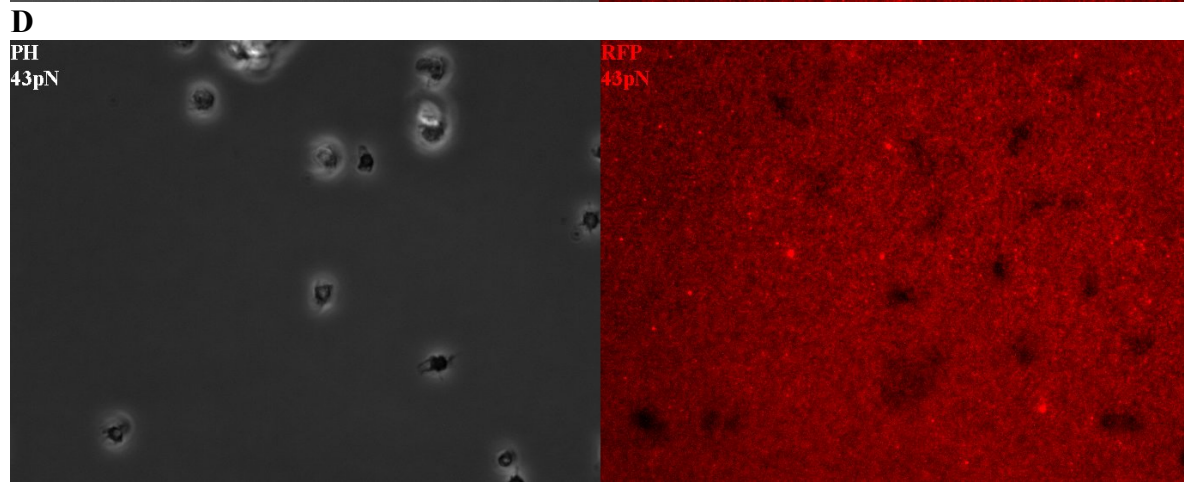
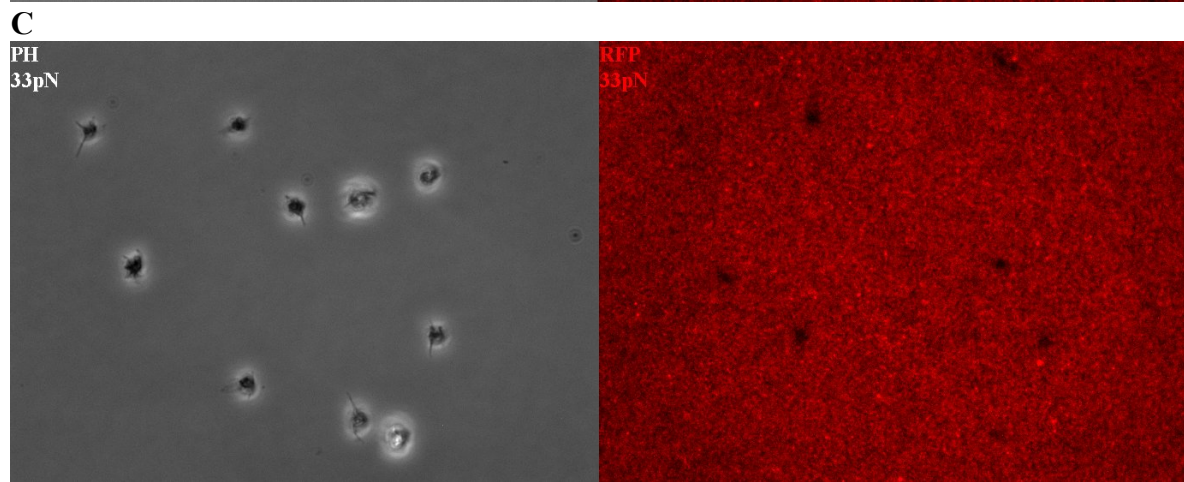
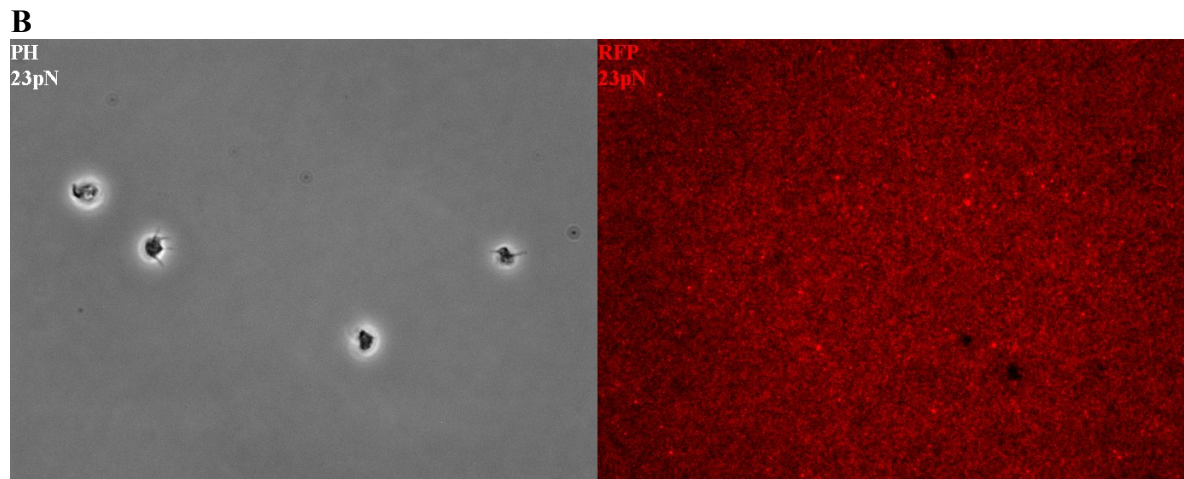


Figure 3.5.1.1 Human platelet mechanobiology on *PLL-g-PEG-Biotin - NA - Biotin-TGT-cRGD 10 %* and the control *PLL-g-PEG-Biotin - NA-FITC - Biotin-cRGD 10 %*.

Spreading behaviour was significantly increased by external integrin activation at a tension threshold of ≥ 55 pN. Interestingly physiological conditions are only able to promote migration at a force ≥ 160 pN while the mechanosensitive stimulus regulating intracellular downstream signaling is shifted to lower tension thresholds with an external integrin activation. Depicted are seven independent experiments and their mean. * = $p < 0.05$.





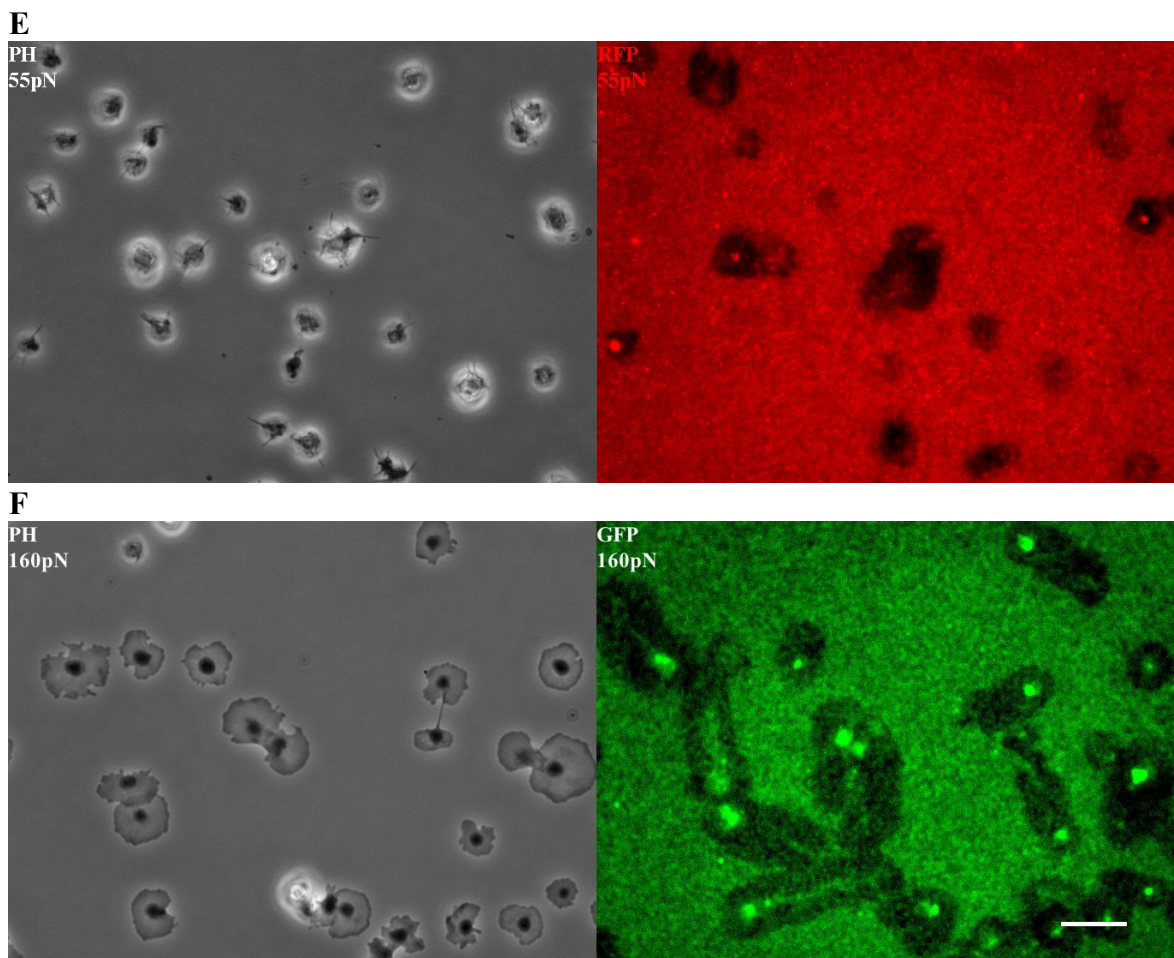
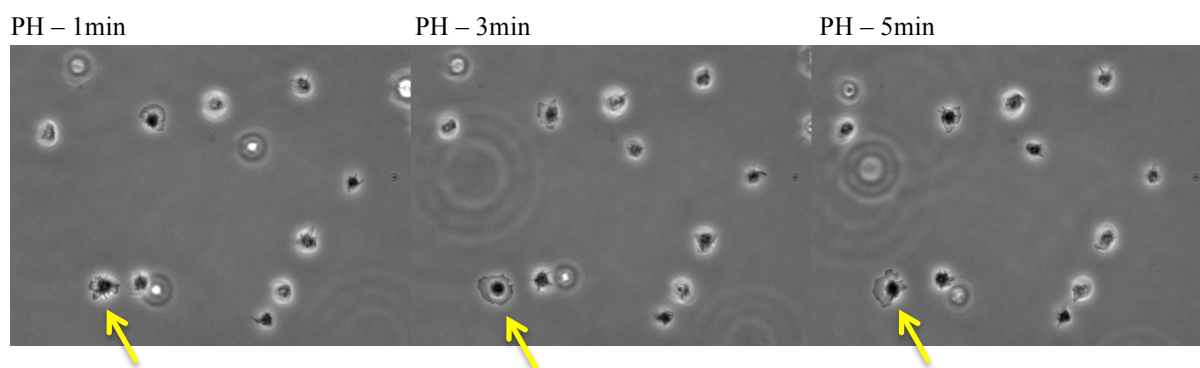


Figure 3.5.1.2: Human platelet mechanobiology on *PLL-g-PEG-Biotin - NA - Biotin-TGT-cRGD 10 %* and the control *PLL-g-PEG-Biotin - NA-FITC - Biotin-cRGD 10 %* under physiological conditions of Ca^{2+} 1mM and Mg^{2+} 1mM.

Clearly evident is the reduced percentage of adherent cells on lower TGTs and the fact that a tension threshold of $> 55\text{pN}$ is required for platelet spreading. Visible are scattered lamellipodia from $\geq 43\text{pN}$. Although the ligand is removed from the surface the tension threshold to preserve permanent spreading is not reached. By visibly comparing the area of removed substrate it seems that the platelets spread at an early time point on 55pN which is revealed when live imaging these cells. Images taken by the Olympus IX 83 with a 100x objective in the RFP/GFP channel after 60 min incubation at 37°C . A) *PLL-g-PEG-Biotin - NA - Biotin-12pN-cRGD 10 %* B) *PLL-g-PEG-Biotin - NA - Biotin-23pN-cRGD 10 %* C) *PLL-g-PEG-Biotin - NA - Biotin-33pN-cRGD 10 %* D) *PLL-g-PEG-Biotin - NA - Biotin-43pN-cRGD 10 %* E) *PLL-g-PEG-Biotin - NA - Biotin-55pN-cRGD 10 %* F) *PLL-g-PEG-Biotin - NA-FITC - Biotin-cRGD 10 %*. Scale bar = $10\ \mu\text{m}$



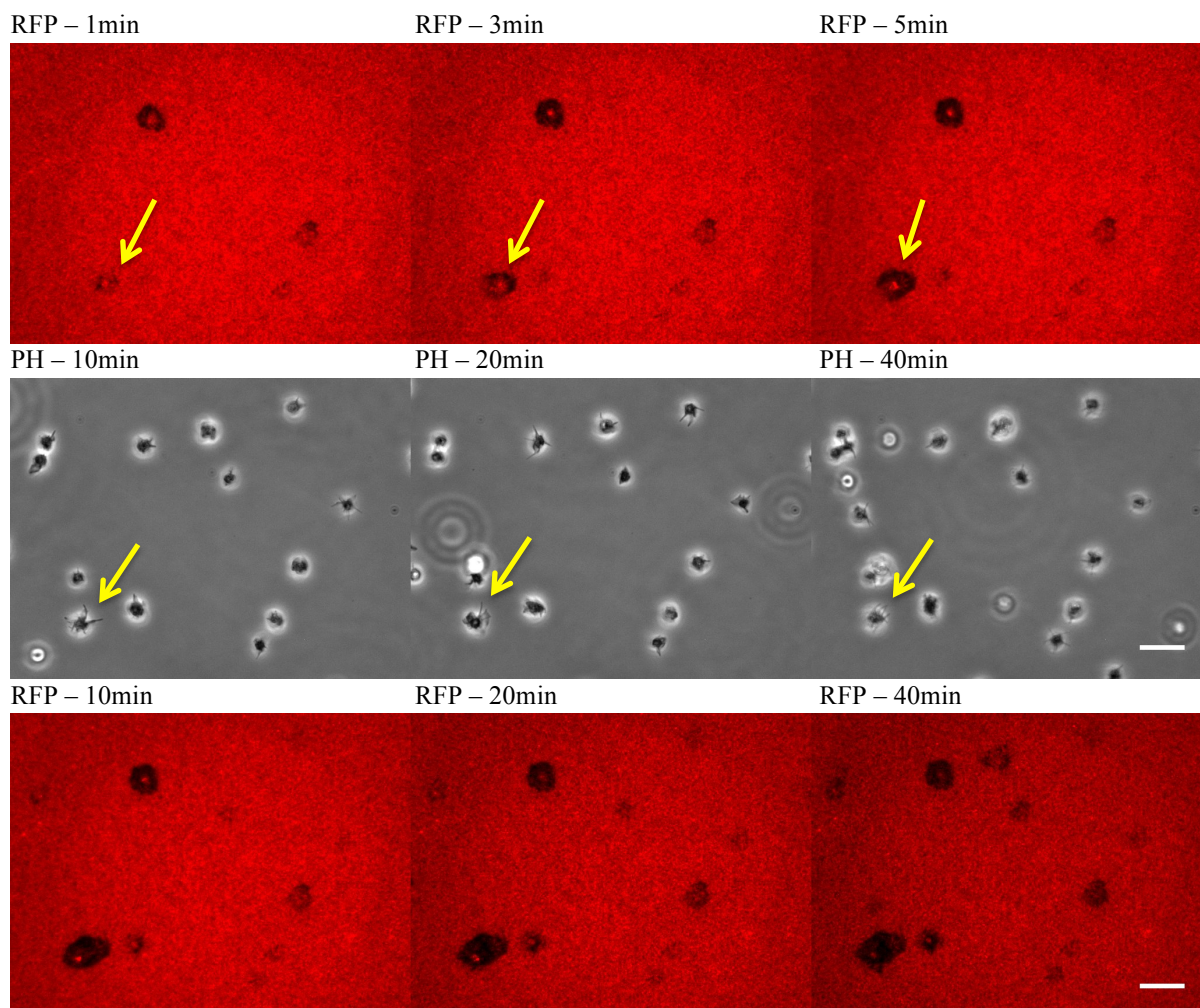


Figure 3.5.1.3: Live imaging of human platelets and investigating mechanobiology on *PLL-g-PEG-Biotin - NA - Biotin-55pN-cRGD 10 %* under physiological conditions of Ca^{2+} 1mM and Mg^{2+} 1mM.

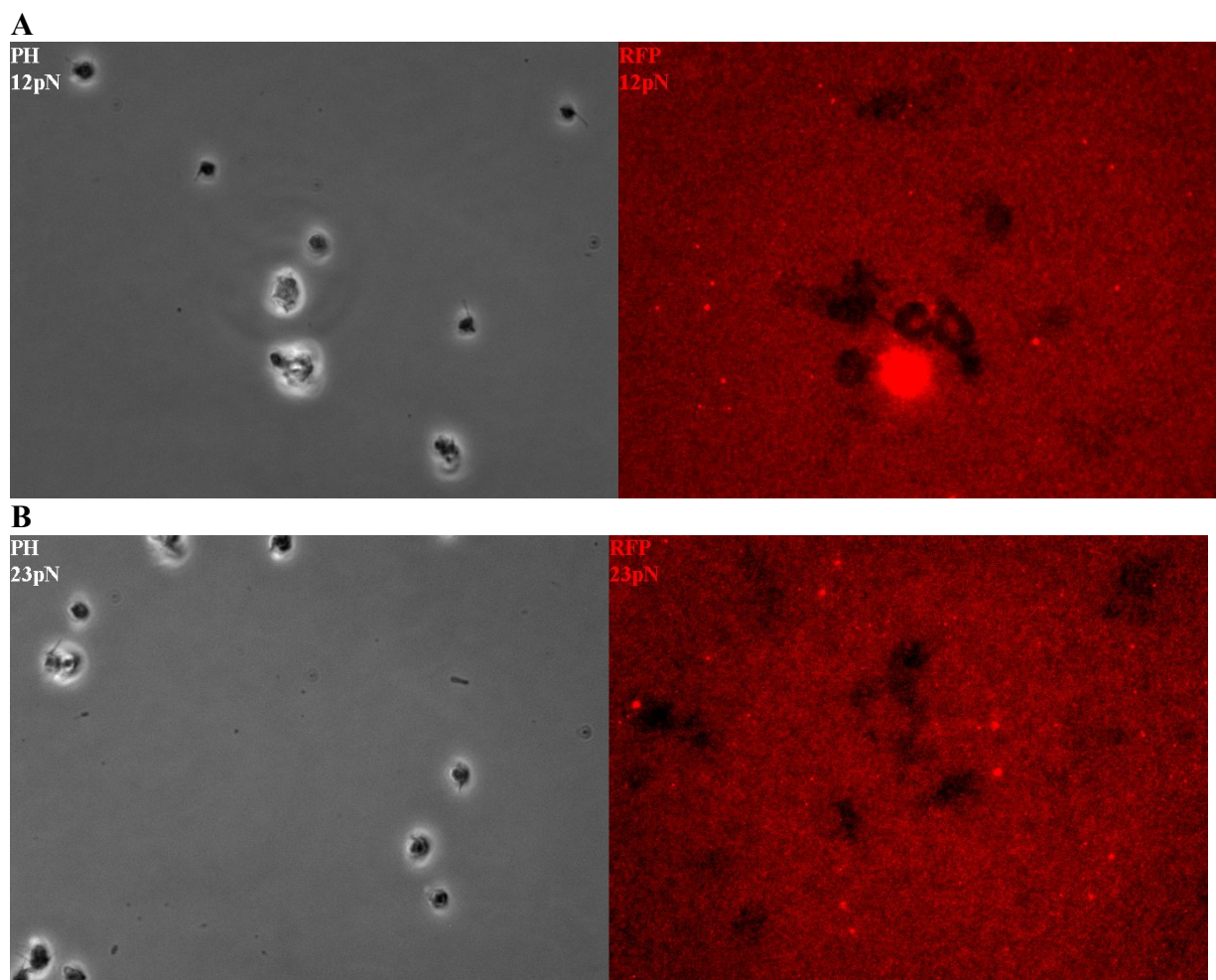
Time lapse depicting six individual images taken at 1,3,5,10,20 and 40 min in the phase contrast (PH) and red fluorescence channel (Fluorophore Cy3) simultaneously while incubated at 37°C. Spreading is clearly evident during the first five minutes, where platelets remove the ligand from the surface, the force however is not sufficient to trigger integrin-mediated downstream signaling. Thus the tension threshold to preserve permanent spreading – and promote migratory behaviour is $> 55\text{pN}$. The yellow arrow indicates an individual platelet with the temporary formation of protrusions/lamellipodia. Scale bar = 10 μm .

As depicted by figure 3.5.1.3 platelets gradually remove more ligand from the surface with increasing tension tolerance under physiological conditions. There seems to be a close correlation between the mechanical probing of the ligand-integrin interaction and the removal of substrate from the surface. Hypothetically there might be an additional recruitment of integrins to evolving filo- and lamellipodia. While platelets removed the ligand from the surface and initially even fully spread on 55pN, the threshold to preserve the lamellipodia failed to be reached.

It is evident from the results that spreading is observed at an early time point after platelet adherence and platelets mechanically probe their microenvironment – however further downstream signaling is required in order to preserve permanent filo- and lamellipodia.

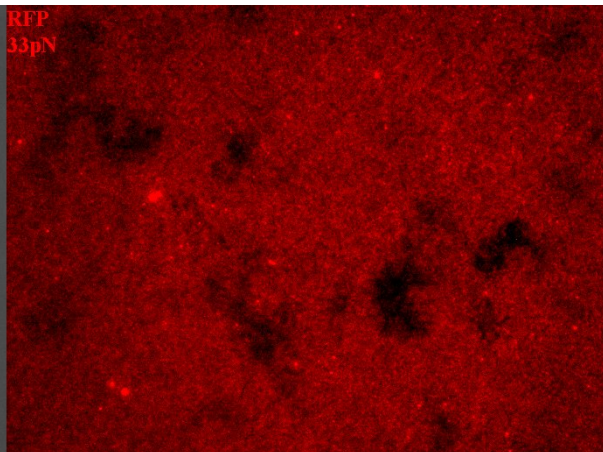
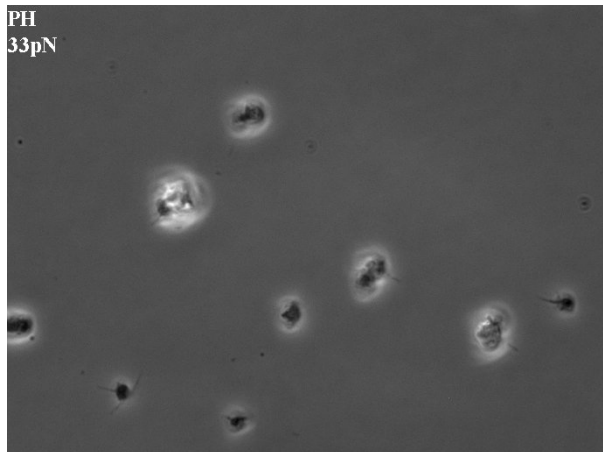
This is an interesting finding by which platelets are initially able to fully spread on 55pN and nonetheless require an additional fine tuneable mechanical trigger in order to be able migrate.

This phenomenon can be actively overcome by an external integrin activation.



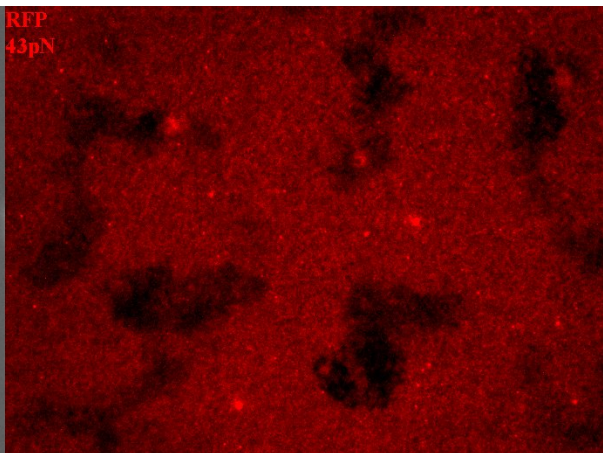
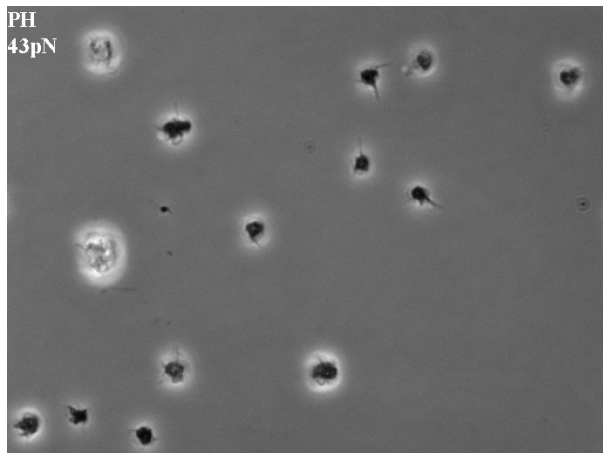
C

PH
33pN



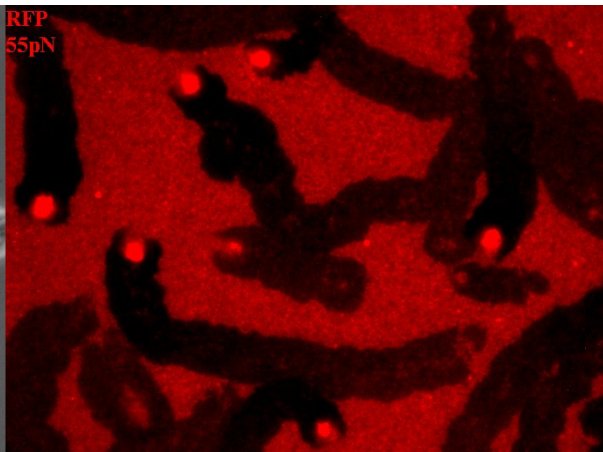
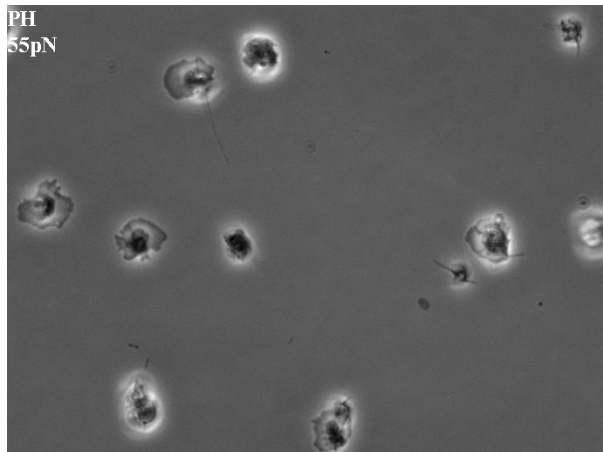
D

PH
43pN



E

PH
55pN



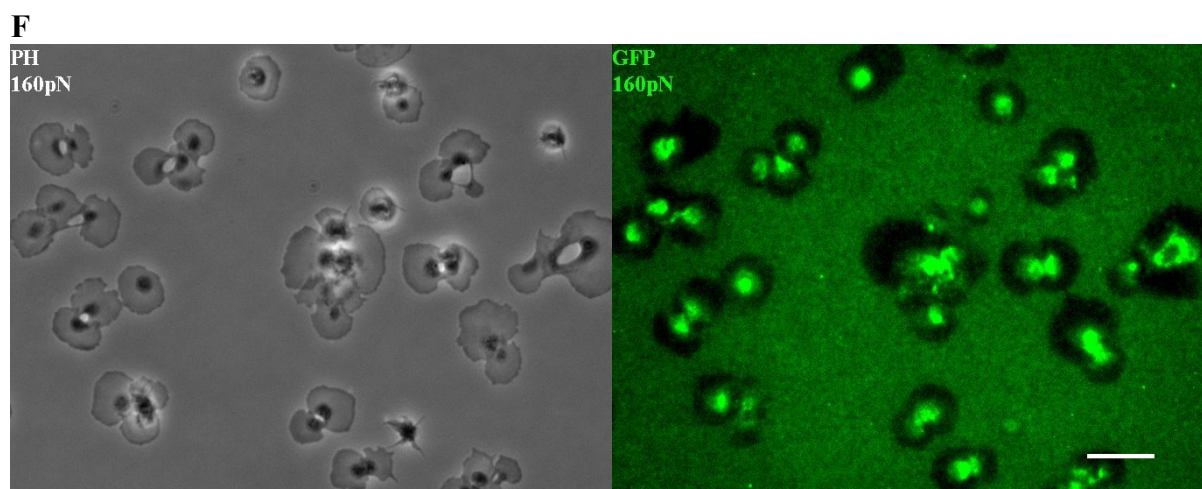


Figure 3.5.1.4: Human platelet mechanobiology on *PLL-g-PEG-Biotin - NA - Biotin-TGT-cRGD 10 %* and the control *PLL-g-PEG-Biotin - NA-FITC - Biotin-cRGD 10 %* with integrin activation by Mn^{2+} 200 μ M.

Clearly evident is the fact that a tension threshold of > 55 pN is required for permanent platelet spreading. Interestingly locomotion can already be observed at 12pN although up until a tension threshold of 43pN the platelets follow a random migratory pattern. Due to the fact that platelets on low tension tolerances only form temporary protrusions and fail to polarize in the direction of migration, the ligand is only unequally removed from the surface. At 55pN the majority of platelets spread, polarized and significantly migrated by fully removing the substrate from the surface. Noticeable is that migration length increases up until 55pN where platelets apply enough mechanical force to remove the ligand from the surface, whereas at 160pN the ligand-integrin interaction and platelets remain in a sessile condition. Images taken by the Olympus IX 83 with a 100x objective in the PH/RFP/GFP channel after 60 min incubation at 37°C. A) *PLL-g-PEG-Biotin - NA - Biotin-12pN-cRGD 10 %* B) *PLL-g-PEG-Biotin - NA - Biotin-23pN-cRGD 10 %* C) *PLL-g-PEG-Biotin - NA - Biotin-33pN-cRGD 10 %* D) *PLL-g-PEG-Biotin - NA - Biotin-43pN-cRGD 10 %* E) *PLL-g-PEG-Biotin - NA - Biotin-55pN-cRGD 10 %* F) *PLL-g-PEG-Biotin - NA-FITC - Biotin-cRGD 10 %*. Scale bar = 10 μ m

Clearly evident from these results is the fact that platelet mechanobiology significantly depends on the force transmitted via the ligand-integrin interaction and that the percentage of integrins in the high affinity state may play a central role for the downstream response. The results in figure 3.5.1.4 D suggest however that a fully spread platelet is not necessarily needed for migration. By analysing the migratory pattern on low tension tolerances ≤ 43 pN it seems that platelets form temporary filopodia and lamellipodia when migrating. However, migration is only observed in the presence of these protrusions thus playing a fundamental role in promoting migration. While Gaertner et al. observed polarization in the direction of locomotion, platelets followed a rather random migratory pattern on the low tension tolerances ≤ 43 pN in which the protrusion pointed in the direction of migration. (Gaertner, Ahmad et al. 2017) This might be explained by the mechanosensitive force transmitted through the ligand-integrin interaction resulting in decreased intracellular signalling in which the threshold for permanent spreading and unidirectional locomotion is not reached.

To summarize the findings of platelet function on the tension gauge tethering system it is important to stress that platelet spreading requires a force greater $\geq 55\text{pN}$ under physiological conditions, while the activated integrins can significantly enhance lamellipodia formation. Under physiological conditions platelets bind to the substrate probing their mechanical environment via the integrin and platelet migration fundamentally depends on mechanical or external integrin activation. Even a fully spread platelet that is already able to remove ligand from the surface needs an additional trigger to induce downstream signalling that will result in the formation of permanent lamellipodia, polarization and unidirectional migration. However, platelet migration was also observed in the presence of temporary protrusion, yet following a different migratory pattern. Thus, these results outline that platelet migration is a condition in which platelets interact with their microenvironment, but an additional mechanical stimulus initiates downstream signalling.

3.5.2 Murine platelet mechanobiology on the tension gauge tethering system

Following murine platelets were seeded on the tension gauge tether and their mechanobiology investigated. The data show a gradually increasing trend of adherent platelets from 33pN - 160pN that can further be enhanced by external integrin activation. The migratory behaviour of murine platelets almost mirrors that of human platelets. The most evident difference in promoting migration is at 43pN for murine platelets. Less force and the smaller size of the murine platelets might explain this phenomenon.

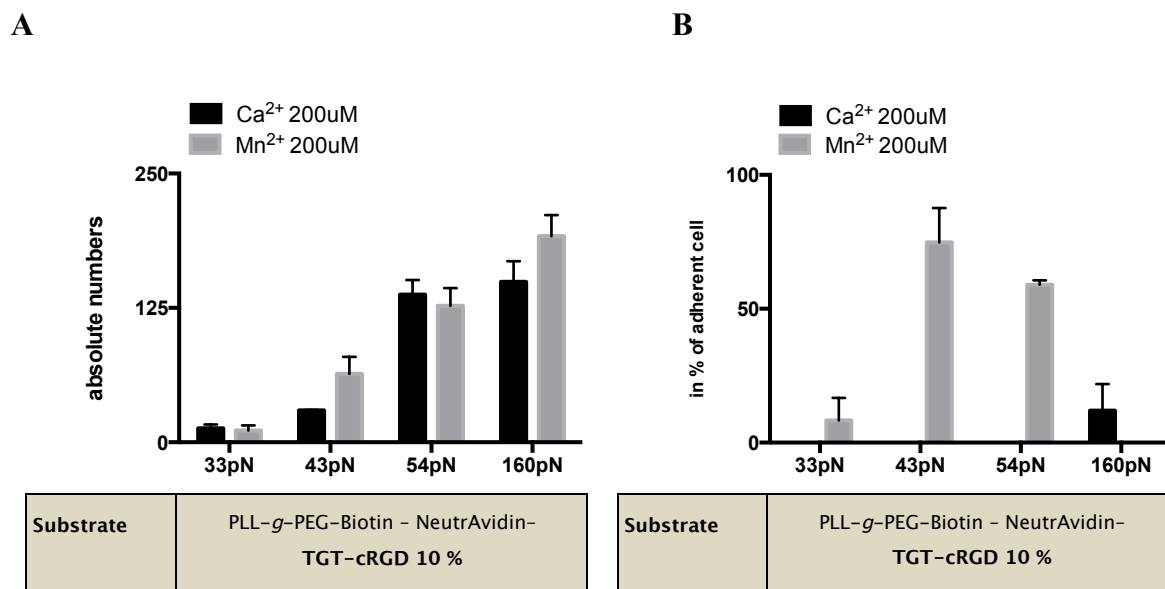


Figure 3.5.2.1: Murine platelet function on *PLL-g-PEG-Biotin - NA - Biotin-TGT-cRGD 10 %* and *PLL-g-PEG-Biotin - NA-FITC - Biotin-cRGD 10%*.

A) Platelet cell counts B) Migration in per cent of adherent cells. A considerable difference to human platelets is that the optimal tension tolerance is at 43pN. Depicted are three independent experiments and their mean. * = $p < 0.05$.

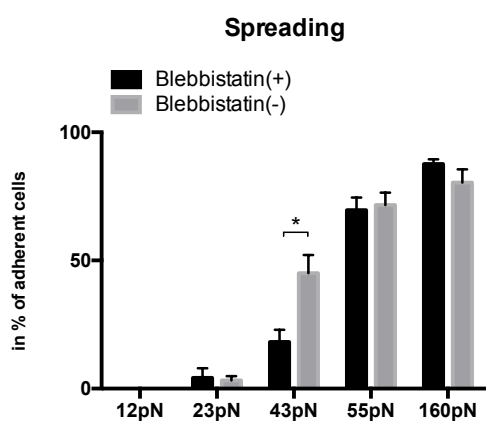
3.6 The influence of pharmacologically inhibiting the contractile machinery of human platelets

The synergy of the mechanosensitive probing via the integrin and the formation of protrusion through the cytoskeletal machinery led to the question of how platelets would react when pharmacologically inhibiting the contractile component: myosin IIa.

Due to the close collaboration of the integrin as a mechanical membrane receptor and the contractile apparatus, platelet function was investigated by pharmacologically inhibiting the myosin IIa with Blebbistatin. The two main cytoskeletal proteins, actin and myosin, not only preserve the cells surface tension, but also fundamentally influence the formation of protrusions. The leading edge of a migrating platelet is mainly depended on actin-polymerization linked to cell-matrix-adhesion-assembly, while the trailing edge is characterised by myosin IIa-mediated contraction and adhesion-disassembly. (Gaertner, Ahmad et al. 2017) The precise coordination of both processes allows the platelet to generate traction force and unidirectional locomotion, while the intracellular repetitive sequences were shown to determine migration speed. (Palecek, Loftus et al. 1997) (Gupton and Waterman-Storer 2006) (Yam, Wilson et al. 2007) (Lämmermann, Bader et al. 2008)

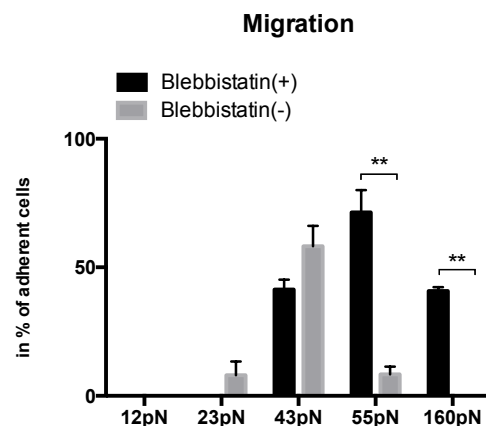
Hypothetically platelets with a myosin IIa inhibition have reduced force and adapt a flatter cell shape, due to reduced overall surface tension. The results show that spreading was only significantly altered on 43pN while the rest of the groups only showed a minor shape change. This is clearly evident by the increased area shown in figure 3.6 D) on intermediate – and low-tension tolerances. Migration was significantly abolished on high-tension surfaces. This is due to the fact that platelets lack the force that is normally applied via the interplay of integrin with the actomyosin network. Alternate intracellular signalling pathways and the predominant role of actin as driving force of locomotion – when silencing myosin – promote migration at a tension threshold of 43pN. On low-tension tolerances, even the different shape configuration does not significantly alter platelet migration behaviour. Of particular interest is the migration velocity – while clearly evident that the inhibition of the myosin machinery results in slower locomotion on intermediate – and high-tension tolerances, the migration on low-tension tolerance (23pN, but not 12pN) takes place in a myosin IIa independent manner.

A



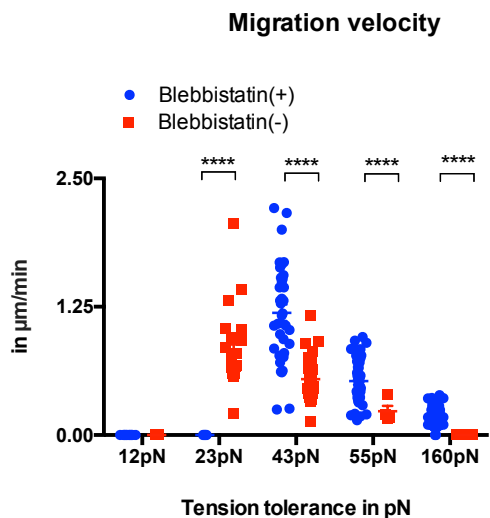
| | |
|------------------|---|
| Substrate | PLL- <i>g</i> -PEG-Biotin - NeutrAvidin- TGT-cRGD 10 % |
| Divalent cations | Ca ²⁺ 1mM Mg ²⁺ 1mM Mn ²⁺ 200 μM |

B



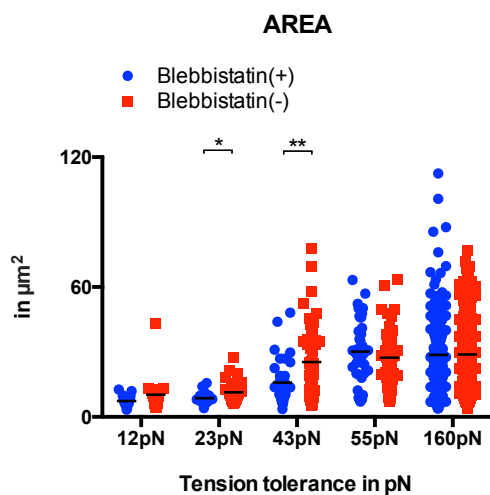
| | |
|------------------|---|
| Substrate | PLL- <i>g</i> -PEG-Biotin - NeutrAvidin- TGT-cRGD 10 % |
| Divalent cations | Ca ²⁺ 1mM Mg ²⁺ 1mM Mn ²⁺ 200 μM |

C



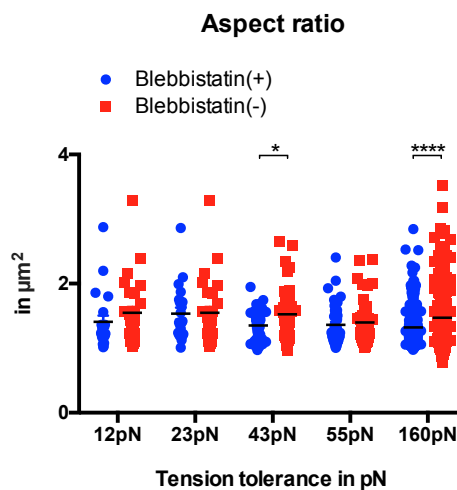
| | |
|------------------|--|
| Substrate | PLL- <i>g</i> -PEG-Biotin - NeutrAvidin- TGT-cRGD 10 % |
| Divalent cations | Ca ²⁺ 1mM Mg ²⁺ 1mM Mn ²⁺ 200 μM |

D



| | |
|------------------|--|
| Substrate | PLL- <i>g</i> -PEG-Biotin - NeutrAvidin- TGT-cRGD 10 % |
| Divalent cations | Ca ²⁺ 1mM Mg ²⁺ 1mM Mn ²⁺ 200 μM |

E



| | |
|------------------|--|
| Substrate | PLL- <i>g</i> -PEG-Biotin - NeutrAvidin- TGT-cRGD 10 % |
| Divalent cations | Ca ²⁺ 1mM Mg ²⁺ 1mM Mn ²⁺ 200 μM |

Figure 3.6: Pharmacological inhibition of myosin IIa by Blebbistatin.

- A) Spreading in per cent of adherent cells, depicting a significant difference on intermediate tension tolerances.
- B) Migration in per cent of adherent cells. Migration was significantly abolished on high tension tolerances, indicating that the force generated is dependent on myosin IIa contraction. Interestingly at a tension threshold of 43pN the generated force is myosin IIa independent. Depicted are five independent experiments and their mean.
* = $p < 0.05$ ** $p < 0.01$
- C) Migration velocity. With decreasing tension tolerance for intermediate - and high tension tolerances, the migration velocity increases among both groups. On low tension tolerances, migration occurs in a myosin IIa independent manner. Depicted are individual cells and their mean. (12pN-B(+) n=0, B(-) n=0; 23pN-B(+) n=0, B(-) n=19; 43pN-B(+) n=36, B(-) n=33; 55pN-B(+) n=39, B(-) n=4; 160pN-B(+) n=175, B(-) n=0) **** = $p < 0.0001$
- D) Depicted is the influence of myosin IIa inhibition on the area
- E) Depicted is the influence of myosin IIa inhibition on the aspect ratio

3.7 Pharmacological blockage of the mechanosensitive channels Piezo1 of human platelets

Platelet mechanotransduction depends on mechanosensitive transmembrane ion channels regulating rapid cationic fluxes. (Coste, Xiao et al. 2012) One such mechanosensitive channel found in platelets is Piezo1 and predominantly regulates Ca^{2+} permeability. As priorly described Ca^{2+} influx plays a pivotal role for platelet function and spreading; in its absence however, migration completely abolishes.

A principle approach to study channel activity is the use of inhibitors - the peptide GsMTx4 (Grammostola spatulata mechanotoxin 4) selectively inhibits Piezo1. (Bae, Sachs et al. 2011) Therefore we investigated human platelets on *PLL-g-PEG-Biotin - NA - Biotin-TGT-cRGD 10 %* and *PLL-g-PEG-Biotin - NA-FITC - Biotin-cRGD 10%* and its effects on the selective blockage of the Piezo I channel.

As evident from figure 3.7A) spreading is merely influenced, however migration is significantly reduced among all groups (see figure 3.7 B)). Apart from the mechanosensitive cation channel Piezo1, platelets also carry ATP-gated P2X1, the transient receptor potential ion channel 6 (TRPC6) as well as the store-operated calcium entry via Stim1-Orai1. (Hassock, Zhu et al. 2002) (Varga-Szabo, Braun et al. 2008) (Mahaut-Smith, Jones et al. 2011) (Nakamura, Sandrock-Lang et al. 2013) (Jones, Evans et al. 2014) (Mahaut-Smith, M. P. (2012) Interestingly migration velocity depicted in figure 3.7.1c was significantly reduced, however did not cease – this may be explained by the fact that the calcium influx is compensated by alternative routes when silencing Piezo1 by GsMTx4. In conclusion it is important to outline the importance of the MSCs for platelet migration, in particular the

migration velocity and further *in vivo* experiments are needed to study the effects of the alternative cationic channels.

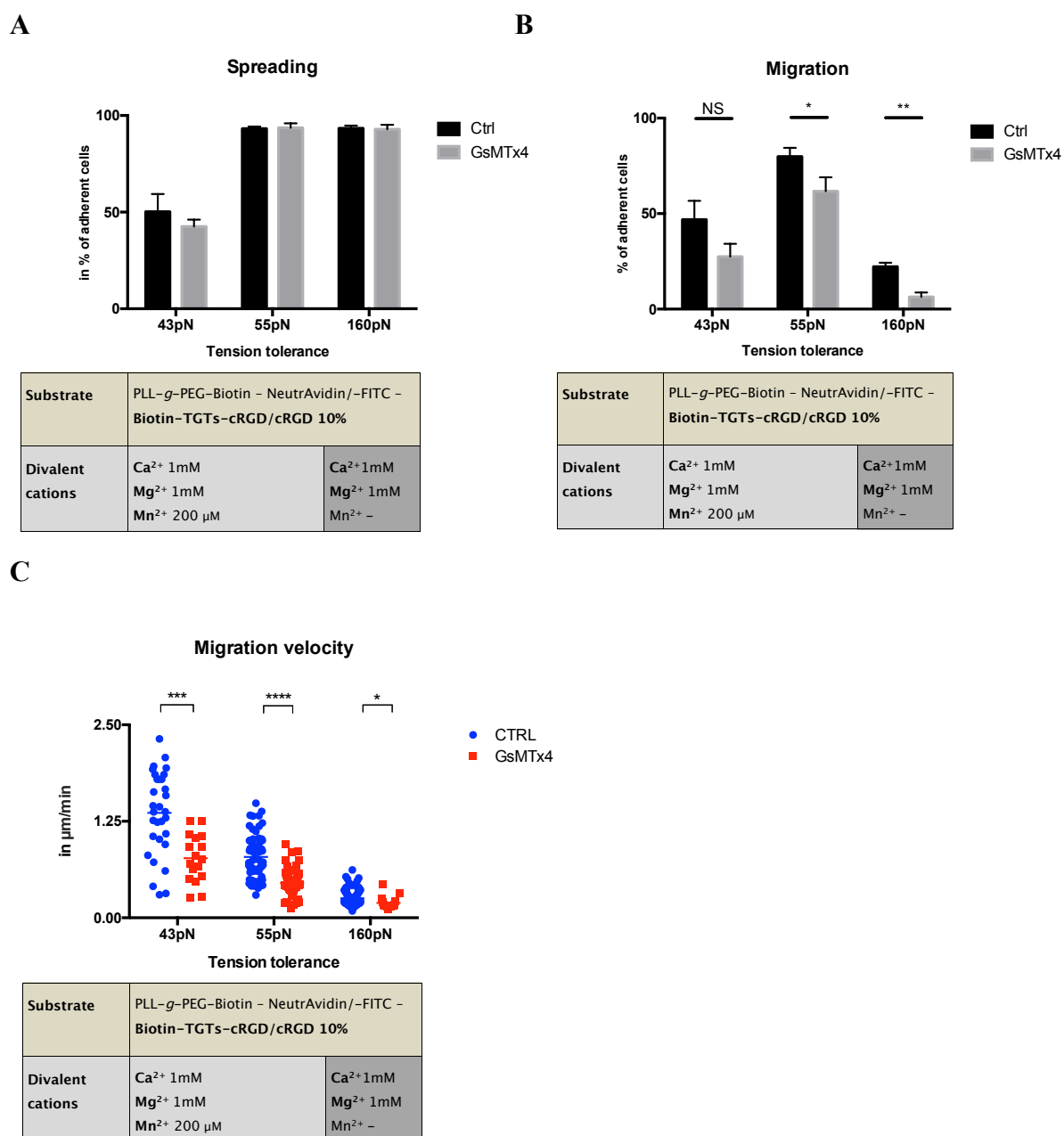


Figure 3.7: Pharmacological inhibition of Piezo1 by GsMTx-4 for human platelets.

A) Spreading in per cent of adherent cells - depicting no significant difference between the tension tolerances.

B) Migration in per cent of adherent cells. Migration was significantly abolished on high-tension tolerances, indicating that the mechanosensitive machinery works in a Ca²⁺-dependant manner. Depicted are five independent experiments and their mean. * = $p < 0.05$ ** $p < 0.01$

C) Migration velocity in $\mu\text{m}/\text{min}$. With decreasing tension tolerance for intermediate and high tension tolerances, the migration velocity increases among both groups. This shows that Piezo I seem to play a key role for Ca²⁺ influx, and thus plays a fundamental role for platelet migration. Depicted are individual cells and their mean. 43pN-Ctrl n=36, GsMTx-4 n=33; 55pN-Ctrl n=39, GsMTx-4 n=4; 160pN-Ctrl n=175, GsMTx-4 n=0) * = $p < 0.015$ *** = $p = 0.0001$ **** = $p < 0.0001$

4 Discussion

The established assay allows to study the complex mechanosensitive effects on platelet function by dynamic visualisation. It specifically focuses on their impact on platelet migration and allows to quantify single molecular forces at the pN scale. Platelet mechanobiology through integrin mediated outside-in signaling plays a pivotal role in triggering a specific tension threshold that significantly alters platelet behaviour.

It is tempting to speculate that platelets *in vivo* constantly scan the vasculature for potential lesions might adhere and spread on the ECM or a maturing blood clot and the mechanical microenvironment determines platelet activation in the presence of adhesive proteins and soluble agonists.

Investigating the diverse mechanisms orchestrating platelet function is fundamental when considering their central role in physiological haemostasis and pathological conditions such as vascular injury, inflammation and atherothrombosis. Platelet mechanobiology consists of a complex bidirectional interaction between the integrins acting as mechanosensitive membrane receptors with the innards of the platelet's contractile machinery. The biophysical constitution of the microenvironment precisely regulates downstream signalling, thereby inducing multiple intra - and extracellular processes.

Over the past few decades several groups intended to elucidate platelet forces using a broad range of approaches: 1) force measurements in maturing blood clots for individual platelets in the order of nanonewton (Jen and McIntire 1982) (Carr and Zekert 1991) (Carr 2003) (Liang, Han et al. 2010) and 2) single molecular forces transmitted via the integrin in the order of piconewton (Stabley, Jurchenko et al. 2011) (Morimatsu, Mekhdjian et al. 2013) (Wang and Ha 2013) (Blakely, Dumelin et al. 2014). Wang et al. introduced the tension gauge tether that is an innovative approach to investigate single molecular forces transmitted via the integrin that was chosen due to its physical – and ligand properties. (Wang and Ha 2013) Two distinct levels of integrin tension were identified using a genetically modified CHO-K1 cell-line: an integrin tension of ~40 pN before focal adhesions (FA) formation in an actomyosin independent manner, whereas through integrin clustering FAs were able to generate a force > 55pN. (Wang, Sun et al. 2015) (Wang, LeVine et al. 2018)

Although previous groups described platelet locomotion (Lowenhaupt, Miller et al. 1973) at sites of inflammation (Feng, Nagy et al. 1998) (Czapiga, Gao et al. 2005) (Pitchford, Momi et al. 2008) and intracellular Ca^{2+} and actin polymerization as two pivotal components, (Kraemer, Borst et al. 2010) (Schmidt, Münzer et al. 2011) (Schmidt, Kraemer et al. 2012) platelet migration has only recently been identified by Gärtner et al. to be an autonomous process in vivo. (Gaertner, Ahmad et al. 2017)

Earlier, Lauffenburger et al. characterized a well-defined sequence of events for migrating cells that follows four repetitive steps: 1) membrane extensions as lamelli- and filopodia at the front (leading edge) 2) ligand adhesion 3) actomyosin mediated contraction 4) substrate release at the rear. (Lauffenburger and Horwitz 1996) Platelets adapt a similar migrating phenotype as seen by other mesenchymal cells – a prerequisite of platelet migration is however that the ligand needs to be removable from the substrate. Gaertner et al. identified the initial platelet spreading morphology to adapt a target like shape with an aspect ratio ≈ 1 . The cells polarized in which the leading edge emerged at one side of a lamellipodia by actin polymerization and – rearrangement, while the rear contracted in a myosin – dependent manner. Due to the platelet's shape change and cytoskeletal rearrangement, the pseudonucleus was now located at the rear of the platelet with an aspect ratio ≈ 2 . A persistently migrating platelet adapted this half-moon like phenotype. Conclusively platelet function strongly depends on the biophysical constitution of the microenvironment, since platelet actomyosin dependent contractile forces have to overcome ligand resistance in order to promote migration in this manner. (Gaertner, Ahmad et al. 2017)

This phenotype of target-like spreading and unidirectional migration was only initially observed on ligand resistances $> 55\text{pN}$, while the threshold was lowered to $\geq 55\text{pN}$ with an external integrin activation. The initial adhesion of platelets with the capability to fully spread and remove the substrate from the surface requires a specific substrate resistance in order to preserve permanent spreading (see figure 4.1). This is consistent with the findings of Zhang et al. who proposed that the ligand-integrin interaction controls a mechanical checkpoint central to platelet activation. This study also used the tension gauge tether, however focusing on the discrimination of soluble – versus platelet bound fibrinogen and its effects on platelet aggregation. (Zhang, Qiu et al. 2018)

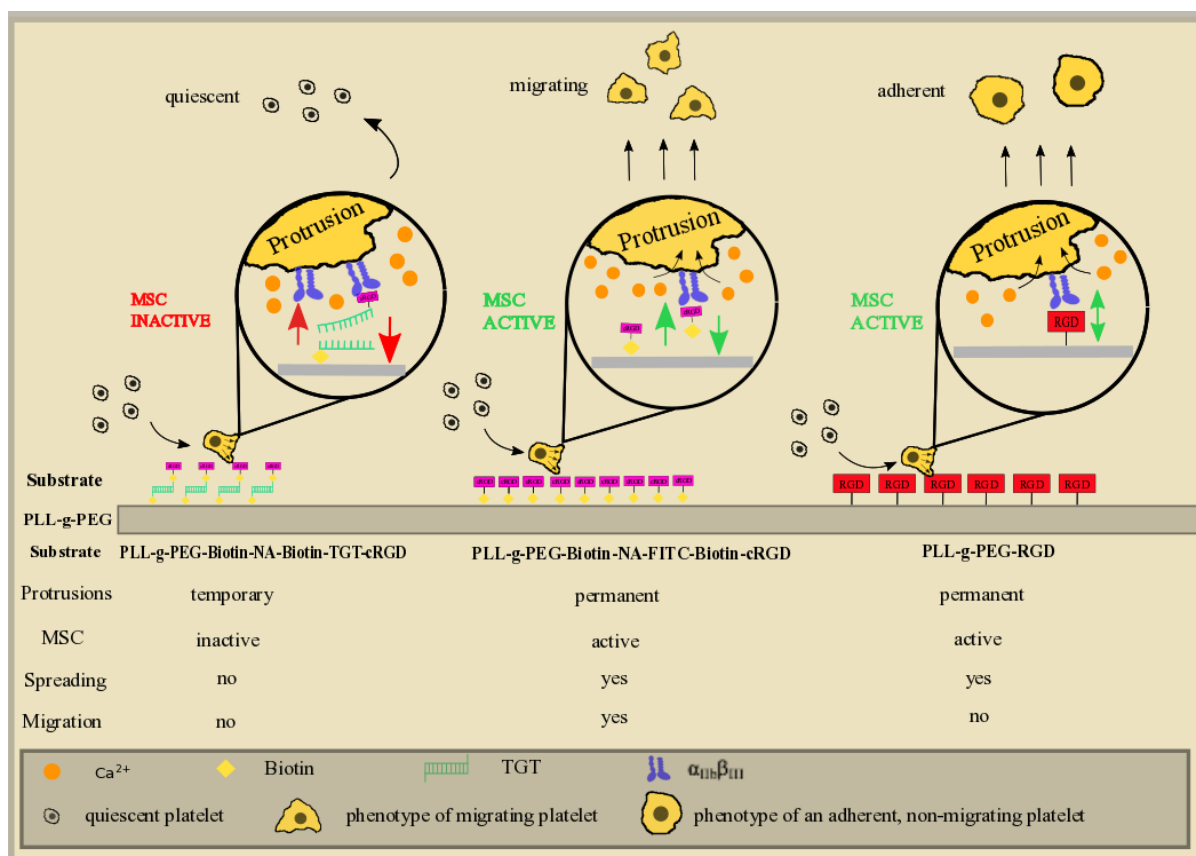


Figure 4.1: Mechanobiology of platelets on varying substrate resistances under physiological conditions (Ca²⁺, Mg²⁺, ADP and TXA₂)

Scenario on the left: Platelets adhere and remove the substrate from the surface – the mechanosensitive channel remains inactive with the formation of temporary protrusions; platelets detach from the surface.

Scenario in the middle: Platelets adhere, spread and migrate, by removing the substrate from the surface – activation of the mechanosensitive channel with formation of permanent protrusions.

Scenario on the right: Platelets adhere and spread, however unable to remove the substrate from the surface – activation of the mechanosensitive channel; platelets remain static.

In accordance with Qiu et al. who outlined the pivotal role of substrate stiffness on platelet function, platelet behaviour under physiological conditions was considerably different on low tension tolerances. High resistance force will stabilize the open, high affinity confirmation of the $\alpha_{IIb}\beta_3$ integrin, however this mechanosensitive checkpoint was not reached on tension tolerances ≤ 55 pN. (Qiu, Brown et al. 2014) Interestingly the quantity of substrate removed from the surface evidenced by the surface-fluorescence-loss of the substrate, followed an increasing trend from 12pN – 55pN. These findings support the hypothesis that the additional recruitment of integrins in FAs and an increase of force over time are determined by a mechanosensitive threshold leading to permanent spreading.

Platelet function was significantly different when the outside-in signalling was circumvented by external integrin activation. The migrating phenotype described by Gaertner et al. was only observed on tension thresholds > 55 pN with an external integrin activation (see figure

4.2). On low ligand resistance, the platelets formed temporary lamellipodia in the direction of locomotion, while following a rather random migratory pattern.

This finding that an activated platelet yet requires an additional mechanosensitive trigger and the fact that platelets may adapt two distinct migratory patterns, may highlight its importance in vivo, where a circulating platelet adheres, partially spreads and migrates on a substrate surface. This phenomenon may be explained by the following: on the one hand the platelet force may overcome ligand resistance and the platelet detaches from the vessel wall, but on the other hand the mechanical microenvironment and maturing blood clot may constitute a resistant network, mechanically and biochemically activating the platelet.

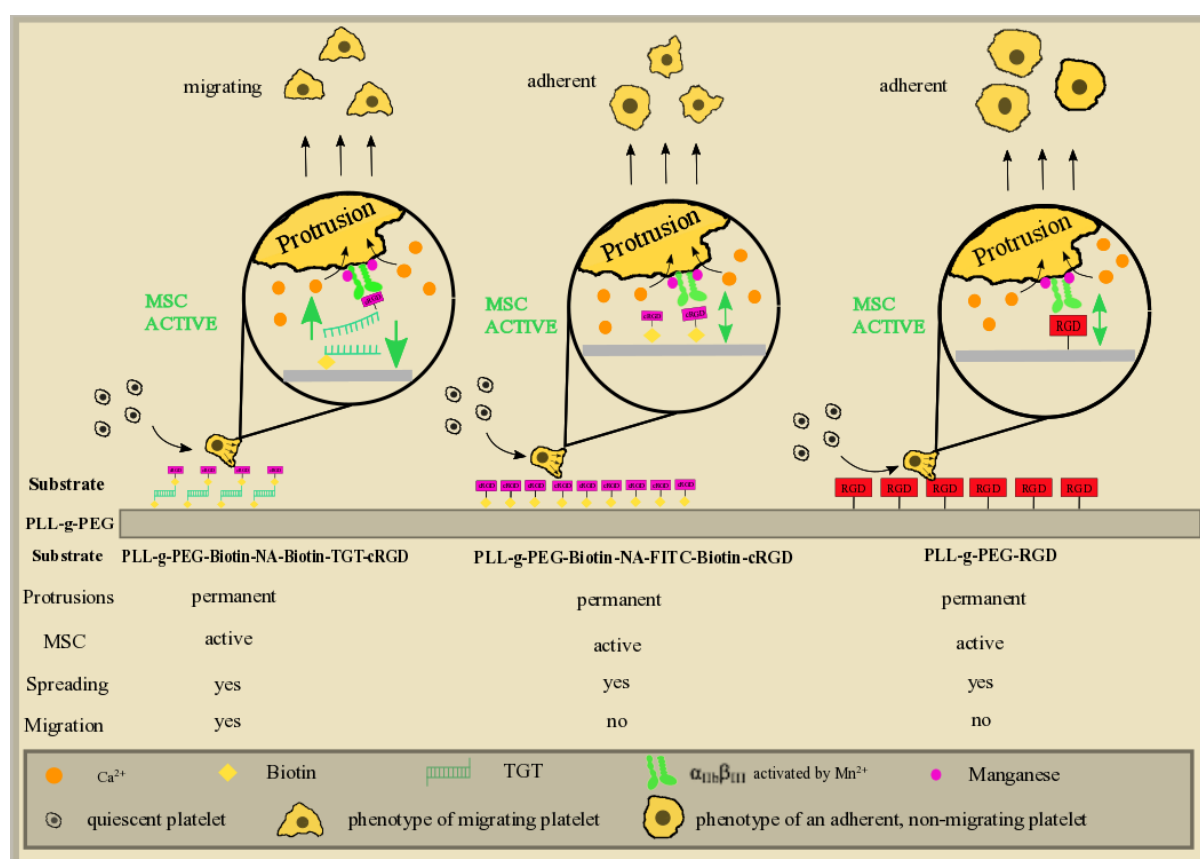


Figure 4.2: Mechanobiology of platelets on varying substrate resistances with an external integrin activation by Manganese

Scenario on the left: Platelets adhere, spread and migrate, by removing the substrate from the surface – activation of the mechanosensitive channel with formation of permanent protrusions.

Scenario in the middle/right: Platelets adhere and spread, however unable to remove the substrate from the surface – activation of the mechanosensitive channel with formation of permanent protrusions; platelets remain static.

Remarkable is the fact that Gaertner et al. only observed migration in the presence of anti-adhesive proteins such as albumin or casein that may modulate the conformational presentation of fibrinogen molecule in vitro. (Gaertner, Ahmad et al. 2017) The presence of

soluble proteins was neither required for migration on cRGDs under physiological conditions, nor on TGTs with an external integrin activation. Interestingly the findings by Qiu et al. and Jirouskova et al. revealed that fibrinogen concentration significantly alters platelet function. Paradoxically high fibrinogen concentrations (100 ug/mL) significantly diminish platelet adhesion that is most likely caused by the spatial organisation of the fibrinogen molecules on the surface altering exposure of substrate binding sites. Our assay guaranteed the single molecular interaction with the integrin by electrostatically aligning the substrate on the surface, thereby explicitly exposing its binding site. In concordance with Qiu et al. but unlike the findings by Jirouskova et al. substrate stiffness and increasing ligand concentrations maximised platelet spreading.

Furthermore, platelet mechanical forces are spatially differently distributed on the plasma membrane. Unlike the findings by Wang et. al who identified the centre of the CHO-K1 cells to be the strongest force across single integrins within motile FAs, in platelets the least force is generated in the middle where the cytoplasm rich pseudonucleus resides. (Wang, Sun et al. 2015) This is clearly evident on the *PLL-g-PEG-Biotin – NA-FITC - Biotin-cRGD 10 %* with a ligand resistance of 160pN under physiological conditions. Migrating platelets revealed the equal removal of substrates at the periphery, while the central part spared a line of substrate. A considerable difference was noticeable on the 55pN with Mn^{2+} . The majority of platelets removed all the substrate from the surface, however initial central substrate lines were also visible. This phenomenon might be explained through the additional recruitment of integrins to the central region with increasing force over time. This hypothesis is supported by the findings of Wang et al. who identified integrin clustering in FAs to exert forces >55 pN in an actomyosin dependent manner. (Wang, Sun et al. 2015)

Additionally, the pharmacological blockage of myosin IIa had no effect on spreading, but migration was significantly reduced. (Gaertner, Ahmad et al. 2017) While platelet migration was considerably reduced on high tension thresholds ≥ 55 pN, ligand resistance was overcome at 43pN with an active myosin IIa inhibition. This confirms that platelet migration on high tension tolerances is mediated in a myosin IIa dependent fashion, but migration on intermediate – and low tension tolerances is mediated via alternative forces.

There exists a considerable body of evidence identifying Ca^{2+} as a central regulatory component of cell migration, mediating actomyosin dependent rearrangements and migratory behaviour. Extracellular Ca^{2+} influx is mediated by the P2X1-receptor, the transient receptor potential ion channel 6 (TRPC6) and store-operated calcium entry via Stim1-Orai1 and plays a fundamental role for MLC-phosphorylation (Ser19) and myosin IIa-activation. (Haddock,

Zhu et al. 2002) (Varga-Szabo, Braun et al. 2008) (Mahaut-Smith, Jones et al. 2011) (Nakamura, Sandrock-Lang et al. 2013) (Jones, Evans et al. 2014) Gaertner et al. described the switch from spreading to migration to be regulated by a Ca^{2+} - mediated myosin IIa dependent rear contraction. Unlike the findings by Gaertner et. al where platelet spreading was retrained, but migration significantly reduced in the absence of extracellular calcium, platelet adherence was completely impaired on *PLL-g-PEG-Biotin – NA-FITC - Biotin-cRGD 10 %* surfaces. This phenomenon might be explained by the fact that our assay was reduced to the core of the fibrinogen molecule, i.e. the RGD sequences exclusively binding to the $\alpha_{\text{IIb}}\beta_3$ integrin. The integrin activation is the key regulatory step for platelet spreading that itself depends on sufficient levels of extracellular Ca^{2+} concentration. In summary this suggests that not only platelet polarization and migration, but also spreading requires extracellular Ca^{2+} .

However, the mechanisms of how mechanosensing via the integrin mediates Ca^{2+} influx in platelets, still remains uninvestigated. The channel modulator GsMTx-4 effectively diminishes platelet migration by blocking the mechanosensitive channel Piezo1. The exact mechanism is not known, however Piezo1 is involved in mechanically mediated extracellular Ca^{2+} influx. (Bowman, Gottlieb et al. 2007) (Bae, Sachs et al. 2011) While human as well as murine platelets revealed a normal spreading behaviour, migration was only abolished on 160pN under physiological conditions. On tension tolerances < 160pN platelets were able to migrate even in the presence of GsMTx-4, however the percentage and velocity of migrating cells were considerably reduced. These findings suggest that platelet spreading and migration might be considered as two different processes. However, due to the fact that the underlying mechanism of how GsMTx-4 inhibits Piezo I is still not known, these findings need to further be investigated by using knockout mice.

By reducing the experimental setup to a minimum, where the integrin $\alpha_{\text{IIb}}\beta_3$ binds a single ligand, our findings confirmed the hypothesis of Gaertner et al. that platelet migration is mediated by four key regulatory mechanisms: 1) Activation with: TXA_2 and ADP or thrombin 2) $\alpha_{\text{IIb}}\beta_3$ integrin as bidirectional mechanosensitive membrane receptor 3) extracellular Ca^{2+} influx 4) actin polymerization and myosin contraction.

In conclusion it is important to emphasize the fact that platelet migration has only recently been identified as an autonomous process in vivo. (Gaertner, Ahmad et al. 2017) Platelet recruitment to sites of injury or inflammation has been described in detail in the literature over the past few decades - however little is known of how platelets perceive their

mechanical microenvironment. The present study identified for the first time how single molecular forces alter platelet function, specifically investigating the effect on platelet migration. By controlling ligand density and tension tolerance the developed assay allows to precisely investigate platelet mechanobiology. Additional experiments will be required to perceive insights in how the mechanosensing influences the behaviour of the contractile apparatus.

It is tempting to picture the clinical benefits these selective modulations of platelet function would imply – clinical catheters and medical implants could be modified in such a way that platelet interaction may be reduced to a minimum.

5 Summary

Background: Platelets play a crucial role in primary hemostasis besides an increasing body of evidence suggesting an active participation in the first line of host defence. Platelets are among the first cells to be encountered at sites of vascular injury or inflammation. These microenvironments expose a myriad of biochemical – as well as biophysical stimuli, activating and directing platelet migration. Autonomous platelet migration has previously been seen with great scepticism and only recently been described by Gärtner et al.. (Gaertner, Ahmad et al. 2017)

The transmembrane protein $\alpha_{IIb}\beta_3$ is the most abundant integrin on the platelet plasma membrane, linking extracellular stimuli to the platelet's innards. It plays a fundamental role for mechanotransduction and thus allows platelets to physically probe their microenvironment. When actomyosin dependent traction forces overcome substrate resistance, platelets start to migrate.

Here we aim to establish a novel imaging based tool to analyse platelet migration and to quantify molecular forces involved in this process.

Results: We established a novel platelet migration assay allowing us to adjust substrate resistance and to measure single integrin-mediated forces at the pN scale. Substrate resistance as well as levels of integrin activation are crucial components for autonomous platelet migration. Following physiological activation (Ca^{2+} , Mg^{2+} , ADP and TXA_2) platelets migrate on surfaces with a substrate resistance of ≈ 160 pN, while a substrate resistance too low (≤ 55 pN) or too high (> 160 pN) abandons the vast majority of migrating platelets. In contrast, when integrins were stabilized in their active conformation, platelet function as well as migratory behaviour were significantly altered.

Besides the central role of the integrin as a surface receptor, pharmacological inhibition of the contractile apparatus as well as the mechanosensitive channels on the platelet plasma membrane have significant effects on platelet function. By inhibiting myosin IIa, migration is abolished on high-tension tolerances (55pN; 160 pN), while platelets migrate in a myosin IIa independent manner on intermediate (43pN) – and low-tension tolerances (23pN). An essential component for actomyosin dependent contraction is the Ca^{2+} flux into the cell via the mechanosensitive channel Piezo1. Inhibition of Piezo1 by GsMTx4 significantly reduced

migration, indicating an important role of mechanosensitive ion channels in platelet migration.

Conclusion: This study identified substrate resistance, the transmembrane integrin $\alpha_{IIb}\beta_3$ and the contractile apparatus as essential components for platelet mechanobiology. When traction forces overcome substrate resistance, platelets form permanent lamellipodia, polarize and migrate.

Thus, this work outlines that platelets mechanically probe their microenvironment by applying traction forces on the encountered substrate. The physical resistance of that substrate is the key component for platelet migration that induces further downstream signalling

Zusammenfassung

Hintergrund: Neben der entscheidenden Rolle in der primären Hämostase, gibt es zunehmend mehr Hinweise, dass Thrombozyten eine Schlüsselrolle in der Immunabwehr spielen. Thrombozyten gehören mit zu den ersten Zellen, die in der Entzündung oder bei Gefäßverletzungen aufzufinden sind. Diese Mikroumgebungen setzen eine Vielzahl von biochemischen – sowie biophysikalischen Stimuli frei, die die Thrombozytenmigration aktivieren und dirigieren. Autonome Thrombozytenmigration wurde zuvor mit großer Skepsis betrachtet und erst kürzlich von Gärtner et al. beschrieben. (Gaertner, Ahmad et al. 2017)

Das Transmembranprotein $\alpha_{IIb}\beta_3$ ist das am häufigsten vorkommende Integrin auf der Plasmamembran der Thrombozyten und verbindet extrazelluläre Stimuli mit dem Innenleben der Thrombozyten. Es spielt eine grundlegende Rolle für die Mechanotransduktion und ermöglicht es den Thrombozyten, ihre Mikroumgebung physikalisch zu prüfen. Wenn Aktomyosin abhängige Zugkräfte den Substratwiderstand überwinden, beginnen Thrombozyten zu wandern.

Durch diese Studie soll eine neuartige, bildbasierte Methode zur Analyse der Thrombozytenmigration etabliert werden, die es uns ermöglicht, die an diesem Prozess involvierten molekularen Kräfte zu quantifizieren.

Ergebnisse: Wir konnten eine neuartige Methode zur Analyse der Thrombozytenmigration entwickeln, bei der wir den Substratwiderstand kontrollieren und individuelle Integrinvermittelte Kräfte in pN messen. Der Substratwiderstand sowie der Grad der Integrinaktivierung sind entscheidende Komponenten für die autonome Thrombozytenmigration. Unter physiologischen Bedingungen (Ca^{2+} , Mg^{2+} , ADP und TXA_2) wandern Thrombozyten auf Oberflächen mit einem Substratwiderstand von ≈ 160 pN, während ein zu niedriger (≤ 55 pN) oder zu hoher Substratwiderstand (> 160 pN) zur Verminderung des Großteils wandernder Thrombozyten führt. Die extrazelluläre Integrinaktivierung bedingt jedoch eine signifikante Veränderung der Thrombozytenfunktion und insbesondere des Migrationsverhaltens.

Neben der zentralen Rolle der Integrine als Oberflächenrezeptoren, haben die pharmakologische Blockade des kontraktilen Apparates sowie der mechanosensitiven Kanäle in der Plasmamembran einen signifikanten Effekt auf die Thrombozytenfunktion. Durch die

Hemmung des Myosin IIa kommt es zur Verminderung der Thrombozytenmigration auf Oberflächen mit hohem Substratwiderstand (55pN; 160 pN), während Thrombozyten auf niedrigen (23pN) - und intermediären (43pN) Substratwiderständen in einer Myosin unabhängigen Art und Weise migrieren. Ein wesentlicher Bestandteil Aktomyosin abhängiger Kontraktion ist der Ca^{2+} Einstrom in die Zelle, bedingt durch den mechanosensitiven Pieszo1 Kanal. Eine Blockade durch GsMTx4 bedingt eine signifikante Reduktion der Migration und liefert Hinweise darauf, dass diese mechanosensitiven Ionenkanäle eine entscheidende Rolle für die Thrombozytenmigration spielen.

Schlussfolgerung: Durch die vorliegende Arbeit konnten der Substratwiderstand, das Transmembranintegrin $\alpha_{\text{IIb}}\beta_3$ sowie der kontraktile Apparat als wesentliche Bestandteile der Thrombozyten - Mechanobiologie identifiziert werden. Wenn die Zugkräfte den Substratwiderstand überwinden, bilden Thrombozyten permanente Lamellipodien, polarisieren und wandern.

Folglich zeigt diese Arbeit, dass Thrombozyten Zugkräfte auf das vorgefundene Substrat ausüben und ihre Mikroumgebung dadurch mechanisch prüfen. Der physikalische Widerstand des Substrats ist die Schlüsselkomponente für die Thrombozytenmigration, die eine nachgeschaltete Signalweitergabe induziert.

6 Bibliography

- Abramowitz, M. and Davidson, M.W. (2020): Microscopy resource center, Website.
URL: <http://www.olympus-lifescience.com/en/microscope-resource/primer/flash/>
- Adair, B. D. and M. Yeager (2002). "Three-dimensional model of the human platelet integrin alpha IIb beta 3 based on electron cryomicroscopy and x-ray crystallography." Proc Natl Acad Sci U S A **99**(22): 14059-14064.
- Arnaout, M. A., S. L. Goodman and J.-P. Xiong (2007). "Structure and mechanics of integrin-based cell adhesion." Current Opinion in Cell Biology **19**(5): 495-507.
- Arnaout, M. A., B. Mahalingam and J. P. Xiong (2005). "Integrin structure, allostery, and bidirectional signaling." Annu Rev Cell Dev Biol **21**: 381-410.
- Askari, J. A., P. A. Buckley, A. P. Mould and M. J. Humphries (2009). "Linking integrin conformation to function." Journal of Cell Science **122**(2): 165.
- Bae, C., F. Sachs and P. A. Gottlieb (2011). "The mechanosensitive ion channel Piezo1 is inhibited by the peptide GsMTx4." Biochemistry **50**(29): 6295-6300.
- Balasubramanian, V. and S. M. Slack (2002). "The effect of fluid shear and co-adsorbed proteins on the stability of immobilized fibrinogen and subsequent platelet interactions." Journal of Biomaterials Science, Polymer Edition **13**(5): 543-561.
- Barnhart, E. L., K.-C. Lee, K. Keren, A. Mogilner and J. A. Theriot (2011). "An Adhesion-Dependent Switch between Mechanisms That Determine Motile Cell Shape." PLOS Biology **9**(5): e1001059.
- Baumgartner, H. R. (1977). "Platelet interaction with collagen fibrils in flowing blood. I. Reaction of human platelets with alpha chymotrypsin-digested subendothelium." Thromb Haemost **37**(1): 1-16.
- Beer, J. H., K. T. Springer and B. S. Coller (1992). "Immobilized Arg-Gly-Asp (RGD) peptides of varying lengths as structural probes of the platelet glycoprotein IIb/IIIa receptor." Blood **79**(1): 117-128.
- Beglova, N., S. C. Blacklow, J. Takagi and T. A. Springer (2002). "Cysteine-rich module structure reveals a fulcrum for integrin rearrangement upon activation." Nat Struct Biol **9**(4): 282-287.
- Bennett, J. S. (1996). "Structural biology of glycoprotein IIb-IIIa." Trends Cardiovasc Med **6**(1): 31-36.

- Bennett, J. S. (2001). "Platelet-fibrinogen interactions." Ann N Y Acad Sci **936**: 340-354.
- Bennett, J. S. (2005). "Structure and function of the platelet integrin α IIb β 3." The Journal of Clinical Investigation **115**(12): 3363-3369.
- Bennett, J. S., B. W. Berger and P. C. Billings (2009). "The structure and function of platelet integrins." J Thromb Haemost **7 Suppl 1**: 200-205.
- Berger, G., J. M. Masse and E. M. Cramer (1996). "Alpha-granule membrane mirrors the platelet plasma membrane and contains the glycoproteins Ib, IX, and V." Blood **87**(4): 1385-1395.
- Bergmeier, W., C. L. Piffath, T. Goerge, S. M. Cifuni, Z. M. Ruggeri, J. Ware and D. D. Wagner (2006). "The role of platelet adhesion receptor GPIIb/IIIa far exceeds that of its main ligand, von Willebrand factor, in arterial thrombosis." Proc Natl Acad Sci U S A **103**(45): 16900-16905.
- Biosciences, B. (2018). "Fluorescence spectral viewer: FITC.", Website
URL: <https://www.bdbiosciences.com/en-us/applications/research-applications/multicolor-flow-cytometry/product-selection-tools/spectrum-viewer>
- Biosciences, B. (2018). "Fluorescence spectral viewer: Cy3.", Website
URL: <https://www.bdbiosciences.com/en-us/applications/research-applications/multicolor-flow-cytometry/product-selection-tools/spectrum-viewer>
- Blair, P. and R. Flaumenhaft (2009). "Platelet alpha-granules: basic biology and clinical correlates." Blood Rev **23**(4): 177-189.
- Blakely, B. L., C. E. Dumelin, B. Trappmann, L. M. McGregor, C. K. Choi, P. C. Anthony, V. K. Duesterberg, B. M. Baker, S. M. Block, D. R. Liu and C. S. Chen (2014). "A DNA-based molecular probe for optically reporting cellular traction forces." Nature Methods **11**: 1229.
- Bland, J. M. and D. G. Altman (2009). "Analysis of continuous data from small samples." BMJ **338**: a3166.
- Boarder, M. R. and S. M. O. Hourani (1998). "The regulation of vascular function by P2 receptors: multiple sites and multiple receptors." Trends in Pharmacological Sciences **19**(3): 99-107.
- Bowman, C. L., P. A. Gottlieb, T. M. Suchyna, Y. K. Murphy and F. Sachs (2007). "Mechanosensitive ion channels and the peptide inhibitor GsMTx-4: history, properties, mechanisms and pharmacology." Toxicon **49**(2): 249-270.
- Brass, L. F., K. M. Wannemacher, P. Ma and T. J. Stalker (2011). "Regulating thrombus growth and stability to achieve an optimal response to injury." Journal of Thrombosis and Haemostasis **9**(s1): 66-75.

- Brass, L. F., L. Zhu and T. J. Stalker (2005). "Minding the gaps to promote thrombus growth and stability." Journal of Clinical Investigation **115**(12): 3385-3392.
- Calderwood, D. A., B. Yan, J. M. de Pereda, B. G. Alvarez, Y. Fujioka, R. C. Liddington and M. H. Ginsberg (2002). "The phosphotyrosine binding-like domain of talin activates integrins." J Biol Chem **277**(24): 21749-21758.
- Calderwood, D. A., R. Zent, R. Grant, D. J. Rees, R. O. Hynes and M. H. Ginsberg (1999). "The Talin head domain binds to integrin beta subunit cytoplasmic tails and regulates integrin activation." J Biol Chem **274**(40): 28071-28074.
- Carman, C. V. and T. A. Springer (2003). "Integrin avidity regulation: are changes in affinity and conformation underemphasized?" Current Opinion in Cell Biology **15**(5): 547-556.
- Carr, M. E., Jr. (2003). "Development of platelet contractile force as a research and clinical measure of platelet function." Cell Biochem Biophys **38**(1): 55-78.
- Carr, M. E., Jr. and S. L. Zekert (1991). "Measurement of platelet-mediated force development during plasma clot formation." Am J Med Sci **302**(1): 13-18.
- Chen, J., A. Salas and T. A. Springer (2003). "Bistable regulation of integrin adhesiveness by a bipolar metal ion cluster." Nat Struct Biol **10**(12): 995-1001.
- Chou, J., N. Mackman, G. Merrill-Skoloff, B. Pedersen, B. C. Furie and B. Furie (2004). "Hematopoietic cell-derived microparticle tissue factor contributes to fibrin formation during thrombus propagation." Blood **104**(10): 3190-3197.
- Ciciliano, J. C., R. Tran, Y. Sakurai and W. A. Lam (2014). "The Platelet and the Biophysical Microenvironment: Lessons from Cellular Mechanics." Thrombosis Research **133**(4): 532-537.
- Cierniewski, C. S., T. Byzova, M. Papierak, T. A. Haas, J. Niewiarowska, L. Zhang, M. Cieslak and E. F. Plow (1999). "Peptide Ligands Can Bind to Distinct Sites in Integrin α IIb β 3 and Elicit Different Functional Responses." Journal of Biological Chemistry **274**(24): 16923-16932.
- Clark, E. A. and J. S. Brugge (1995). "Integrins and signal transduction pathways: the road taken." Science **268**(5208): 233-239.
- Clemetson, K. J. and J. M. Clemetson (2001). "Platelet collagen receptors." Thromb Haemost **86**(1): 189-197.
- Coller, B. S. (2015). " α IIb β 3: structure and function." Journal of Thrombosis and Haemostasis **13**(S1): S17-S25.

- Coller, B. S. and S. J. Shattil (2008). "The GPIIb/IIIa (integrin α IIb β 3) odyssey: a technology-driven saga of a receptor with twists, turns, and even a bend." Blood **112**(8): 3011-3025.
- Coons, A. H., Creech, H.J., Jones R.N., Berliner, E. (1942). "The Demonstration of Pneumococcal Antigen in Tissues by the Use of Fluorescent Antibody." The Journal of Immunology **45**(3): 159.
- Coons, A. H. and M. H. Kaplan (1950). "Localization of antigen in tissue cells; improvements in a method for the detection of antigen by means of fluorescent antibody." J Exp Med **91**(1): 1-13.
- Cornelissen, I., D. Palmer, T. David, L. Wilsbacher, C. Concengco, P. Conley, A. Pandey and S. R. Coughlin (2010). "Roles and interactions among protease-activated receptors and P2ry12 in hemostasis and thrombosis." Proc Natl Acad Sci U S A **107**(43): 18605-18610.
- Coste, B., B. Xiao, J. S. Santos, R. Syeda, J. Grandl, K. S. Spencer, S. E. Kim, M. Schmidt, J. Mathur, A. E. Dubin, M. Montal and A. Patapoutian (2012). "Piezo proteins are pore-forming subunits of mechanically activated channels." Nature **483**(7388): 176-181.
- Coughlin, S. R. (2005). "Protease-activated receptors in hemostasis, thrombosis and vascular biology." J Thromb Haemost **3**(8): 1800-1814.
- Craig, D., M. Gao, K. Schulten and V. Vogel (2004). "Structural Insights into How the MIDAS Ion Stabilizes Integrin Binding to an RGD Peptide under Force." Structure **12**(11): 2049-2058.
- Critchley, D. R. (2009). "Biochemical and structural properties of the integrin-associated cytoskeletal protein talin." Annu Rev Biophys **38**: 235-254.
- Czapiga, M., J. L. Gao, A. Kirk and J. Lekstrom-Himes (2005). "Human platelets exhibit chemotaxis using functional N-formyl peptide receptors." Exp Hematol **33**(1): 73-84.
- D'Souza, S. E., M. H. Ginsberg, T. A. Burke and E. F. Plow (1990). "The ligand binding site of the platelet integrin receptor GPIIb-IIIa is proximal to the second calcium binding domain of its alpha subunit." J Biol Chem **265**(6): 3440-3446.
- Davey, M. G. and E. F. LÜScher (1967). "Actions of Thrombin and Other Coagulant and Proteolytic Enzymes on Blood Platelets." Nature **216**: 857.
- Davi, G. and C. Patrono (2007). "Platelet activation and atherothrombosis." N Engl J Med **357**(24): 2482-2494.
- De Clerck, F. (1986). "Blood platelets in human essential hypertension." Agents Actions **18**(5-6): 563-580.

- De Clerck, F., B. Xhonneux, J. Leysen and P. A. Janssen (1984). "Evidence for functional 5-HT₂ receptor sites on human blood platelets." Biochem Pharmacol **33**(17): 2807-2811.
- Diener Plasma-surface-technology (2020): Zepto Flyer, Website
URL: https://d3krux2s64mzgx.cloudfront.net/fileadmin/user_upload/Downloads/Niederdruckplasma/Zepto.pdf
- Doggett, T. A., G. Girdhar, A. Lawshe, D. W. Schmidtke, I. J. Laurenzi, S. L. Diamond and T. G. Diacovo (2002). "Selectin-like kinetics and biomechanics promote rapid platelet adhesion in flow: the GPIb(alpha)-vWF tether bond." Biophys J **83**(1): 194-205.
- Dubois, C., L. Panicot-Dubois, G. Merrill-Skoloff, B. Furie and B. C. Furie (2006). "Glycoprotein VI-dependent and -independent pathways of thrombus formation in vivo." Blood **107**(10): 3902.
- Duperray, A., R. Berthier, E. Chagnon, J. Ryckewaert, M. Ginsberg, E. Plow, and G. Marguerie (1987). "Biosynthesis and processing of platelet GPIIb-IIIa in human megakaryocytes." The Journal of Cell Biology **104**(6): 1665-1673.
- Elbert, D. L. and J. A. Hubbell (1998). "Self-assembly and steric stabilization at heterogeneous, biological surfaces using adsorbing block copolymers." Chem Biol **5**(3): 177-183.
- Farrell, D. H., P. Thiagarajan, D. W. Chung and E. W. Davie (1992). "Role of fibrinogen alpha and gamma chain sites in platelet aggregation." Proceedings of the National Academy of Sciences **89**(22): 10729.
- Feng, D., J. A. Nagy, K. Pyne, H. F. Dvorak and A. M. Dvorak (1998). "Platelets Exit Venules by a Transcellular Pathway at Sites of F-Met Peptide-Induced Acute Inflammation in Guinea Pigs." International Archives of Allergy and Immunology **116**(3): 188-195.
- Fitzgerald, L. A. and D. R. Phillips (1985). "Calcium regulation of the platelet membrane glycoprotein IIb-IIIa complex." J Biol Chem **260**(20): 11366-11374.
- Fukata, M., M. Nakagawa and K. Kaibuchi (2003). "Roles of Rho-family GTPases in cell polarisation and directional migration." Current Opinion in Cell Biology **15**(5): 590-597.
- Gachet, C. (2006). "Regulation of platelet functions by P₂ receptors." Annu Rev Pharmacol Toxicol **46**: 277-300.
- Gachet, C. (2008). "P₂ receptors, platelet function and pharmacological implications." Thromb Haemost **99**(3): 466-472.
- Gaertner, F., Z. Ahmad, G. Rosenberger, S. Fan, L. Nicolai, B. Busch, G. Yavuz, M. Luckner, H. Ishikawa-Ankerhold, R. Hennel, A. Benechet, M. Lorenz, S. Chandraratne, I. Schubert, S. Helmer, B. Striednig, K. Stark, M. Janko, R. T. Bottcher, A. Verschoor, C. Leon, C. Gachet, T. Gudermann, Y. S. M. Mederos, Z. Pincus, M. Iannacone, R. Haas, G.

- Wanner, K. Lauber, M. Sixt and S. Massberg (2017). "Migrating Platelets Are Mechano-scavengers that Collect and Bundle Bacteria." *Cell* **171**(6): 1368-1382 e1323.
- Geiger, B., A. Bershadsky, R. Pankov and K. M. Yamada (2001). "Transmembrane crosstalk between the extracellular matrix--cytoskeleton crosstalk." *Nat Rev Mol Cell Biol* **2**(11): 793-805.
- Gibbins, J. M., M. Okuma, R. Farndale, M. Barnes and S. P. Watson (1997). "Glycoprotein VI is the collagen receptor in platelets which underlies tyrosine phosphorylation of the Fc receptor gamma-chain." *FEBS Lett* **413**(2): 255-259.
- Gingras, A. R., N. Bate, B. T. Goult, L. Hazelwood, I. Canestrelli, J. G. Grossmann, H. Liu, N. S. Putz, G. C. Roberts, N. Volkmann, D. Hanein, I. L. Barsukov and D. R. Critchley (2008). "The structure of the C-terminal actin-binding domain of talin." *Embo j* **27**(2): 458-469.
- Gingras, A. R., N. Bate, B. T. Goult, B. Patel, P. M. Kopp, J. Emsley, I. L. Barsukov, G. C. K. Roberts and D. R. Critchley (2010). "Central Region of Talin Has a Unique Fold That Binds Vinculin and Actin." *The Journal of Biological Chemistry* **285**(38): 29577-29587.
- Gleissner, C. A., P. von Hundelshausen and K. Ley (2008). "Platelet chemokines in vascular disease." *Arterioscler Thromb Vasc Biol* **28**(11): 1920-1927.
- Good, N. E., G. D. Winget, W. Winter, T. N. Connolly, S. Izawa and R. M. Singh (1966). "Hydrogen ion buffers for biological research." *Biochemistry* **5**(2): 467-477.
- Gupton, S. L. and C. M. Waterman-Storer (2006). "Spatiotemporal Feedback between Actomyosin and Focal-Adhesion Systems Optimizes Rapid Cell Migration." *Cell* **125**(7): 1361-1374.
- Hantgan, R. R., C. Paumi, M. Rocco and J. W. Weisel (1999). "Effects of ligand-mimetic peptides Arg-Gly-Asp-X (X = Phe, Trp, Ser) on alphaIIb beta3 integrin conformation and oligomerization." *Biochemistry* **38**(44): 14461-14474.
- Hartwig, J. H. (2013). Chapter 8 - The Platelet Cytoskeleton. *Platelets (Third Edition)*. A. D. Michelson, Academic Press: 145-168.
- Harvey, B. J., C. Perez and M. Levitus (2009). "DNA sequence-dependent enhancement of Cy3 fluorescence." *Photochem Photobiol Sci* **8**(8): 1105-1110.
- Hassock, S. R., M. X. Zhu, C. Trost, V. Flockerzi and K. S. Authi (2002). "Expression and role of TRPC proteins in human platelets: evidence that TRPC6 forms the store-independent calcium entry channel." *Blood* **100**(8): 2801.
- Herman, B. (1998). "Fluorescence Microscopy." *Current Protocols in Cell Biology* **00**(1): 4.2.1-4.2.10.

- Herzenberg, L. A., R. G. Sweet and L. A. Herzenberg (1976). "Fluorescence-activated Cell Sorting." Scientific American **234**(3): 108-118.
- Holmsen, H. and H. J. Weiss (1979). "Secretable storage pools in platelets." Annu Rev Med **30**: 119-134.
- Hu, D. D., C. A. White, S. Panzer-Knodle, J. D. Page, N. Nicholson and J. W. Smith (1999). "A new model of dual interacting ligand binding sites on integrin alphaIIb beta3." J Biol Chem **274**(8): 4633-4639.
- Hughes, P. E. and M. Pfaff (1998). "Integrin affinity modulation." Trends Cell Biol **8**(9): 359-364.
- Hynes, R. O. (1992). "Integrins: Versatility, modulation, and signaling in cell adhesion." Cell **69**(1): 11-25.
- Hynes, R. O. (2002). "Integrins: bidirectional, allosteric signaling machines." Cell **110**(6): 673-687.
- Italiano, J. E., P. Lecine, R. A. Shivdasani and J. H. Hartwig (1999). "Blood Platelets Are Assembled Principally at the Ends of Proplatelet Processes Produced by Differentiated Megakaryocytes." The Journal of Cell Biology **147**(6): 1299-1312.
- Jackson, S. P. (2007). "The growing complexity of platelet aggregation." Blood **109**(12): 5087-5095.
- Jackson, S. P. (2011). "Arterial thrombosis--insidious, unpredictable and deadly." Nat Med **17**(11): 1423-1436.
- Janesick, J. R., T. Elliott, S. Collins, M. M. Blouke and J. Freeman (1987). Scientific Charge-Coupled Devices, Optical Engineering 26(8), 268692.
- Janesick, J.R., (2001). Scientific Charge-Coupled Devices, J.R. Janesick, SPIE-The International Society for Optical Engineering, pp. 22-42.
- Jedlitschky, G., A. Greinacher and H. K. Kroemer (2012). "Transporters in human platelets: physiologic function and impact for pharmacotherapy." Blood **119**(15): 3394-3402.
- Jen, C. J. and L. V. McIntire (1982). "The structural properties and contractile force of a clot." Cell Motil **2**(5): 445-455.
- Jirouskova, M., J. K. Jaiswal and B. S. Coller (2007). "Ligand density dramatically affects integrin alpha IIb beta 3-mediated platelet signaling and spreading." Blood **109**(12): 5260-5269.

- Jiroušková, M., J. K. Jaiswal and B. S. Coller (2007). "Ligand density dramatically affects integrin α IIb β 3-mediated platelet signaling and spreading." Blood **109**(12): 5260.
- Jones, S., R. J. Evans and M. P. Mahaut-Smith (2014). " Ca^{2+} Influx through P2X1 Receptors Amplifies P2Y1 Receptor-Evoked Ca^{2+} Signaling and ADP-Evoked Platelet Aggregation." Molecular Pharmacology **86**(3): 243.
- Junt, T., H. Schulze, Z. Chen, S. Massberg, T. Goerge, A. Krueger, D. D. Wagner, T. Graf, J. E. Italiano, Jr., R. A. Shivdasani and U. H. von Andrian (2007). "Dynamic visualization of thrombopoiesis within bone marrow." Science **317**(5845): 1767-1770.
- Kahn, M. L., M. Nakanishi-Matsui, M. J. Shapiro, H. Ishihara and S. R. Coughlin (1999). "Protease-activated receptors 1 and 4 mediate activation of human platelets by thrombin." J Clin Invest **103**(6): 879-887.
- Kee, M. F., D. R. Myers, Y. Sakurai, W. A. Lam and Y. Qiu (2015). "Platelet mechanosensing of collagen matrices." PLoS One **10**(4): e0126624.
- Kenausis, G. L., J. Vörös, D. L. Elbert, N. Huang, R. Hofer, L. Ruiz-Taylor, M. Textor, J. A. Hubbell and N. D. Spencer (2000). "Poly(l-lysine)-g-Poly(ethylene glycol) Layers on Metal Oxide Surfaces: Attachment Mechanism and Effects of Polymer Architecture on Resistance to Protein Adsorption." The Journal of Physical Chemistry B **104**(14): 3298-3309.
- Keren, K., Z. Pincus, G. M. Allen, E. L. Barnhart, G. Marriott, A. Mogilner and J. A. Theriot (2008). "Mechanism of shape determination in motile cells." Nature **453**(7194): 475-480.
- Kieffer, N. and D. R. Phillips (1990). "Platelet Membrane Glycoproteins: Functions in Cellular Interactions." Annual Review of Cell Biology **6**(1): 329-357.
- Kim, C., F. Ye and M. H. Ginsberg (2011). "Regulation of Integrin Activation." Annual Review of Cell and Developmental Biology **27**(1): 321-345.
- Klinger, M. H. and W. Jelkmann (2002). "Role of blood platelets in infection and inflammation." J Interferon Cytokine Res **22**(9): 913-922.
- Klugerman, M. R. (1965). "Chemical and Physical Variables Affecting the Properties of Fluorescein Isothiocyanate and Its Protein Conjugates." The Journal of Immunology **95**(6): 1165.
- Konkle, B. A. (2011). "Acquired disorders of platelet function." Hematology Am Soc Hematol Educ Program **2011**: 391-396.
- Kononova, O., R. I. Litvinov, D. S. Blokhin, V. V. Klochkov, J. W. Weisel, J. S. Bennett and V. Barsegov (2017). "Mechanistic Basis for the Binding of RGD- and AGDV-Peptides to the Platelet Integrin α IIb β 3." Biochemistry **56**(13): 1932-1942.

- Kraemer, B. F., O. Borst, E. M. Gehring, T. Schoenberger, B. Urban, E. Ninci, P. Seizer, C. Schmidt, B. Bigalke, M. Koch, I. Martinovic, K. Daub, T. Merz, L. Schwanitz, K. Stellos, F. Fiesel, M. Schaller, F. Lang, M. Gawaz and S. Lindemann (2010). "PI3 kinase-dependent stimulation of platelet migration by stromal cell-derived factor 1 (SDF-1)." *J Mol Med (Berl)* **88**(12): 1277-1288.
- Kroll, M. H., J. D. Hellums, L. V. McIntire, A. I. Schafer and J. L. Moake (1996). "Platelets and shear stress." *Blood* **88**(5): 1525.
- Kroll, M. H. and A. I. Schafer (1989). "Biochemical mechanisms of platelet activation." *Blood* **74**(4): 1181-1195.
- Kunapuli, S. P. (1998). "Multiple P2 receptor subtypes on platelets: a new interpretation of their function." *Trends Pharmacol Sci* **19**(10): 391-394.
- Lam, W. A., O. Chaudhuri, A. Crow, K. D. Webster, T.-D. Li, A. Kita, J. Huang and D. A. Fletcher (2011). "Mechanics and contraction dynamics of single platelets and implications for clot stiffening." *Nature materials* **10**(1): 61-66.
- Lämmermann, T., B. L. Bader, S. J. Monkley, T. Worbs, R. Wedlich-Söldner, K. Hirsch, M. Keller, R. Förster, D. R. Critchley, R. Fässler and M. Sixt (2008). "Rapid leukocyte migration by integrin-independent flowing and squeezing." *Nature* **453**(7191): 51-55.
- Lauffenburger, D. A. and A. F. Horwitz (1996). "Cell migration: a physically integrated molecular process." *Cell* **84**(3): 359-369.
- Lee, J. O., P. Rieu, M. A. Arnaout and R. Liddington (1995). "Crystal structure of the A domain from the alpha subunit of integrin CR3 (CD11b/CD18)." *Cell* **80**(4): 631-638.
- Léon, C., A. Eckly, B. Hechler, B. Aleil, M. Freund, C. Ravanat, M. Jourdain, C. Nonne, J. Weber, R. Tiedt, M.-P. Gratacap, S. Severin, J.-P. Cazenave, F. Lanza, R. Skoda and C. Gachet (2007). "Megakaryocyte-restricted α MYH9 inactivation dramatically affects hemostasis while preserving platelet aggregation and secretion." *Blood* **110**(9): 3183.
- Li, N., N. H. Wallen, M. Ladjevardi and P. Hjemdahl (1997). "Effects of serotonin on platelet activation in whole blood." *Blood Coagul Fibrinolysis* **8**(8): 517-523.
- Li, Z., M. K. Delaney, K. A. O'Brien and X. Du (2010). "Signaling during platelet adhesion and activation." *Arterioscler Thromb Vasc Biol* **30**(12): 2341-2349.
- Liang, X. M., S. J. Han, J.-A. Reems, D. Gao and N. J. Sniadecki (2010). "Platelet retraction force measurements using flexible post force sensors." *Lab on a Chip* **10**(8): 991-998.
- Lichtman, J. W. and J. A. Conchello (2005). "Fluorescence microscopy." *Nat Methods* **2**(12): 910-919.

- Liston, E. M., L. Martinu and M. R. Wertheimer (1993). "Plasma surface modification of polymers for improved adhesion: a critical review." Journal of Adhesion Science and Technology **7**(10): 1091-1127.
- Litvinov, R. I., D. H. Farrell, J. W. Weisel and J. S. Bennett (2016). "The Platelet Integrin α IIb β 3 Differentially Interacts with Fibrin Versus Fibrinogen." J Biol Chem **291**(15): 7858-7867.
- Lowenhaupt, R. W., M. A. Miller and H. I. Glueck (1973). "Platelet migration and chemotaxis demonstrated in vitro." Thrombosis Research **3**(5): 477-487.
- Luo, B. H., C. V. Carman and T. A. Springer (2007). "Structural basis of integrin regulation and signaling." Annu Rev Immunol **25**: 619-647.
- Ma, Y. Q., J. Qin and E. F. Plow (2007). "Platelet integrin α IIb β 3: activation mechanisms." Journal of Thrombosis and Haemostasis **5**(7): 1345-1352.
- Maeda, H., N. Ishida, H. Kawauchi and K. Tsujimura (1969). "Reaction of fluorescein-isothiocyanate with proteins and amino acids. I. Covalent and non-covalent binding of fluorescein-isothiocyanate and fluorescein to proteins." J Biochem **65**(5): 777-783.
- Mahaut-Smith, M. P., S. Jones and R. J. Evans (2011). "The P2X1 receptor and platelet function." Purinergic Signalling **7**(3): 341-356.
- Massberg, S., S. Eisenmenger, G. Enders, F. Krombach and K. Messmer (1998). "Quantitative analysis of small intestinal microcirculation in the mouse." Res Exp Med (Berl) **198**(1): 23-35.
- Massberg, S., M. Gawaz, S. Gruner, V. Schulte, I. Konrad, D. Zohlhofer, U. Heinzmann and B. Nieswandt (2003). "A crucial role of glycoprotein VI for platelet recruitment to the injured arterial wall in vivo." J Exp Med **197**(1): 41-49.
- May, A. E., P. Seizer and M. Gawaz (2008). "Platelets: inflammatory firebugs of vascular walls." Arterioscler Thromb Vasc Biol **28**(3): s5-10.
- McNicol, A. and S. J. Israels (1999). "Platelet dense granules: structure, function and implications for haemostasis." Thromb Res **95**(1): 1-18.
- Mehrbod, M., S. Trisno and Mohammad R. K. Mofrad (2013). "On the Activation of Integrin α IIb β 3: Outside-in and Inside-out Pathways." Biophysical Journal **105**(6): 1304-1315.
- Meijering, E., O. Dzyubachyk and I. Smal (2012). "Methods for cell and particle tracking." Methods Enzymol **504**: 183-200.

- Mody, N. A. and M. R. King (2008). "Platelet Adhesive Dynamics. Part II: High Shear-Induced Transient Aggregation via GPIIb/IIIa-vWF-GPIIb/IIIa Bridging." Biophysical Journal **95**(5): 2556-2574.
- Morimatsu, M., A. H. Mekhdjian, A. S. Adhikari and A. R. Dunn (2013). "Molecular Tension Sensors Report Forces Generated by Single Integrin Molecules in Living Cells." Nano Letters **13**(9): 3985-3989.
- Moroi, M., S. M. Jung, M. Okuma and K. Shinmyozu (1989). "A patient with platelets deficient in glycoprotein VI that lack both collagen-induced aggregation and adhesion." Journal of Clinical Investigation **84**(5): 1440-1445.
- Mory, A., S. W. Feigelson, N. Yarali, S. S. Kilic, G. I. Bayhan, R. Gershoni-Baruch, A. Etzioni and R. Alon (2008). "Kindlin-3: a new gene involved in the pathogenesis of LAD-III." Blood **112**(6): 2591.
- Moser, M., B. Nieswandt, S. Ussar, M. Pozgajova and R. Fassler (2008). "Kindlin-3 is essential for integrin activation and platelet aggregation." Nat Med **14**(3): 325-330.
- Mould, A. P., S. J. Barton, J. A. Askari, S. E. Craig and M. J. Humphries (2003). "Role of ADMIDAS cation-binding site in ligand recognition by integrin alpha 5 beta 1." J Biol Chem **278**(51): 51622-51629.
- Moy, V. T., E. L. Florin and H. E. Gaub (1994). "Intermolecular forces and energies between ligands and receptors." Science **266**(5183): 257-259.
- Mustard, J. F., R. L. Kinlough-Rathbone and M. A. Packham (1989). "Isolation of human platelets from plasma by centrifugation and washing." Methods Enzymol **169**: 3-11.
- Myers, D. R., Y. Qiu, M. E. Fay, M. Tennenbaum, D. Chester, J. Cuadrado, Y. Sakurai, J. Baek, R. Tran, J. C. Ciciliano, B. Ahn, R. G. Mannino, S. T. Bunting, C. Bennett, M. Briones, A. Fernandez-Nieves, M. L. Smith, A. C. Brown, T. Sulchek and W. A. Lam (2017). "Single-platelet nanomechanics measured by high-throughput cytometry." Nat Mater **16**(2): 230-235.
- Nakamura, L., K. Sandrock-Lang, C. Speckmann, T. Vraetz, M. Bührle, S. Ehl, J. W. M. Heemskerk and B. Zieger (2013). "Platelet secretion defect in a patient with stromal interaction molecule 1 deficiency." Blood **122**(22): 3696.
- Ni, H., C. V. Denis, S. Subbarao, J. L. Degen, T. N. Sato, R. O. Hynes and D. D. Wagner (2000). "Persistence of platelet thrombus formation in arterioles of mice lacking both von Willebrand factor and fibrinogen." J Clin Invest **106**(3): 385-392.
- Ni, H., P. S. Yuen, J. M. Papalia, J. E. Trevithick, T. Sakai, R. Fassler, R. O. Hynes and D. D. Wagner (2003). "Plasma fibronectin promotes thrombus growth and stability in injured arterioles." Proc Natl Acad Sci U S A **100**(5): 2415-2419.

- Nieswandt, B., B. Aktas, A. Moers and U. J. Sachs (2005). "Platelets in atherothrombosis: lessons from mouse models." *J Thromb Haemost* **3**(8): 1725-1736.
- Nieswandt, B., W. Bergmeier, V. Schulte, K. Rackebrandt, J. E. Gessner and H. Zirngibl (2000). "Expression and function of the mouse collagen receptor glycoprotein VI is strictly dependent on its association with the FcRgamma chain." *J Biol Chem* **275**(31): 23998-24002.
- Nieswandt, B., M. Moser, I. Pleines, D. Varga-Szabo, S. Monkley, D. Critchley and R. Fassler (2007). "Loss of talin1 in platelets abrogates integrin activation, platelet aggregation, and thrombus formation in vitro and in vivo." *J Exp Med* **204**(13): 3113-3118.
- Niiya, K., E. Hodson, R. Bader, V. Byers-Ward, J. A. Koziol, E. F. Plow and Z. M. Ruggeri (1987). "Increased surface expression of the membrane glycoprotein IIb/IIIa complex induced by platelet activation. Relationship to the binding of fibrinogen and platelet aggregation." *Blood* **70**(2): 475-483.
- Nishida, N., C. Xie, M. Shimaoka, Y. Cheng, T. Walz and T. A. Springer (2006). "Activation of leukocyte beta2 integrins by conversion from bent to extended conformations." *Immunity* **25**(4): 583-594.
- O'Neill, K., N. Aghaeepour, J. Spidlen and R. Brinkman (2013). "Flow cytometry bioinformatics." *PLoS computational biology* **9**(12): e1003365-e1003365.
- Offermanns, S. (2006). "Activation of platelet function through G protein-coupled receptors." *Circ Res* **99**(12): 1293-1304.
- Ono, A., E. Westein, S. Hsiao, W. S. Nesbitt, J. R. Hamilton, S. M. Schoenwaelder and S. P. Jackson (2008). "Identification of a fibrin-independent platelet contractile mechanism regulating primary hemostasis and thrombus growth." *Blood* **112**(1): 90-99.
- Oria, R., T. Wiegand, J. Escribano, A. Elosegui-Artola, J. J. Uriarte, C. Moreno-Pulido, I. Platzman, P. Delcanale, L. Albertazzi, D. Navajas, X. Trepas, J. M. García-Aznar, E. A. Cavalcanti-Adam and P. Roca-Cusachs (2017). "Force loading explains spatial sensing of ligands by cells." *Nature* **552**(7684): 219-224.
- Palecek, S. P., J. C. Loftus, M. H. Ginsberg, D. A. Lauffenburger and A. F. Horwitz (1997). "Integrin-ligand binding properties govern cell migration speed through cell-substratum adhesiveness." *Nature* **385**(6616): 537-540.
- Pawley, J.B. (2006): Handbook of biological confocal microscopy, J.B. Pawley(Ed.), 3 Aufl., Springer Science+Buisness Media, LCC pp.918-931.
- Perfetto, S. P., P. K. Chattopadhyay and M. Roederer (2004). "Seventeen-colour flow cytometry: unravelling the immune system." *Nature Reviews Immunology* **4**(8): 648-655.

- Phillips, D. R. and A. K. Baughan (1983). "Fibrinogen binding to human platelet plasma membranes. Identification of two steps requiring divalent cations." J Biol Chem **258**(17): 10240-10246.
- Pincus, Z. and J. A. Theriot (2007). "Comparison of quantitative methods for cell-shape analysis." J Microsc **227**(Pt 2): 140-156.
- Pitchford, S. C., S. Momi, S. Baglioni, L. Casali, S. Giannini, R. Rossi, C. P. Page and P. Gresele (2008). "Allergen induces the migration of platelets to lung tissue in allergic asthma." Am J Respir Crit Care Med **177**(6): 604-612.
- Pollard, T. D., K. Fujiwara, R. Handin and G. Weiss (1977). "CONTRACTILE PROTEINS IN PLATELET ACTIVATION AND CONTRACTION*." Annals of the New York Academy of Sciences **283**(1): 218-236.
- Puklin-Faucher, E., M. Gao, K. Schulten and V. Vogel (2006). "How the headpiece hinge angle is opened: New insights into the dynamics of integrin activation." J Cell Biol **175**(2): 349-360.
- Puklin-Faucher, E. and M. P. Sheetz (2009). "The mechanical integrin cycle." J Cell Sci **122**(Pt 2): 179-186.
- Qiu, Y., A. C. Brown, D. R. Myers, Y. Sakurai, R. G. Mannino, R. Tran, B. Ahn, E. T. Hardy, M. F. Kee, S. Kumar, G. Bao, T. H. Barker and W. A. Lam (2014). "Platelet mechanosensing of substrate stiffness during clot formation mediates adhesion, spreading, and activation." Proceedings of the National Academy of Sciences of the United States of America **111**(40): 14430-14435.
- Qiu, Y., J. Ciciliano, D. R. Myers, R. Tran and W. A. Lam (2015). "Platelets and physics: How platelets “feel” and respond to their mechanical microenvironment." Blood Reviews **29**(6): 377-386.
- Reichmann, J. (2017). "Handbook of optical filters for fluorescence microscopy." Website, URL: <http://www.chroma.com/resources-support/downloads/filter-handbook>
- Reid, G., P. Wielinga, N. Zelcer, I. van der Heijden, A. Kuil, M. de Haas, J. Wijnholds and P. Borst (2003). "The human multidrug resistance protein MRP4 functions as a prostaglandin efflux transporter and is inhibited by nonsteroidal antiinflammatory drugs." Proc Natl Acad Sci U S A **100**(16): 9244-9249.
- Riggs, J. L., R. J. Seiwald, J. H. Burckhalter, C. M. Downs and T. G. Metcalf (1958). "Isothiocyanate Compounds as Fluorescent Labeling Agents for Immune Serum." The American Journal of Pathology **34**(6): 1081-1097.
- Rius, M., W. F. Thon, D. Keppler and A. T. Nies (2005). "Prostanoid transport by multidrug resistance protein 4 (MRP4/ABCC4) localized in tissues of the human urogenital tract." J Urol **174**(6): 2409-2414.

- Ruggeri, Z. M. (1997). "Mechanisms initiating platelet thrombus formation." Thromb Haemost **78**(1): 611-616.
- Ruggeri, Z. M. (2002). "Platelets in atherothrombosis." Nat Med **8**(11): 1227-1234.
- Ruggeri, Z. M. (2007). "The role of von Willebrand factor in thrombus formation." Thromb Res **120 Suppl 1**: S5-9.
- Ruoslahti, E. (1996). "RGD and other recognition sequences for integrins." Annu Rev Cell Dev Biol **12**: 697-715.
- Ruoslahti, E. and M. D. Pierschbacher (1986). "Arg-Gly-Asp: a versatile cell recognition signal." Cell **44**(4): 517-518.
- Sabnis, R. W. (2015). Fluorescein-5-isothiocyanate (FITC). Handbook of Fluorescent Dyes and Probes: 219-223.
- Sakariassen, K. S., P. F. Nievelstein, B. S. Coller and J. J. Sixma (1986). "The role of platelet membrane glycoproteins Ib and IIb-IIIa in platelet adherence to human artery subendothelium." Br J Haematol **63**(4): 681-691.
- Sanborn, M. E., B. K. Connolly, K. Gurunathan and M. Levitus (2007). "Fluorescence properties and photophysics of the sulfoindocyanine Cy3 linked covalently to DNA." J Phys Chem B **111**(37): 11064-11074.
- Sanchez-Cortes, J. and M. Mrksich (2009). "The platelet integrin α IIb β 3 binds to the RGD and AGD motifs in fibrinogen." Chem Biol **16**(9): 990-1000.
- Santoro, S. A. and W. J. Lawing, Jr. (1987). "Competition for related but nonidentical binding sites on the glycoprotein IIb-IIIa complex by peptides derived from platelet adhesive proteins." Cell **48**(5): 867-873.
- Savage, B., F. Almus-Jacobs and Z. M. Ruggeri (1998). "Specific synergy of multiple substrate-receptor interactions in platelet thrombus formation under flow." Cell **94**(5): 657-666.
- Savage, B., E. Saldivar and Z. M. Ruggeri (1996). "Initiation of platelet adhesion by arrest onto fibrinogen or translocation on von Willebrand factor." Cell **84**(2): 289-297.
- Schindelin, J., I. Arganda-Carreras, E. Frise, V. Kaynig, M. Longair, T. Pietzsch, S. Preibisch, C. Rueden, S. Saalfeld, B. Schmid, J. Y. Tinevez, D. J. White, V. Hartenstein, K. Eliceiri, P. Tomancak and A. Cardona (2012). "Fiji: an open-source platform for biological-image analysis." Nat Methods **9**(7): 676-682.

- Schmidt, E.-M., P. Münzer, O. Borst, B. F. Kraemer, E. Schmid, B. Urban, S. Lindemann, P. Ruth, M. Gawaz and F. Lang (2011). "Ion channels in the regulation of platelet migration." Biochemical and Biophysical Research Communications **415**(1): 54-60.
- Schmidt, E. M., B. F. Kraemer, O. Borst, P. Münzer, T. Schönberger, C. Schmidt, C. Leibrock, S. T. Towhid, P. Seizer, D. Kuhl, C. Stournaras, S. Lindemann, M. Gawaz and F. Lang (2012). "SGK1 Sensitivity of Platelet Migration." Cellular Physiology and Biochemistry **30**(1): 259-268.
- Schwartz, M. A., M. D. Schaller and M. H. Ginsberg (1995). "Integrins: Emerging Paradigms of Signal Transduction." Annual Review of Cell and Developmental Biology **11**(1): 549-599.
- Schwarz Henriques, S., R. Sandmann, A. Strate and S. Koster (2012). "Force field evolution during human blood platelet activation." J Cell Sci **125**(Pt 16): 3914-3920.
- Semple, J. W., J. E. Italiano, Jr. and J. Freedman (2011). "Platelets and the immune continuum." Nat Rev Immunol **11**(4): 264-274.
- Shattil, S. J., C. Kim and M. H. Ginsberg (2010). "The final steps of integrin activation: the end game." Nat Rev Mol Cell Biol **11**(4): 288-300.
- Sheriff, J., D. Bluestein, G. Girdhar and J. Jesty (2010). "High-shear stress sensitizes platelets to subsequent low-shear conditions." Ann Biomed Eng **38**(4): 1442-1450.
- Shimaoka, M., J. Takagi and T. A. Springer (2002). "Conformational regulation of integrin structure and function." Annu Rev Biophys Biomol Struct **31**: 485-516.
- Shimaoka, M., T. Xiao, J. H. Liu, Y. Yang, Y. Dong, C. D. Jun, A. McCormack, R. Zhang, A. Joachimiak, J. Takagi, J. H. Wang and T. A. Springer (2003). "Structures of the alpha L I domain and its complex with ICAM-1 reveal a shape-shifting pathway for integrin regulation." Cell **112**(1): 99-111.
- Smith, J. W., R. S. Piotrowicz and D. Mathis (1994). "A mechanism for divalent cation regulation of beta 3-integrins." J Biol Chem **269**(2): 960-967.
- Smyth, S. S., E. D. Reis, H. Väänänen, W. Zhang and B. S. Coller (2001). "Variable protection of β 3-integrin-deficient mice from thrombosis initiated by different mechanisms." Blood **98**(4): 1055.
- Springer, T. A. and J. H. Wang (2004). "The three-dimensional structure of integrins and their ligands, and conformational regulation of cell adhesion." Adv Protein Chem **68**: 29-63.
- Springer, T. A., J. Zhu and T. Xiao (2008). "Structural basis for distinctive recognition of fibrinogen gammaC peptide by the platelet integrin α IIb β 3." J Cell Biol **182**(4): 791-800.

- Stabley, D. R., C. Jurchenko, S. S. Marshall and K. S. Salaita (2011). "Visualizing mechanical tension across membrane receptors with a fluorescent sensor." *Nat Methods* **9**(1): 64-67.
- Stenberg, P. E., R. P. McEver, M. A. Shuman, Y. V. Jacques and D. F. Bainton (1985). "A platelet alpha-granule membrane protein (GMP-140) is expressed on the plasma membrane after activation." *J Cell Biol* **101**(3): 880-886.
- Stephens, D. J. and V. J. Allan (2003). "Light Microscopy Techniques for Live Cell Imaging." *Science* **300**(5616): 82.
- Tadokoro, S., S. J. Shattil, K. Eto, V. Tai, R. C. Liddington, J. M. de Pereda, M. H. Ginsberg and D. A. Calderwood (2003). "Talin Binding to Integrin β Tails: A Final Common Step in Integrin Activation." *Science* **302**(5642): 103.
- Takagi, J., B. M. Petre, T. Walz and T. A. Springer (2002). "Global conformational rearrangements in integrin extracellular domains in outside-in and inside-out signaling." *Cell* **110**(5): 599-511.
- Tozer, E. C., R. C. Liddington, M. J. Sutcliffe, A. H. Smeeton and J. C. Loftus (1996). "Ligand Binding to Integrin α Ib β 3 Is Dependent on a MIDAS-like Domain in the β 3 Subunit." *Journal of Biological Chemistry* **271**(36): 21978-21984.
- Ussar, S., H. V. Wang, S. Linder, R. Fassler and M. Moser (2006). "The Kindlins: subcellular localization and expression during murine development." *Exp Cell Res* **312**(16): 3142-3151.
- Valdramidou, D., M. J. Humphries and A. P. Mould (2008). "Distinct roles of beta1 metal ion-dependent adhesion site (MIDAS), adjacent to MIDAS (ADMIDAS), and ligand-associated metal-binding site (LIMBS) cation-binding sites in ligand recognition by integrin alpha2beta1." *J Biol Chem* **283**(47): 32704-32714.
- Vanhoutte, P. M. and R. A. Cohen (1983). "The elusory role of serotonin in vascular function and disease." *Biochem Pharmacol* **32**(24): 3671-3674.
- Varga-Szabo, D., A. Braun, C. Kleinschnitz, M. Bender, I. Pleines, M. Pham, T. Renné, G. Stoll and B. Nieswandt (2008). "The calcium sensor STIM1 is an essential mediator of arterial thrombosis and ischemic brain infarction." *The Journal of Experimental Medicine* **205**(7): 1583.
- Varga-Szabo, D., I. Pleines and B. Nieswandt (2008). "Cell adhesion mechanisms in platelets." *Arterioscler Thromb Vasc Biol* **28**(3): 403-412.
- Vorchheimer, D. A., J. J. Badimon and V. Fuster (1999). "Platelet glycoprotein IIb/IIIa receptor antagonists in cardiovascular disease." *Jama* **281**(15): 1407-1414.

- Wagner, C. L., M. A. Mascelli, D. S. Neblock, H. F. Weisman, B. S. Coller and R. E. Jordan (1996). "Analysis of GPIIb/IIIa receptor number by quantification of 7E3 binding to human platelets." Blood **88**(3): 907-914.
- Wang, X. and T. Ha (2013). "Defining single molecular forces required to activate integrin and notch signaling." Science **340**(6135): 991-994.
- Wang, X., J. Sun, Q. Xu, F. Chowdhury, M. Roein-Peikar, Y. Wang and T. Ha (2015). "Integrin Molecular Tension within Motile Focal Adhesions." Biophys J **109**(11): 2259-2267.
- Wang, Y., D. N. LeVine, M. Gannon, Y. Zhao, A. Sarkar, B. Hoch and X. Wang (2018). "Force-activatable biosensor enables single platelet force mapping directly by fluorescence imaging." Biosensors & bioelectronics **100**: 192-200.
- Wegener, K. L., A. W. Partridge, J. Han, A. R. Pickford, R. C. Liddington, M. H. Ginsberg and I. D. Campbell (2007). "Structural basis of integrin activation by talin." Cell **128**(1): 171-182.
- Weisel, J. W., C. Nagaswami, G. Vilaire and J. S. Bennett (1992). "Examination of the platelet membrane glycoprotein IIb-IIIa complex and its interaction with fibrinogen and other ligands by electron microscopy." J Biol Chem **267**(23): 16637-16643.
- Weiss, E. J., J. R. Hamilton, K. E. Lease and S. R. Coughlin (2002). "Protection against thrombosis in mice lacking PAR3." Blood **100**(9): 3240-3244.
- Wiederschain, G. Y. (2011). "The Molecular Probes handbook. A guide to fluorescent probes and labeling technologies." Biochemistry (Moscow) **76**(11): 10-97.
- Wong, C. H., C. N. Jenne, B. Petri, N. L. Chrobok and P. Kubes (2013). "Nucleation of platelets with blood-borne pathogens on Kupffer cells precedes other innate immunity and contributes to bacterial clearance." Nat Immunol **14**(8): 785-792.
- Xiao, T., J. Takagi, B. S. Coller, J. H. Wang and T. A. Springer (2004). "Structural basis for allostery in integrins and binding to fibrinogen-mimetic therapeutics." Nature **432**(7013): 59-67.
- Xiong, J.-P., T. Stehle, B. Diefenbach, R. Zhang, R. Dunker, D. L. Scott, A. Joachimiak, S. L. Goodman and M. A. Arnaout (2001). "Crystal Structure of the Extracellular Segment of Integrin α V β 3." Science (New York, N.Y.) **294**(5541): 339-345.
- Xiong, J. P., T. Stehle, S. L. Goodman and M. A. Arnaout (2003). "New insights into the structural basis of integrin activation." Blood **102**(4): 1155-1159.

- Xiong, J. P., T. Stehle, R. Zhang, A. Joachimiak, M. Frech, S. L. Goodman and M. A. Arnaout (2002). "Crystal structure of the extracellular segment of integrin alpha Vbeta3 in complex with an Arg-Gly-Asp ligand." Science **296**(5565): 151-155.
- Yam, P. T., C. A. Wilson, L. Ji, B. Hebert, E. L. Barnhart, N. A. Dye, P. W. Wiseman, G. Danuser and J. A. Theriot (2007). "Actin–myosin network reorganization breaks symmetry at the cell rear to spontaneously initiate polarized cell motility." The Journal of Cell Biology **178**(7): 1207-1221.
- Ye, F., C. Kim and M. H. Ginsberg (2011). "Molecular mechanism of inside-out integrin regulation." J Thromb Haemost **9 Suppl 1**: 20-25.
- Yeaman, M. R. (2014). "Platelets: at the nexus of antimicrobial defence." Nat Rev Microbiol **12**(6): 426-437.
- Zhang, Y., Y. Qiu, A. T. Blanchard, Y. Chang, J. M. Brockman, V. P. Ma, W. A. Lam and K. Salaita (2018). "Platelet integrins exhibit anisotropic mechanosensing and harness piconewton forces to mediate platelet aggregation." Proc Natl Acad Sci U S A **115**(2): 325-330.
- Zhang, Y., Y. Qiu, A. T. Blanchard, Y. Chang, J. M. Brockman, V. P.-Y. Ma, W. A. Lam and K. Salaita (2018). "Platelet integrins exhibit anisotropic mechanosensing and harness piconewton forces to mediate platelet aggregation." Proceedings of the National Academy of Sciences **115**(2): 325.
- Zhou, Y., K. K. Chan, T. Lai and S. Tang (2013). "Characterizing refractive index and thickness of biological tissues using combined multiphoton microscopy and optical coherence tomography." Biomedical optics express **4**(1): 38-50.
- Zhu, J., B. H. Luo, T. Xiao, C. Zhang, N. Nishida and T. A. Springer (2008). "Structure of a complete integrin ectodomain in a physiologic resting state and activation and deactivation by applied forces." Mol Cell **32**(6): 849-861.
- Zhu, J., J. Zhu, A. Negri, D. Provasi, M. Filizola, B. S. Coller and T. A. Springer (2010). "Closed headpiece of integrin alphaIIb beta3 and its complex with an alphaIIb beta3-specific antagonist that does not induce opening." Blood **116**(23): 5050-5059.

7 Eidesstaatliche Erklärung

Ich erkläre hiermit an Eides statt, dass ich die an der Medizinischen Fakultät der Ludwig-Maximilians-Universität München eingereichte Arbeit mit dem Titel:

The role of mechanosensing in platelet function

am Klinikum der Ludwig-Maximilians-Universität München
Medizinische Klinik und Poliklinik I

selbst verfasst, alle Teile eigenständig formuliert und keine fremden Textteile übernommen habe, die nicht als solche gekennzeichnet sind. Kein Abschnitt der Doktorarbeit wurde von einer anderen Person formuliert und bei der Abfassung wurden keine anderen als die in der Abhandlung aufgeführten Hilfsmittel benutzt.

Ich habe an keiner anderen Stelle einen Antrag auf Zulassung zur Promotion gestellt oder bereits einen Dokortitel auf der Grundlage des vorgelegten Studienabschlusses erworben und mich auch nicht einer Doktorprüfung erfolglos unterzogen.

Die Arbeit habe ich bislang an keiner Hochschule als Bestandteil einer Prüfungs- oder Qualifikationsleistung vorgelegt.

Die Dissertation wurde ohne Hinzuziehung einer kommerziellen Promotionsberatung erstellt.

Die Promotionsordnung der Medizinischen Fakultät der Ludwig-Maximilians-Universität München ist mir bekannt. Die Bedeutung der eidesstattlichen Erklärung und die strafrechtlichen Folgen einer unrichtigen oder unvollständigen eidesstattlichen Erklärung sind mir bekannt.

Ben Raude

Berlin, den 12.07.2021